

Institut für Nutzpflanzenwissenschaften und Ressourcenschutz

**Studies on the effect of exogenous amino acid
application on nematodes**

Dissertation

zur Erlangung des Grades

Doktor der Agrarwissenschaften (Dr. agr.)

der Landwirtschaftlichen Fakultät

der Rheinischen Friedrich-Wilhelms-Universität Bonn

vorgelegt von

Roman Christopher Blümel

aus Essen

Bonn, 2020

Referent: Prof. Dr. Florian Grundler

Korreferent: Prof. Dr. Johannes Hallmann

Tag der mündlichen Prüfung: 30.10.2019

Angefertigt mit Genehmigung der Landwirtschaftlichen Fakultät der Universität Bonn

ABSTRACT

Plant-parasitic nematodes are considered as key pathogens in agricultural crop production. They cause substantial yield losses in numerous crops and across all climatic regions worldwide. Antagonistic effects on various life stages of economically relevant plant-parasitic nematode species were reported for different amino acids (aa). In order to screen for effects induced by exogenous application and to reveal their underlying mechanistic methionine (Met), lysine (Lys), threonine (Thr), isoleucine (Ile), 2-ketobutyric acid (Ket), homoserine (Hom) and tryptophan (Trp) were tested on the free-living nematode *Caenorhabditis elegans* and the plant-parasite *Heterodera schachtii*.

Try applications reduced the activity and development of *C. elegans*, whereas only Ket affected the activity of *H. schachtii*. Interestingly, soaking J2 stage nematodes in aa solutions for twenty-four hours, induced a sex ratio change for both Lys isomers. The strongest effects were observed when aa were supplemented to the nutrient-medium in a monoxenic culture of the host plant, *Arabidopsis thaliana*. This approach reduced the number of female nematodes per plant for Iso, Met, Thr, and Ket. Additionally, slight negative effects could be detected on the adult female sizes. Interestingly, these effective aa all belong to the aspartate pathway. Herein, in particular the plant inherent enzyme methionine- γ -lyase (MGL) was identified as possible key functional element.

Pflanzenparasitäre Nematoden gehören zu den wichtigsten Schaderregern im landwirtschaftlichen Pflanzenbau. Sie verursachen weltweit substanzienlen Ertragsverluste in unterschiedlichen Kulturen und klimatische Regionen. Antagonistische Effekte gegen verschiedene Lebensstadien ökonomisch relevanter Nematodenspezies wurden für verschiedene Aminosäuren (aa) beschrieben. Um durch exogene Applikation indizierte Effekte aufzuzeigen und die ihnen zugrunde liegenden Mechanismen zu untersuchen, wurden Methionin (Met), Lysin (Lys), Threonin (Thr), Isoleucin (Ile), 2-Ketobuttersäure (Ket), Homoserin (Hom) and Tryptophan (Trp) gegen den freilebenden Nematoden *Caenorhabditis elegans* sowie den pflanzenparasitären Nematoden *Heterodera schachtii* getestet.

In den Studien konnten Effekte die aus dem direkten Kontakt juveniler Nematoden mit applizierten Substanzen resultieren von denjenigen Effekten abgegrenzt werden die als sekundäre Folge der Wirtspflanzenbehandlung auftraten. Try beeinträchtigte Aktivität und Entwicklung von *C. elegans*, wohingegen sich Ket nur auf die Aktivität von *H. schachtii* auswirkte. Die 24 stündige Inkubation von *H. schachtii* J2 in wässrigen D-Lys und L-Lys Lösungen induzierte eine Umkehr des Geschlechterverhältnisses. Die stärksten Effekte wurden jedoch durch Zugabe der Testsubstanzen in das Nährmedium der Wirtspflanze *A. thaliana* hervorgerufen. An Iso, Met, Thr, und Ket behandelten Pflanzenwurzeln war die Anzahl weiblicher Nematoden signifikant reduziert. Des Weiteren war eine leichte Abnahme des Körperumfangs erkennbar. Alle wirksamen aa sind eng verwandte und funktional verknüpfte Metabolite innerhalb des sogenannten Aspartat Stoffwechselweges. Weitergehende molekulare Studien deuten klar auf eine kritische funktionale Beteiligung des Enzyms Methionin- γ -lyase (MGL) hin.

TABLE OF CONTENTS

Abstract	2
1 Index	9
1.1 Figures	9
1.2 Tables	11
1.3 Abbreviations	12
2 Introduction	18
2.1 Animal and plant model organisms	18
2.1.1 <i>Heterodera schachtii</i>	18
2.1.2 <i>Caenorhabditis elegans</i>	20
2.1.3 <i>Arabidopsis thaliana</i>	21
2.2 Amino acids	23
2.2.1 Characterization and classification	23
2.2.2 Chemical and physical characterization properties	24
2.3 Aa metabolism and transport of plants	26
2.3.1 Description of biosynthesis pathway	29
2.3.2 Regulation of the Aspartate Pathway	33
2.3.3 Aa transport in plants	35
2.4 Aa in nematode-hostplant interactions	37
2.4.1 Aa requirements of nematodes	37
2.4.2 The participation of aa transporters in host-nematode interactions	37
2.4.3 Influence of quantitative aa levels in host plants on nematode parasitism	39
2.5 Applied nematode control techniques	39
2.5.1 Chemical nematode control	40
2.5.2 Plant derived nematode control	40
2.5.3 Biological nematode control	41
2.6 Effects of exogenously applied aa on nematodes	43

2.6.1 Effects reported for methionine	43
2.6.2 Effects reported for other aa	44
2.6.3 Summary on aa induced effects on nematodes	45
3 Materials	46
3.1 Biological materials	46
3.2 Chemicals	47
3.3 Plastic and glassware	50
3.4 Instruments / machines	52
3.5 Purchased kits	54
3.6 Software	55
4 Methods	56
4.1 Preparation of test compound solutions	56
4.2 Experiments with <i>C. elegans</i>	56
4.2.1 Culture establishment and maintenance of <i>C. elegans</i>	57
4.2.2 Tests for effects on the activity of <i>C. elegans</i>	59
4.2.3 Effects on the development of <i>C. elegans</i>	60
4.3 Experiments with <i>Heterodera schachtii</i>	61
4.3.1 Maintenance and preparation	61
4.3.2 Maintenance and preparation of <i>A. thaliana</i>	63
4.3.3 Infection assay analyses	64
4.3.4 Activity test in solution	65
4.3.5 24h incubation of nematodes prior to inoculation	66
4.3.6 Knops'-medium supplemented with test compounds	67
4.3.7 Detailed analysis of the infection and development of <i>H. schachtii</i>	69
4.3.8 Infection assays with SALK_081563c and mtol-1 mutant lines	70
4.3.9 Gene expression analysis by NEMATIC	72
4.3.10 Gene expression analysis by qRT-PCR	73

5 Results	81
5.1 <i>C. elegans</i> experiments	81
5.1.1 Effects on the activity	81
5.1.2 Effects on the development	82
5.2 <i>H. schachtii</i> experiments	84
5.2.1 Effects on the activity	84
5.2.2 24h incubations of <i>H. schachtii</i>	85
5.2.3 Treatment of <i>A. thaliana</i>	89
5.2.4 Detailed infection and development analysis	96
5.2.5 Gene expression analysis by NEMATIC	97
5.2.6 qRT-PCR	100
6 Discussion	108
6.1 Effects induced by direct contact	109
6.1.1 Implications of the nematode biology for compound exposures	109
6.1.2 Effects on the activity of <i>C. elegans</i> and <i>H. schachtii</i>	110
6.1.3 Effects on the development of <i>C. elegans</i>	111
6.1.4 Effects on the parasitism of <i>H. schachtii</i>	112
6.2 Effects on <i>H. schachtii</i> induced by treatments of the host plant <i>A. thaliana</i>	113
6.2.1 Effects induced by supplementing aa to Knops'-medium on <i>A. thaliana</i>	113
6.2.2 Effects on the parasitism of <i>H. schachtii</i>	114
6.2.3 Detailed infection and development analysis	114
6.2.4 Effects on the quantitative and qualitative nutritional situation	115
6.3 Analysis with regard to the aspartate pathway	116
6.3.1 The involvement of the aspartate pathway	116
6.3.2 Regulation of the aspartate pathway in the syncytium	117
6.3.3 Transcriptional changes in aa treated <i>A. thaliana</i> roots	118
6.3.4 Examining the influence of MGL	121

6.4 Final conclusion	122
7 References	123
8 Appendix	133
8.1 Materials and methods	133
8.1.1 NGM-medium	133
8.1.2 LB-medium	133
8.1.3 M9 buffer	134
8.1.4 Bleach solution	134
8.1.5 S-Basal complete medium	135
8.1.6 Knops'-medium	136
8.1.7 DNA extraction from plant	138
8.1.8 The NEMATIC analysis	138
8.1.9 Primer design using Primer 3	140
8.2 Results	141
8.2.1 Results for experiments on <i>C. elegans</i>	141
8.2.2 Results on <i>H. schachtii</i>	142

1 INDEX

1.1 Figures

Figure 1 L-Lys structural formula	24
Figure 2 D-Lys structural formula	24
Figure 3 L-Met structural formula	24
Figure 4 D-Met structural formula	24
Figure 5 L-Thr structural formula	25
Figure 6 D-Thr structural formula	25
Figure 7 L-Trp structural formula	25
Figure 8 D-Trp structural formula	25
Figure 9 L-Ile structural formula	25
Figure 10 D-Ile structural formula	25
Figure 11 L-Hom structural formula	26
Figure 12 2-Ketobutyric acid structural formula	26
Figure 13 Aspartate pathway diagram	28
Figure 14 Schematic diagram of a funnel	62
Figure 15 Female and male <i>H. schachtii</i> body shape	65
Figure 16 <i>C. elegans</i> activity test	82
Figure 17 <i>H. schachtii</i> activity test	85
Figure 18 24h incubation: adult nematodes per plant	86
Figure 19 24h incubation: syncytium and female sizes	88
Figure 20 24h incubation in the absence of ZnCl ₂ and HgCl ₂	89
Figure 21 Aa treated <i>A. thaliana</i> : invasion rate analysis	91
Figure 22 Aa treated <i>A. thaliana</i> : adult nematodes per plant	92
Figure 23 Aa treated <i>A. thaliana</i> : measurement of female sizes	93
Figure 24 Aa treated <i>A. thaliana</i> : measurement of syncytium sizes	94
Figure 25 Aa treated <i>A. thaliana</i> : no. of eggs per cyst	95
Figure 26 NEMATIC analysis	98
Figure 27 RNA integrity, quantity and purification test	101
Figure 28 DNA digestion confirmation in RNA samples 1/3	102
Figure 29 DNA digestion confirmation in RNA samples 2/3	102
Figure 30 DNA digestion confirmation in RNA samples 3/3	102

Figure 31 PCR on <i>H. schachtii</i> infected <i>A. thaliana</i> cDNA	103
Figure 32 PCR on <i>H. schachtii</i> cDNA	103
Figure 33 qRT-PCR: Gene expression in aa treated uninfected <i>A. thaliana</i> roots	105
Figure 34 qRT-PCR: Gene expression in aa treated infected <i>A. thaliana</i> roots	106

1.2 Tables

Table 1 Test compound concentrations - <i>C. elegans</i> activity	59
Table 2 Test compound concentrations - <i>C. elegans</i> development	60
Table 3 Test compound concentration - <i>H. schachtii</i> activity and 24 hr incubation	66
Table 4 Final compound concentrations in the Knops'-medium	68
Table 5 Primer set used for SALK_081563c homozygosity determination	72
Table 6 DNase digestion reaction protocol - “RQ1 RNase-free DNase”	74
Table 7 Thermo cycler protocol for cDNA synthesis	75
Table 8 PCR master mix protocol	76
Table 9 Thermocycler protocol for primer specificity analysis	77
Table 10 Aspartate family primer set	78
Table 11 qRT-PCR protocol - gene expression and primer primer efficiency	79
Table 12 qRT-PCR master mix	80
Table 13 <i>C. elegans</i> development effects	83
Table 14 24 hr incubations of nematodes prior to inoculation – total numbers	87
Table 15 <i>A. thaliana</i> on enriched Knops'-medium - main root lengths	90
Table 16 Daily close up analysis of the <i>H. schachtii</i> infection process	96
Table 17 NEMATIC – detailed differential gene expressions	99
Table 18 KPO ₄ buffer	133
Table 19 NGM-medium	133
Table 20 LB-medium	134
Table 21 M9-buffer	134
Table 22 Bleach solution	135
Table 23 Trace Metal Solution	135
Table 24 S-Basal solution	136
Table 25 S-Basal complete solution	136
Table 26 Knops'-medium protocol	137
Table 27 Knops'-medium stock solutions	137
Table 28 1 M Tris	138
Table 29 Marker gene dataset analysed with NEMATIC	138
Table 30 NEMATIC – detailed gene expression fold changes	148

1.3 Abbreviations

°C	degree Celsius
µg	microgram
µl	microliter
µM	micrometer
1 st	first
2 nd	second
3 rd	third
7 th	seventh
<i>A. thaliana</i>	<i>Arabidopsis thaliana</i>
aa	amino acids
AAPs (also AtAAPs)	amino acid permeases
ACC	1-aminocyclopropane-1-carboxylic Acid
acetyl-CoA	acetylcoenzyme A
ACO	ACC-oxidase
ACS	ACC-synthase
ACT	actin
AHAS	acetohydroxyacid synthase
AK	aspartate kinase
APC	amino acid-polyamine-choline
<i>Aphelenchoides</i> sp.	<i>Aphelenchoides</i> species
Arg	arginine
approx	approximately
AS	anthranilate synthase
Asn	asparagine
Asp	aspartic acid
AtLHT1	<i>Arabidopsis thaliana</i> lysine histidine transporter
AtMGL	<i>Arabidopsis thaliana</i> methionine-gamma-lyase
ATP	adenosine triphosphate

BCAT	branched-chain aminotransferase
bp	base pair
<i>C. elegans</i>	<i>Caenorhabditis elegans</i>
CATs (also AtCAT)	cationic amino acid transporters
CBL	cystathionine β -lyase
cDNA	complementary deoxyribonucleic acid
cds	coding sequences
cf.	confer to
CGS	cystathionine gamma synthase
cm	centimeter
CO ₂	carbon dioxide
col-0	columbia-0
-COOH	carboxyl group
CTAB	cetrimoniumbromide
Cys	cysteine
ddH ₂ O	double-distilled water
DHAD	dihydroxyacid dehydratase
DHPS	dihydrodipicolinate synthase
DLM	DL-methionine
DL-M	DL-methionine
DL-Met	DL-methionine
DANN	deoxyribonucleic acid
dpi	days past infection
dps	days past seeding
EC	electronic annotation
<i>et al.</i>	<i>et aliae</i> ; and others
EtOH	ethanol
G	gram
G3P	D-glyceraldehyde 3-phosphate
Gln	glutamine

Glu	glutamic acid
Gly	glycine
-H	hydrogen atom
<i>H. schachtii</i>	<i>Heterodera schachtii</i>
H ₂ O	water
ha	hectare
HCl	hydrogen chloride
His	histidine
HK	homoserine kinase
Hom	homoserine
h	hours
HSD	homoserine dehydrogenase
i.e.	<i>id est</i> ; this means
IGPS	indole-3-Glycerol Phosphate Synthase
Ile	isoleucine
ISC	initial syncytial cell
J2	second stage juveniles
JA-Ile	jasmonate-isoleucine
KARI	ketol acid reductoisomerase
kb	kilo bases
Ket	2-ketobutyric acid
kg	kilogram
KOH	potassium hydroxide
L	liter
L (1-4)	larvae stage 1-4 regarding <i>C. elegans</i>
LB	lysogeny broth
Ler-0	Landsberg
Leu	leucine
LN ₂	liquid nitrogen
LTHR (also AtLTHR)	L-threonine

Lys	Lysine
M	Molar
<i>M.</i>	<i>Meloidogyne</i>
Met	methionine
mg	milligram
MGL	methionine- γ -lyase
min	minute
ml	milliliter
MM	H-Met-Met-OH
mm	millimeter
mM	millimol
mm ²	square millimeter
MMT	AdoMet:MetS-methyltransferase
MoA	mode of action
MS	methionine synthase
MTA	5-methylthioadenosine
N	Nitrogen
n	number
no	number
NAMP	nematode associated molecular pattern
NaOCl	sodium hypochlorite
NASC	The Nottingham <i>Arabidopsis</i> Stock Centre
NEMATIC	Nematode-Arabidopsis Transcriptomic Interaction Compendium
NGM	nematode growth medium
-NH ₂	amino group
nmol	nanomole
no	number
OMR1	theronine dehydratase/deaminase
OPH	O-phosphohomoserine
PAI	phosphoribosylanthranilate isomerase

PAMP	pathogen-associated molecular pattern
PAT	phosphoribosylanthranilate transferase
PCR	polymerase chain reaction
Phe	phenylalanine
Pro	proline
qRT-PCR	quantitative real time polymerase chain reaction
RIN	RNA integrity number
RNA	ribonucleic acid
rpm	rounds per minute
RT	reverse transcriptase
RT-PCRs	real time polymerase chain reaction
SAH	S-adenosylhomocysteine
SAM	S-adenosylmethionine
SAMS	S-adenosylmethionine synthase
sec	second
Ser	serine
SMC	S-adenosylmethionine S-methylcysteine
SMM	S-methlymethionine
TAIR	The <i>Arabidopsis</i> Information Resource
T-DNA	transfer deoxyribonucleic acid
THA	threonine aldolase
Thr	threonine
Trp	tryptophan
TrpS	tryptophan synthase
TS	threonine synthase
Tyr	tyrosine
V	voltage
v.	version
Val	valine
W	untreated control

WS	Wassilewskija
ZnCl ₂	zinc chloride
α KB	α -ketobutyrate

2 INTRODUCTION

Plant-parasitic nematodes cause considerable economic losses across all crops in agricultural systems worldwide. Today's nematode control in crop production is mainly composed of cultivation methods, chemical active substances, biocontrol and resistant or tolerant crop varieties. Even though diverse tools are available, the overall control efficacy remains insufficient (Chitwood, 2003). The necessity to reduce yield losses by plant-parasitic nematodes in commercial agricultural results in an open demand for new and in particular non-chemical nematode control options. The control potential of aa has been investigated for the first time in 1962 (Overman and Woltz, 1962). Over the next decades continuous research revealed multiple effects against a broad spectrum of nematode species. The most promising candidate aa were selected and their effects against nematodes were studied in detail under *in vitro* conditions.

2.1 Animal and plant model organisms

2.1.1 *Heterodera schachtii*

Invisible to the human eye, plant-parasitic nematodes gain increasing attention and importance in commercial agriculture. Although these pathogens are microscopically small, they attack in numbers and can induce tremendous damage. Plant-parasitic nematodes feed on plant roots from the outside as ectoparasites or enter the root tissue and feed inside of it as endoparasites. Endoparasitic nematode species can be further divided into a migratory and a sedentary fraction. Among those, sedentary endoparasitic nematodes are considered as the economically most important root pathogens (Wyss and Grundler, 1992). They comprise cyst nematodes (*Heterodera* spp., *Globodera* spp.) and root-knot nematodes (*Meloidogyne* spp.) (Williamson and Gleason, 2003). Sedentary plant-parasitic nematode species establish feeding site structures inside of host plant roots, that impair or block the xylem and phloem based nutrient and water transport. Additionally, penetrating the root leaves open wounds in the epidermis that function as entrance gates for secondary fungal, bacterial and viral infections.

Heterodera spp. have a broad host range, also including cruciferous plants like *Arabidopsis thaliana* (Williamson and Gleason, 2003, Sijmons *et al.* 1991). The cyst nematode *Heterodera schachtii* is an obligate biotroph endoparasite, showing an initial migratory and a sedentary life stage (Wyss and Grundler, 1992b). At the life cycle's beginning, eggs containing second

stage juveniles (J2) are located inside a cyst, the swollen dead body of a female nematode. J2 hatch from the eggs and emerge into the soil. They migrate actively through towards the plant roots, sensing their target by chemotaxis. J2 primarily invade at growing root tips and emergence sites of lateral roots (Wyss and Zunke, 1986). Cyst nematodes use the stylet, a needle like organ, to penetrate into the root. After successful penetration the J2 migrate intracellularly towards the vascular cylinder by piercing the cell walls (Wyss and Zunke, 1986). Here they stop and induce a complex feeding structure, the syncytium (Grundler *et al.*, 1998). The J2 pierce potential cells until a suitable cell is located to establish the syncytium, referred to as the initial syncytial cell (ISC). Afterwards, the stylet is inserted 3-4 μ m, by very careful thrusting movements and stays protruded inside for seven hours (h) (Wyss and Zunke, 1986; Sijmons *et al.*, 1991). Within this phase, cell wall material is deposited around the stylet tip, at affected cell wall areas and in neighboring cells. Moreover, membrane fragments condense and plasmodesmata are modified, forming cell wall openings. In further consequence, the gradual plasmodesmata widening leads to protoplast fusion of neighboring cells accompanied with cell wall degradation. The outer syncytial cells undergo a progressive fusion process with their neighboring cells (Grundler *et al.*, 1998). In summary, the syncytium is a nematode induced, multi-nucleic feeding structure of fused cells, with greatly thickened outer syncytial walls. It is the only source of nutrients including essential aa for the sedentary living *H. schachtii* (Szakasits *et al.*, 2009). After syncytium establishment *H. schachtii* loses its migratory ability and enters the sedentary phase. Subsequently, *H. schachtii* molts three times including sex determination. It is a long-term debate if *H. schachtii* underlies a genotypic or phenotypic sex determination. It was postulated that the quantitative availability of nutrients within the syncytium affects the sex determination. In this, a beneficial situation is thought to favor the development of females over males (Grundler, 1989; Grundler *et al.*, 1991). This might arise from markedly different quantitative nutrient uptake of male and female *H. schachtii*, whereas females take up 29 times more food than males (Müller *et al.*, 1981).

Nematodes that develop into males show a vermiform shape inside the J3 cuticles before they finally emerge into the soil to search and mate with females. Opposed to males, female nematodes do not leave the roots, but expand in size and develop the characteristic egg shape, cf. figure 15. The adult female bodies are finally filled with multiple hundred eggs before they die and remain as egg filled cysts in the soil (Sijmons *et al.*, 1991).

2.1.2 *Caenorhabditis elegans*

Caenorhabditis elegans is a worldwide distributed free-living nematode and a key model organism in different scientific fields. This species can be cultured on agar plates or in solution in large numbers. The short life cycle (3.5 days at 20°C) enables a quick experimental succession. In general, the easy cultivable bacterium *E. coli* yields as *in vitro* food source. Herein, the uracil auxotroph mutant strain OP50 is used to restrict an overgrowth of the bacteria on the plates (Brenner *et al.*, 1974). Since *C. elegans* is composed of relatively few cells, it is a functional model organism for lineage, pattern and genomic studies (Felix, 2008). In fact, the first fully sequenced genome of a multicellular organism was the one of *C. elegans*, underlining its suitability for genomic studies (The *C. elegans* sequencing consortium, 1998). Moreover, the transparent body provides optimal preconditions for examinations of all tissues and organs over the whole lifecycle by light microscopy.

The developmental speed and thus the length of the different lifecycle stages is temperature dependent. At 20°C the embryogenesis lasts approximately (approx.) 16h. Protected by the impermeable egg shell, it continues independent and outside of the mother. In general, the eggs are being laid at the 24-cell stage. At the time point of hatching, the L1 typically shows 558 nuclei. The further development includes four larval stages with a molt at the end of each. The L1 stage lasts for 16h, followed by L2-L4 at 12h each. Prior to each molt, the larvae remain in a quiescent state of feeding and locomotive arrest, called the lethargus period (Cassada and Russell, 1975; Byerly *et al.*, 1976; Raizen *et al.*, 2008). The sex is determined within the L4 stage. Adult hermaphrodites begin to produce progeny 12h after the molt from L4, for a period of 2-3 days. During food shortage and high population densities, an alternative lifecycle can be activated. In this, the L2 do not molt into L3 but enter a morphological identifiable stage with arrested development, called the dauer stage. This describes a facultative, reversible developmental arrest in response to unfavorable external conditions. The dauer cuticle has a greater protection against chemicals, the uptake of food stops and the locomotion is reduced. This dauer stage is reversible, regained food accessibility induces a resumption of feeding followed by molting to the L4 stage (Cassada and Russell, 1975).

When screening candidate substances for their nematicidal potential, the aim is to identify those substances that selectively affect plant-parasitic species. The free living and bacterivore *C. elegans* is an off-target organism, representing the group of not plant-parasitic

species. Screening effects of candidate substances on *C. elegans* and *H. schachtii* can accordingly identify substances that exclusively affect plant-parasitic species.

2.1.3 *Arabidopsis thaliana*

The small cruciferous *Arabidopsis thaliana* is a member of the mustard family. The natural distribution includes Europe, Asia and North America with diverse ecosystems from high elevations over tropical to cold northern climates (Meyerowitz, 1987; Meinke *et al.*, 1998).

The leaves are oriented in a rosette of 2-10cm in diameter. Dependent on the environmental conditions, the lifecycle takes six weeks from germination to maturation of the new seeds (Pang and Meyerowitz, 1987). The main stem is equipped with side branches and topped by a raceme inflorescence with multiple side flowers. Additional secondary side stems develop from the rosette (Meyerowitz, 1987). The maximum height is 30-40cm. The small seeds are generated and located in siliques, with an average weight of 20µg and diameter of 0.5mm (Meyerowitz, 1987; Meinke *et al.*, 1998). The root is partitioned into epidermis, cortex, endodermis, and a vascular cylinder surrounding pericycle (Dolan *et al.*, 1993).

A. thaliana can be considered as the major model organism in plant science. The most commonly used ecotypes are Columbia (col-0), Landsberg (Ler-0) and Wassilewskija (WS). It can be cultured on agar-medium and soil, under sterile *in vitro* as well as greenhouse conditions. The outstanding suitability for science erases from its suitability for molecular and genetic analysis. This involves the analysis of conserved processes of eukaryotes, biological structures and functions, as well as most importantly for this study the detailed analysis of host-pathogen interactions (Sijmons *et al.*, 1991; Meinke *et al.*, 1998; The *Arabidopsis* genome initiative, 2000). Driven by ‘The *Arabidopsis* genome initiative’ the complete *Arabidopsis* genome was sequenced and finally published in 2000 as the first fully sequenced plant genome. It is organized in five chromosomes, coding for 25.498 genes of 11.000 families (The *Arabidopsis* genome initiative, 2000; Meinke *et al.*, 1998). Enabled by this pioneer work, the uncomplicated generation of mutants by chemical and insertional mutagenesis and the global availability of mutants from seed banks provide a powerful research tool.

In the 1990s, *A. thaliana* was utilized to establish a model system to study host-plant-pathogen interactions. Successful infections were reported for the bacteria *Xanthomonas campestris* (Simpson and Johnson, 1990) and *Pseudomonas syringae* (Whalen *et al.*, 1991),

the fungus *Sclerotinia sclerotiorum* (Dickman and Mitra, 1992), *Peronospora parasitica* (Koch and Slusarenko, 1990), the cyst nematode species *Heterodera schachtii*, *H. trifolii* and *H. cajani*, the root-knot nematode species *Meloidogyne incognita* and *M. arenaria* and the migratory living *Paratylenchus penetrans* (Sijmons *et al.*, 1991). The combination of *H. schachtii* and *A. thaliana* provided the best functionality for *in vitro* studies of nematode-host and in particular cyst-nematode-host interactions. This sterile, monoxenic *in vitro* model system is setup under controlled temperature and light conditions. Plants are cultured in Petri dishes on Knops'-medium, enabling the plant to develop a long main root at a late development of lateral roots. Knops'-medium and roots are both translucent, enabling macro- and microscopic analysis of the nematode migration, invasion, infection and parasitism process. Among others parameters the invasion rate, time point of ISC establishment, number of male and female nematodes per plant and female and syncytium sizes can be studied.

Two *A. thaliana* mutant lines were used for this study, mto1-1 and SALK_081563c. Both carry mutations within the aspartate family pathway, altering the Met and Thr levels. Mto1-1 was isolated in 1994 by screening for ethionine resistant mutants, a toxic analogue of Met (Inaba *et al.*, 1994). The mutation is located in the Cystathione-gamma-synthase (CGS), restricting its down regulation in response to excess Met accumulations (Chiba *et al.*, 1999). Aa quantifications revealed 10-40-fold increased Met and slightly reduced Thr concentrations in aerial parts during vegetative growth. Only minor growth deficiencies were observed for mto1-1 (Inaba *et al.*, 1994)

SALK_081563c resulted from a genome wide *Agrobacterium* mediated T-DNA mutagenesis project of *A. thaliana* (Alonso *et al.*, 2003). According to ‘The *Arabidopsis* Information Resource’ (TAIR), this mutant carries a homozygous insertion in the threonine synthase (TS), the first enzyme unique to the Thr pathway. Studies revealed that knock outs and downs of TS generally result in elevated Met and lowered Thr levels. In contrast to this, mutants with impaired CGS activity or abundance have a lower Met but rather slightly affected Thr level, cf. 2.3.2.1. Nevertheless, there are no actual results and analysis available for this particular mutant.

The experimental work with these two mutants did not reveal any significant effects. For this reason, the results were attached as supplementary data, see chapter 8.2.2.8.

2.2 Amino acids

2.2.1 Characterization and classification

Aa are of fundamental importance, since every protein of every living organism contains at least one or more polypeptide chains, which are polymers of in-line covalently joined aa. In this, twenty different proteinogenic aa are used that differ in their primary structure, i.e. their individual aa succession (Knippers, 2006). This primary structure determines the polypeptide chain folding according to the diverse chemical characteristics of the different incorporated aa. With the exception of glycine, the common chemical structure of these organic compounds consists of a carboxyl group (-COOH), an amino group (-NH₂) and one hydrogen atom (-H) bound to one α-carbon (Stryer *et al.*, 2013; Pollard and Earnshaw, 2008). The α-carbon is an asymmetrical center, due to the β-carbon and the proton bound to it.

Accordingly, two possible configurations occur: enantiomeric L-isomers and D-isomers. In nature L-isomers are of major relevance, because only these isomers are used for protein synthesis in the vast majority of metabolic processes (Stryer *et al.*, 2013; Pollard and Earnshaw, 2008). Nevertheless, recent findings suggest possible relevant physiological functions of D-isomers in *A. thaliana* (Gördes *et al.*, 2013). Each aa, except for proline, has a characteristic side chain called R-group. Aa differ in size, physical configuration, electrical charge, ability to form hydrogen bridges, hydrophobic character and chemical reactivity based on its chemical structure (Mueller-Esterl, 2009; Stryer *et al.*, 2013). Most aa are dipolar ions, therefore the amino-group is protonated and the carboxyl-group is dissociated under neutral pH conditions (Stryer *et al.*, 2013). Aa are amphotytes, hence they can act as acids and bases at the same time.

Two major subgroups can be separated, the not-proteinogenic and the proteinogenic aa, which are the aa used for protein synthesis. Multiple hundred not-proteinogenic aa occur in nature. Most of them are precursor metabolites or derivatives of proteinogenic aa. Only a minor number has independent relevant functions. Interestingly, especially in plants many not-proteinogenic aa with mostly unknown functions are present (Mueller-Esterl, 2009). According to the polarity of their R-groups, the 20 proteinogenic aa can be distinguished in subgroups (Mueller-Esterl, 2009; Stryer *et al.*, 2013):

- 1) aa with unpolar side-chains (Gly, Ala, Val, Leu, Ile, Met, Pro, Phe, Tyr and Trp)
- 2) aa with polar side-chains (Ser, Thr, Cys, Asn and Gln)
- 3) aa with charged side-chains (Asp, Glu, Lys, Arg and His)

Animals cannot self-synthesize all 20 proteinogenic aa. Those aa that cannot be synthesized are called essential aa. Since their availability is essential for survival they have to be taken up within the diet. The set of essential aa is organism dependent and will be discussed specifically for nematodes in chapter 2.4.1.

2.2.2 Chemical and physical characterization properties

The very background of the function and suitability of compounds in biological processes is determined by their individual chemical and physical composition. Therefore, the relevant characteristics of all test compounds will be listed below:

Proteinogenic aa:

- 1) Lysine C₆H₁₄N₂O₂

Lys is highly hydrophilic due to the polar side-chain. Under neutral pH-conditions it is positively charged and has a primary amino-group attached to the end (Stryer, *et al.*, 2013). Additionally, the side-chain can be modified by methylation (Knippers, 2006).

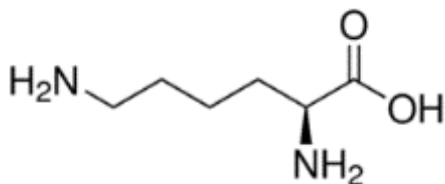


Figure 1 L-Lys structural formula

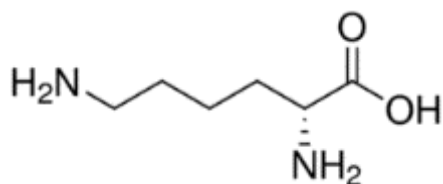


Figure 2 D-Lys structural formula

- 2) Methionine C₅H₁₁NO₂S

Met is a hydrophobic aa. The mostly aliphatic side-chain has an attached thioether group. Therefor it is one of the two existing proteinogenic aa with an incorporated sulfur atom, together with Cysteine (Stryer, *et al.*, 2013).

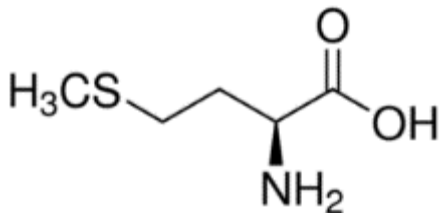


Figure 3 L-Met structural formula

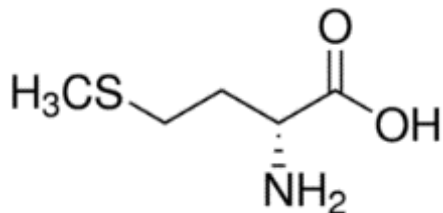


Figure 4 D-Met structural formula

Met was applied in this study as DL-Met and MM. MM is the dipeptide of Met. The two connected Met molecules must be detached before they are accessible for metabolic

processes. DL-Met is composed of the L-isomer and the D-isomer of which the latter is only limited available for metabolically processes.

3) Threonine C₄H₉NO₃

Thr is polar but uncharged. It carries a hydroxyl group that is bound to a hydrophobic side-chain. This group forms hydrogen bond linkages, making Thr hydrophilic. Moreover, Thr has an additional center of asymmetry (Knippers, 2006; Stryer, *et al.*, 2013).

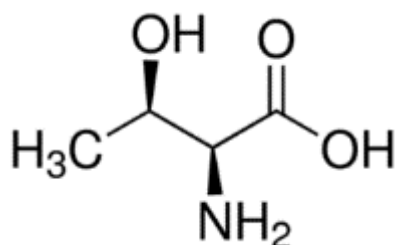


Figure 5 L-Thr structural formula

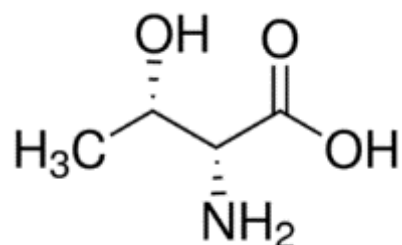


Figure 6 D-Thr structural formula

4) Tryptophan C₁₁N₁₂N₂O₂

Trp belongs to the hydrophobic aa with aromatic side-chains. It has an indole ring attached by a methyl group, which is constructed by two rings and a NH-group. Trp is the a very rare proteinogenic aa. Nevertheless, it is an essential element of the active center of certain enzymes (Knippers, 2006; Stryer, *et al.*, 2013).

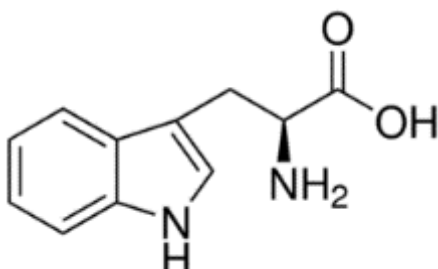


Figure 7 L-Trp structural formula

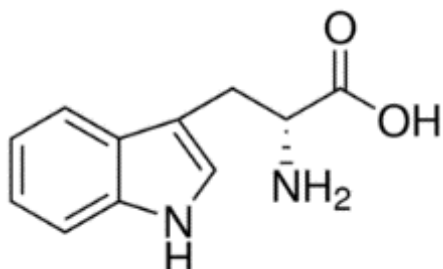


Figure 8 D-Trp structural formula

5) Isoleucine C₆H₁₃NO₂

Ile is hydrophobic. Its side-chain is equipped with an additional chirality center. Same as Val and Leu, Ile has relatively long hydrocarbon sidechains (Stryer, *et al.*, 2013).

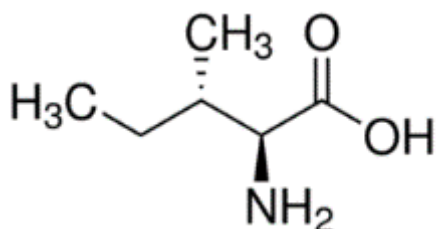


Figure 9 L-Ile structural formula

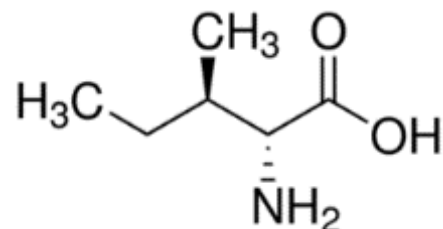


Figure 10 D-Ile structural formula

Not-proteinogenic aa and compounds:

- 6) Homoserine C₄H₉NO₃

Hom belongs to the not-proteinogenic aa. Its chemical structure enables the formation of a closed ring structure of 5 elements. This characteristic restricts the suitability for protein syntheses (Knippers, 2006).

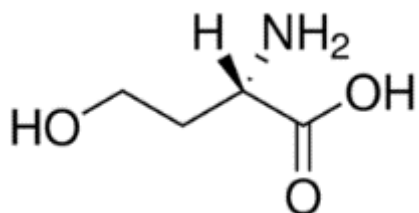


Figure 11 L-Hom structural formula

- 7) 2-Ketobutyric acid C₄H₆O₃

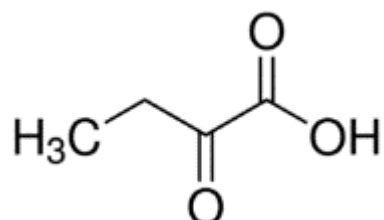


Figure 12 2-Ketobutyric acid structural formula

2.3 Endogenous aa metabolism

According to the results of this work, aa needed to be preliminary taken up by the plant before strong effects on nematodes were induced. Additionally, it was observed that treating *A. thaliana* with aa changed the expression of aspartate family related marker genes. These changes might be inductive for the impairing effects on female nematodes. To elaborate the underlying mechanistic, it could be relevant to involve the enzymatic set up and regulatory system of the aspartate family pathway of plants. Therefore, a comprehensive description on the aspartate pathway will be given hereafter. At first, the synthesis and catabolism routes of all relevant pathway enzymes and intermediate metabolites will be explained. Afterwards, the regulatory interactions between the pathway branches and enzymes will be discussed.

2.3 Aa metabolism and transport of plants

The metabolic pathways of Lys, Met, Thr, Ile originate from a single common precursor substrate: aspartate. This very metabolic region is called “aspartate pathway”, see figure 13.

Herein, the individual pathway branches compete for the carbon/amino skeletons of aspartate (Amir, 2010). This competition underlies a complex structure of regulatory interactions that dynamically balance the enzymatic synthesis and degradation of Lys, Thr, Met, Ile and other related metabolites. To reduce complexity, hereafter the term “aspartate pathway” refers only to those pathways that are located downstream of homoserine, namely the Met, Sam, Thr and Ile branches.

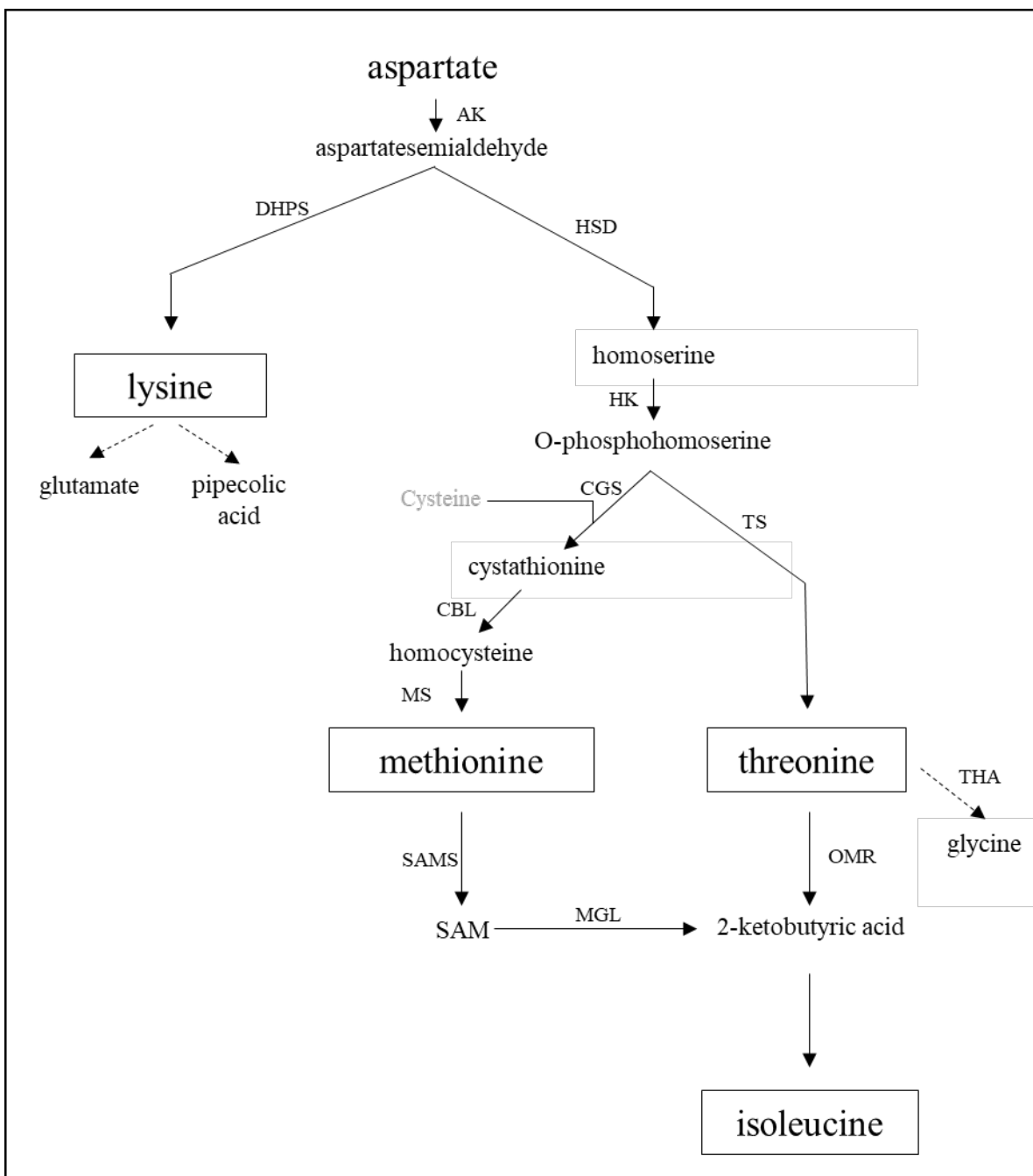


Figure 13 Aspartate pathway diagram Simplified diagram of relevant aspartate family pathway metabolites and enzymes of *A. thaliana*. The individual Lys, Met, Thr and Ile branches separate downstream of aspartate. Indicated are the gene families: aspartate kinase (Ak), cystathionine β -lyase (CBL), S cystathionine γ -synthase (CGS), Dihydronicotinate synthase (DHPS), homoserine kinase (HK), homoserine dehydrogenase (HSD), methionine synthase (MS), S-adenosylmethionine synthase (SAMS), threonine dehydratase/deaminase (OMR), threonine aldolase (THA), threonine synthase (TS) and Met- γ -lyase (MGL). Arrows (\rightarrow) mark the major synthesis succession direction.

2.3.1 Description of biosynthesis pathway

2.3.1.1 Aspartate

Originating from aspartate, the aspartate kinase (AK) forms 3-aspartyl phosphate before the enzyme aspartate semialdehyde dehydrogenase catalyzes the conversion to aspartate-semialdehyde (Amir and Galili, 1999). From this metabolite onwards the catabolism splits into the Lys and Thr/Met-Ile branches.

2.3.1.2 Lysine

The first enzyme unique to the Lys biosynthesis pathway is dihydronicotinate synthase (DHPS). It forms 2,3-dihydronicotinate from aspartate-semialdehyde by a condensation reaction. DHPS appears as the most influential regulatory enzyme within the Lys pathway because it is highly feedback sensitive (Amir and Galili, 1999).

Lys is catabolized via the saccharine pathway into glutamic and acetyl-CoA. Subsequently the derivatives are introduced into the citric acid cycle. The Lys catabolism involves seed, root and floral developmental processes and may also be involved in abiotic stress responses (Arruda *et al.*, 2000; Galili, 2002). *In vivo*, elevated Lys levels invariably generate an elevation Lys catabolism (Arruda *et al.*, 2000).

2.3.1.3 O-Phosphohomoserine

Aspartate-semialdehyde is converted in multiple steps into O-phosphohomoserine (OPH), the common substrate of the Thr and Met biosynthesis pathways. In detail, the homoserine dehydrogenase (HSD) catalyzes the conversion of aspartate-semialdehyde into homoserine before the homoserine kinase (HK) forms OPH. OPH is the branch point metabolite upstream of the individual Thr and Met biosynthesis pathways (Amir and Galili, 1999).

2.3.1.4 Methionine

The first enzyme unique to the Met branch is the cystathione γ -synthase (CGS; EC.2.5.1.48). CGS catalyzes the conversion of the cysteine sulfur compound and forms cystathione. In the next step, cystathione β -lyase (CBL) generates homocysteine, that is finally converted into Met by the methionine synthase (MS) comprising a methyl-group from 5-methyltetrahydrofolate (Kim and Leutsek, 2000; Amir, 2010).

Met is a fundamental compound for various metabolic and cellular processes. For this reason, its biosynthesis and catabolism are tightly regulated. Tracing experiments revealed, that Met is incorporated into S-methylmethionine, S-adenosylmethionine, S-methylcysteine (SMC) and Ile (Rebeille *et al.*, 2006). The Met branch is equipped with three salvage cycles and divides into two catabolic pathways.

The first catabolic pathway is the only interconnection between the Met and the Thr pathway branches. In this, Met- γ -lyase (MGL; EC 4.4.1.11) catalyzes the degradation into CH₃SH, NH₃ and α -ketobutyrate (α KB), which is also formed downstream of Thr. In the following, α KB channels into the Ile biosynthesis, as identified by ¹³C labeling experiments. Accordingly, the Met and Thr pathways both yield substrate for the synthesis of Ile. Even though it is the only direct link between the two main branches of the aspartate pathway, the metabolic relevance is unclear. Possibly it participates in the degradation of S-methylmethionine (SMM), a metabolite that accumulates under elevated Met concentrations. High SMM concentrations induce stress for the plant, possibly as a consequence of the very high synthesis costs of one ATP per molecule. In this situation the MGL→Ile branch could be utilized to synthesize Ile and SMC for additional nitrogen/carbon, sulfide- and methyl-group storage purposes.

Alternatively Met can be transformed by S-adenosylmethionine synthase (SAMS; EC 2.5.1.6) into S-adenosylmethionine (SAM) (Kim and Leutsek, 2000), the activated form of Met. The SAM catabolism involves numerous different derivatives of highest relevance in metabolic and cellular processes, such as the biosynthesis of polyamines, nicotinamines and the plant hormone ethylene. Additionally, it is the methyl group donor for most methylation reactions (Sauter *et al.*, 2013).

The biosynthesis of ethylene involves two enzymatic steps. First, SAM transformation into 5-methylthioadenosine (MTA) and 1-aminocyclopropane-1-carboxylic Acid (ACC) by ACC-synthase (ACS; EC 4.4.1.14). Secondly, ACC-oxidase (ACO) converts ACC into CO₂, HCN, H₂O and ethylene under the consumption of O₂ and ascorbate. Ethylene is a plant hormone and acts as a regulator and manipulator of diverse development, growth and senescence processes from seed germination to fruit ripening. Additionally, it is a stress hormone in response to abiotic and biotic stresses (Bleeker and Kende, 2000; Sauter *et al.*, 2013).

MTA is a by-product of polyamine and ethylene synthesis and the initial substrate of the Yang cycle, also known as Met salvage cycle (Miyazaki and Yang, 1987). Its basic function is to recycle sulfur atoms and simultaneously detoxify MTA, leading to the recovery of Met. The Yang cycle is a succession of six enzymatic conversions under consumption of H₂O, ATP, O₂ and additional, yet unidentified substrates accompanied with the release of adenine, H₂O, P_i, HCOOH and keto acid.

Two additional cyclic pathways are present for Met recycling: The SMM-cycle and the SAM-cycle. The latter utilizes S-adenosylhomocysteine (SAH) originating from SAM consuming methylation reactions. After the conversion of SAH into Homocysteine, MS finally catabolizes its methylation and thus the restoration of Met (Sauter *et al.*, 2013). S-methylmethionine (SMM) is synthesized from Met and SAM in the SMM-cycle, catalyzed by AdoMet:Met S-methyltransferase (MMT; EC 2.1.1.12). It functions as a methyl group-donor for the methylation-reaction of Homocysteine during Met synthesis (Mudd and Datko, 1986; Ranocha *et al.*, 2000).

2.3.1.5 Threonine

OPH is converted into Thr and inorganic phosphate in a single step by threonine synthase (TS), a gene family with two members (TS; EC:4.2.3.1) (Amir, 2010). Early studies on *Pisum sativum* and *Hordeum vulgare* located TS to the chloroplasts (Wallsgrove *et al.*, 1983), which still remains to be confirmed. Afterwards, the Thr catabolism splits into three catabolic pathways:

- 1) the enzymatic driven reversible transformation into glycine and acetaldehyde by threonine aldolase (THA; EC:4.1.2.5), according to functional analysis in *Escherichia coli* (Liu *et al.*, 1998).
- 2) the formation 2-amino-3-oxobutyrate by threonine dehydrogenase.
- 3) the degradation towards Ile synthesis, initiated by the Thr dehydratase/deaminase (OMR1; EC:4.3.1.19) (Joshi *et al.*, 2006).

2.3.1.6 Isoleucine

The Ile pathway of plants was most extensively studied in *A. thaliana*. When degrading Thr, OMR1 converts Thr to 2-Ketobutyrate (2-Keto) and methanethiol (Joshi and Jander, 2009).

This is the first step that is unique to the Ile pathway, originating from Thr. Another four enzymatic driven conversions by dihydroxyacid dehydratase (DHAD), ketol acid reductoisomerase (KARI), acetohydroxyacid synthase (AHAS) and branched-chain aminotransferase (BCAT) follow, before 2-oxobutanoate is finally condensed with one pyruvate molecule and then transformed into Ile. Exclusively in plants, these four intermediate enzymes are also part of the valine synthesis (Yu *et al.*, 2013).

2.3.1.7 Tryptophan

The unique Trp biosynthesis pathway diverts from chorismate and involves conversion reactions by six enzymes starting with Anthranilate Synthase (AS) (Radwanski and Last, 1995; Romero *et al.*, 1995; Barends *et al.*, 2008; Maeda and Dudareva, 2012). Overall, it consumes one amino donor (preferentially Gln), phosphoribosylpyrophosphate and yields D-glyceraldehyde 3-phosphate (G3P), 2H₂O, CO₂, pyruvate, Glu and PPi (Kirschner *et al.*, 1987; Radwanski and Last, 1995; Romero *et al.*, 1995; Barends *et al.*, 2008; Maeda and Dudareva, 2012). In plants the Trp derivatives are incorporated into auxin, phytoalexins, glucosinolates, and indole- as well as anthranilate-derived alkaloids biosynthesis. Accordingly, the Trp involves plant development, pathogen defense response reactions and plant insect interactions by volatile particles, effective in insect attraction (Radwanski and Last, 1995).

It had been demonstrated for a broad range of plant species that AS is feedback inhibited by Trp (Poulsen and Verpoorte, 1991). Accordingly, Trp regulates its own biosynthesis by interfering with the first enzyme unique to its own pathway. Studies on *Salmonella typhimurium* showed that Trp binds to the AS α subunit and restricts the conformational change (Morollo and Eck, 2001).

As apparent from this, the set up and regulation of the aspartate pathway is complex. The derivatives incorporated into diverse biological processes can trigger significant effects across the whole plant. It has to be considered, that nematode targeting effects of interest will always be accompanied by diverse additional effects on various biological processes.

2.3.2 Regulation of the Aspartate Pathway

2.3.2.1 The OPH branchpoint and the Met branch

The aspartate family pathway of plants underlies a multidimensional regulation system. This involves developmentally, environmentally and metabolic biochemically driven gene expression regulations. The hereafter explained regulatory interactions between the Thr, Met, Lys and Ile biosynthesis and catabolic pathways refer to the enzymatic metabolic setup, as described above. In this, primarily the regulatory interdependences downstream of OPH will be introduced.

The first enzyme downstream of Asp is the AK, regulated by substrate level driven feedback inhibitions induced by Thr, Lys, and SAM (Rognes *et al.*, 1980; Amir and Galili, 1999). Hereafter, the Lys and Thr/Met-Ile pathways separate. Both enzymes of this branchpoint are feedback inhibited, DHPS by Lys and HSK by Thr (Galili, 1995; Arruda *et al.*, 2000). In fact, the Lys and Thr synthesis ratios depend on competition between the enzymes DHPS and HSD for their limited common substrate aspartate-semialdehyde (Shaul and Galili, 1993; Galili, 1995).

The next main regulatory mechanism is located downstream of OPH, where the Met and the Thr pathways split. The allosteric enzyme TS and the two-substrate enzyme CGS compete for their common substrate OPH at this branchpoint (Curien *et al.*, 2003; Hesse *et al.*, 2004). Simplified, the balance between Thr and Met abundance functions according to the seesaw mechanism: Elevated levels of one aa and decreased levels of the other will be balanced via CGS and TS. This regulatory concert had recently been comprehensively reviewed and described by Amir (2010), the most relevant findings will be introduced below.

An *in-silico* modeling approach determined, a 1:7 CGS/TS enzyme ratio in an illuminated chloroplast leaf cell. Concurrently both enzymes have similar kinetic efficiencies towards OPH (Curien *et al.*, 2003). This finding accompanied by additional enzyme affinity calculations imply, that the primary usage of OPH for TS is enzyme concentration dependent (Amir, 2010). Mutant analysis and studies with transgenic plants suggest an alternate regulation. Experiments on potato, transformed with a constitutive TS-antisense expression showed only 45% of the wildtype Thr level but a 239-fold increase in Met (Zeh *et al.*, 2001). Moreover, the TS deficient *A. thaliana* mutant mto2-1 had 22-fold increased Met levels accompanied with markedly reduced Thr levels (Bartlem *et al.*, 2000). An inverted approach, with the constitutive expression of a CGS antisense construct in *A. thaliana*, showed a 20-fold accumulated OPH level, a 20-fold decreased CGS activity with a 35% decreased Met

level, but only a 4-fold increased Thr content (Gakiere *et al.*, 2000). Finally, studies on aa synthesis rates in AK feedback insensitive transgenic tobacco significantly increased Thr but did not affect Met levels (Shaul and Galili, 1992). These results indicate a higher affinity of TS towards OPH than for CGS.

Arabidopsis mutant analysis focusing on additional enzymes of the Met pathway revealed little impact on Thr levels. The mutant mto1-1 is deficient in feedback inhibition CGS under elevated Met concentrations. This resulted in increased Met and SAM levels. The SAMS3 deficient mto3 line had increased Met and decreased SAM amounts. Interestingly, in both mutants the Thr level was rather unaffected (Inaba *et al.*, 1994; Shen *et al.*, 2002). An activation of TS by SAM is therefore questionable *in vivo* (Amir, 2010).

Regarding Met synthesis, CGS might only play a minor rate limiting role, as described by Amir (2002). This assumption is based on the observations that:

- 1) impaired TS induced highly elevated Met levels without an increase of CGS protein levels
- 2) decreased CGS-levels only led to a relatively low decrease in Met amounts
- 3) CGS overexpression was found to be negatively correlated with Met levels in roots and flowers, but positively correlated in young leaves (Amir *et al.*, 2002).

Moreover, it had been demonstrated, that the expression of a Met insensitive CGS in tobacco resulted in increased Met, however unchanged Thr, Asp, Lys and Ile levels (Hacham *et al.*, 2006).

Of outstanding impact for the regulation of the Thr and Met pathways is the metabolic level of SAM. A transit peptide equips TS with SAM-sensitivity, resulting in the allosteric activation of TS in response to SAM (Curien *et al.*, 1996; Curien *et al.*, 1998). Additionally, the CGS-mRNA-stability is impaired by SAM and S-adenosly-L-ethionine (Chiba *et al.*, 2003; Onouchi *et al.*, 2005). Accordingly, elevated SAM levels (and hence its precursor Met) induce the synthesis of Thr, leading to reduced OPH availability for the in addition post-transcriptionally impaired CGS (Curien *et al.*, 1996; Amir *et al.*, 2002). Summarized, the SAM abundance directs the global substrate flux between the competitive Thr and Met branches.

2.3.2.2 The Thr catabolism towards Ile synthesis

TD, the first enzyme unique to Ile biosynthesis is feedback inhibited via a sigmoidal α,β -elimination reaction by Ile and valine (Samach *et al.*, 1991; Gallagher *et al.*, 1998). Worth to mention, that this was one of the first discovered allosteric inhibition mechanisms (Samach *et al.*, 1991). Accordingly, Ile levels feedback regulate the substrate influx into its own synthesis pathway. Nevertheless, the described pathway connection SAM→MGL→Ile is not affected by the TD inhibition. Given that all related aa, namely Lys, Thr, Met, regulate their substrate influx at their first pathway specific enzyme, it is likely that this also applies to the MGL initiated connection between SAM and Ile.

Summarized, the aspartate pathway underlies a multilayered regulatory system in which certain metabolites and feedback mechanisms are of outstanding importance. TS is of highest relevance for Thr branch, whereas CGS is of primary importance for the Met pathway. Additionally, the abundance of SAM induces up and down regulations of whole pathway branches.

2.3.3 Aa transport in plants

The described aa metabolism requires a highly efficient transporter system for distribute *de novo* synthesized and exogenously acquired aa within the plant. Aa transporters facilitate the long and short distance transport between different cells, cell compartments and plant organs as well as the uptake of exogenous aa into the roots. Hereafter, the role of aa transporters in aa uptake into the roots, the long and short distance transport and their general involvement in pathogen attacks will be examined. More comprehensive reviews taking in account all aspects related to plant aa transporter were recently published (Liu and Bush, 2006; Tegeder and Rentsch 2010; Tegeder, 2012; Pratelli and Pilot, 2014; Tegeder, 2014).

The *Arabidopsis* genome contains approx. 100 genes coding for aa transporters, belonging to the superfamily amino acid-polyamine-choline (APC) transporters family and the UmamiT family. Herein, the APC and AAAP families with their two members cationic aa transporters (CATs) and aa permeases 1-8 (AAPs) are of outstanding importance (Pratelli and Pilot, 2014 and references herein). Aa transporters mainly differ in their expressional localization, substrate specificity and affinity. This broad diversity ensures that all proteogenic aa can be transported (Tegeder, 2014 and references herein). Nevertheless, Gln

and Asp are preferentially used for long distance transport. These diverse transporters form a multidimensional transportation system that functions as described hereafter.

Aa can be imported into the root by active transport and exit them by passive diffusion, mainly at the apical region (Jones and Darrah, 1994). So far, four aa transporters were demonstrated to participate in the uptake of aa into the roots: AtAAP1 (Lee *et al.*, 2007), AtAAP5 (Svennerstam *et al.*, 2008), AtLHT1 (Hirner *et al.*, 2006; Svennerstam *et al.*, 2008) and AtProT2 (Lehmann *et al.*, 2011). After intake, the organic N compounds are transported apo- and symplastically towards the central cylinder (Rentsch *et al.*, 2007). This plant compartment is enclosed by an apoplastic border, the Caspary strip. Due to the exclusively symplastically passages, apoplastically located aa need to be initially actively imported into the symplast. After the passage, the aa are released by export/efflux into the apoplast of the central cylinder (Tegeder, 2014). The following nutrient translocation within the plant basically involves the transpiration driven long distance xylem root-shoot-leaf transport, the source-sink phloem transport and the radial xylem to phloem transfer.

De novo synthesized and/or exogenously imported aa can remain in the roots for further utilization, be transported to the root tips via phloem or be transported into the leafs by xylem transpiration stream. The bidirectional transporter AtSIAR1 participates in xylem loading in the latter (Ladwig *et al.*, 2012). Beside of aa uptake by the roots, leaf mesophyll cells are the main organ for aa *de novo* synthesis. From the mesophyll cells aa are further distributed towards the sink tissues by concentration gradient driven phloem mass flow. They enter the sieve elements by apo- and symplastically loading (Lalonde *et al.*, 2003; Rentsch *et al.*, 2007; Tegeder, 2014). Symplastically the aa diffuse along the concentration gradient through the plasmodesmata. Apoplastic loading requires the initial uptake into the companion cells. In both cases, the aa must enter the companion cells sieve elements.

Additional to phloem loading in the leafs, aa can be shifted by radial solute exchange from xylem to phloem during long-distance transfer. Herein, aa first exit the xylem into the xylem parenchyma cells. They can either be exported or translocated towards the phloem within the apoplast, or they enter the xylem companion cells followed by symplastical transport into the phloem parenchyma cells before they enter the apoplast. Finally, they are loaded into the sieve element-companion cells (van Bel, 1990; Tegeder, 2014).

Accordingly, exogenously applied aa can be taken up and transported into all plant organs, including pathogen infection and feeding sites.

2.4 Aa in nematode-hostplant interactions

2.4.1 Aa requirements of nematodes

Animals cannot synthesize all aa and those aa that are essential have to be taken up within the nutrition. Unfortunately, very little attention had been paid to identify the specific set of essential aa for nematodes. For the free-living nematode *Caenorhabditis briggsae* Lys, Trp, Met, Thr, Leu, Ile, phenylalanine (Phe), histidine (His) and valine (Val) were identified as essential aa (Vanfleteren, 1973). This corresponds to the set of essential aa determined for *Aphelenchoides* sp., namely Met and His accompanied with a limited dietary requirement for phenylalanine-tyrosine, Thr, Lys and Leu-Iso (Balasubramanian and Myers, 1971).

Only indirect conclusions may be drawn for sedentary plant-parasitic nematodes based on the pathogen induced differentiated expression of aa transporter, related metabolic enzymes and the aa composition in the feeding sites, adjacent tissue or whole roots and plants. This erases from the circumstance, that the nematode induced and controlled syncytia and giant cells are their sole nutrient source. Accordingly, the aa quantities and ratios herein are determinant for the nematode survival and should represent the nutritional aa requirements. Indeed, this composition of free aa in *H. schachtii* feeding sites differs between the individual life stages, as apparent from the work of Krauthausen and Wyss (1982). Almost identical changes in their composition were consistently quantified in both, *Raphanus sativus* and *Brassica napus* between different nematode stages.

2.4.2 The participation of aa transporters in host-nematode interactions

According to their mode of life, sedentary obligate biotrophic pathogens like cyst and gall nematodes must be capable to import aa and nutrients from the apoplast into the feeding site (Yang *et al.*, 2013), possibly by high jacking the plant transporter system. *Vice versa*, host plants aim to retain or redistribute their nutrients (Pratelli and Pilot, 2014). So far, AAP1-8, AtCAT1, AtCAT6 and individual UmamiT were identified as major participants in this host-pathogen nutrient competition.

H. schachtii syncytium gene expression analysis in *A. thaliana* roots demonstrated the involvement of aa transporters in nematode development and root parasitism. AtAAP1-4, AtAAP6 and AtAAP8 transcript levels were elevated in cyst nematode feeding sites and promoter::GUS lines additionally visualized and proofed their expression in the syncytium (not for AtAAP1). Application of T-DNA mutants induced impaired numbers of females for

AtAAP1,2 and 8 (Elashry *et al.*, 2013). The expression of AtAAP3 and AtAAP6 was also localized to gall nematode feeding sites, in particular *M. incognita* galls and giant cells. On aap3 and app6 deficient SALK lines, the infestation rate of the first generation was reduced, accompanied with an increased number of males. Second generation juveniles, originated from females on mutant plants, showed a reduced juvenile emergence, storage lipid amount and infectivity (Marella *et al.*, 2013).

Another approach examined the gene expression profile of *A. thaliana* upon *M. incognita* infection over 4 weeks by ATH1 GeneChip. Herein, 50 transporter genes were observed to be differentially expressed. Follow up analysis demonstrated an increased expression, of AtAAP6 specifically in the galls. Overall, a generally reduced expression of peptide transporters was accompanied by an increase of aa transporters (Hammes *et al.*, 2005). A comparable analysis on *A. thaliana* infected by *H. schachtii*, identified only seven up regulated aa transporters at 3dpi. Moreover, only AtAAP6 and AtPIP2;5 were commonly up regulated in both studies, i.e. by *M. incognita* and *H. schachtii* infections of *A. thaliana* (Puthoff *et al.*, 2003; Hammes *et al.*, 2005). Promoter analysis together with RT-PCRs demonstrated the AtCAT6 expression in the plasma membranes of plant sink tissues and upregulated in *M. incognita* feeding sites. Moreover, knock out lines showed that this transporter is not essential for the feeding sites establishment and maintenance (Hammes *et al.*, 2006).

AtLHT1 acts as modulator of plant defense responses, enhancing the resistance to different pathogens. Herein, the transporter controls the distribution of Gln during basal and systemic defense responses (Liu *et al.*, 2010). During virulent *Pseudomonas syringae* infections of *A. thaliana*, among few others AtCAT1, AtLHT1, AtLHT7 and AAP3 were upregulated. Interestingly, the application of pathogen-associated molecular patterns (PAMPs) in the absence of bacteria also induced the expression of AtCAT1, AtLHT1, AtLHT7, suggesting an involvement in effector triggered plant defense responses (Yang *et al.*, 2013).

In a first hypothetical model, Bartlem (2013) outlined a basic model of a “phloem to giant cell” aa transport succession. Herein, UmamiT transporters (postulated but not unambiguously proven) would unload aa from the phloem into the apoplast and afterwards AAP6 and CAT5 import these into the giant cells (Hammes *et al.*, 2005, 2006; Bartlem *et al.*, 2013).

The application of single aa transporter gene knock out lines appeared to be inefficient, with few exceptions. The broad substrate specificity and partial redundancy of transporters implies, that single transporter knock outs are compensated by others (Fischer *et al.*, 2002; Hammes *et al.*, 2006; Elashry *et al.*, 2013; Yang *et al.*, 2013), an effect that could be overcome by the application of multiple gene knock out mutants.

2.4.3 Influence of quantitative aa levels in host plants on nematode parasitism

It was observed, that the natural quantitative abundance of individual aa in host roots can affect the nematode development. Quantitatively different levels of certain aa in the roots of selected *Brassica napus* ecotypes, were demonstrated to provide favorable conditions for either male or female development. In this regard, high glutamine concentrations were correlated to a pronounced development of females. *Vice versa*, ecotypes with elevated Met, Lys, and Try levels in roots supported the development of male nematodes (Betka *et al.*, 1991). In contrast to this, artificially induced changes of the total aa amounts within the syncytium did not influence the female development. Herein it was postulated, that the quality and not the quantity may be decisive (Grundler *et al.*, 1991).

Previous work revealed increased aa levels in nematode infected roots of different plant species, whereas *H. schachtii* feeding sites showed decreased levels of total aa (Doney *et al.*, 1970; Hanounik and Osborne, 1975; Grundler *et al.* 1991). This may be due to an imbalanced import and *de novo* synthesis towards the aa withdrawal rate by the nematode. The finding that *H. schachtii* infections led to decreased aa concentrations in the phloem of *Brassica oleracea* (Hol *et al.*, 2013) reveals that the global aa balance of plants is disturbed upon nematode attacks.

2.5 Applied nematode control techniques

Beside of classical agricultural cultivation techniques such as crop rotation, flooding or solarization nematode control techniques may be divided into three main groups: chemical, biological and the usage of tolerant and resistant plant varieties. Even though numerous chemical actives, biological agents and tolerant or resistant varieties are available, no unique solution offers 100% nematode control and yield protection. To achieve the best possible protection, all of those strategies have to be used combined in integrated approaches.

2.5.1 Chemical nematode control

Many different chemical substances are available for nematode control. The currently most relevant active ingredients and modes of action (MoA) are: Oxamyl (MoA: Acetylcholinesterase inhibitor), Abamectin (Glutamate-gated chloride channel (GluCl) allosteric modulators), Fluopyram (Complex II inhibitor - of the mitochondrial respiratory chain), Fluensulfone (-), Ethoprop (Acetylcholinesterase inhibitor), Spirotetramat (Acetyl-CoA carboxylase inhibitor) and Thiodicarb (Acetylcholinesterase inhibitor). Additional new substances like Fluazaindolizine (-) are currently under development.

Chemical nematicides may be applied as granules, soil fumigants, soil or foliar sprays, through drip systems, by drenching, seed treatments or even stem ingestions. Most chemical actives act relatively quick at high efficacy levels against a broad spectrum of nematode species. Compared to living biological agents, most chemical nematicides have a more durable shelf life and their functionality is less impacted by differing soil types, microbial competition, and climatic conditions.

Environmental and human safety concerns decrease the global societal acceptance of chemical plant protection products. As a result, legislative measures continuously restrict the use of various substances, a process that will continue. For this reason, it will most likely be necessary in the mid-term future to replace a substantial fraction of the currently predominant chemical nematode control by biological solutions and additional tolerant and resistant varieties.

2.5.2 Plant derived nematode control

Another option to control nematodes is to make use of resistant and tolerant crop varieties. The genetics-based control delivered by the plant itself reduces yield losses on infested sites compared to nematode susceptible varieties. Some high performing varieties may even render the use of chemical nematicides unnecessary, offering an environmentally friendly alternative. Host tolerance or resistance against nematodes relies on native or introgressed resistance genes (R genes), for instance Mi-1.2 in tomato and PI 88788 in soybean.

Mi-1.2 confers resistance against *Meloidogyne incognita*, *M. javanica* and *M. arenaria* (Milligan *et al.*, 1998) and additionally efficacy against phloem feeding insects such as whiteflies and aphids. The mechanism relies on the induction of a necrotic hypersensitive response upon a virulence gene product recognition at the site of nematode invasion

(Williamson and Kumar, 2006). The triggered host plant cell death effectively inhibits giant cell growth resulting in the death of invading sensitive nematode species. Mi-1 is heat sensitive and can lose functionality under heat stress conditions (Marques de Carvalho *et al.*, 2015).

PI88788 is a native R gene of the soybean cultivar Peking and mediates resistance against *Heterodera glycines*. This gene was successfully transferred into high performing commercially soybean cultivars by classical cross breeding. Currently almost all *H. glycines* resistant cultivars rely on this single R gene PI88788. As a result, the selection pressure on *H. glycines* field populations is extremely high. Indeed, a population shift towards less susceptible *H. glycines* races in response to continuous cropping of PI88788 soy varieties is already occurring in the field (McCarville *et al.*, 2017).

Overall, only a limited number of R genes is available, all of them with a narrow nematode species target range. It is quite challenging to discover new functional R genes, optimally with new mode of actions. Once identified, candidate traits must be transferred into commercially suitable varieties by classical breeding or biotech approaches. This process may easily take years, if even being finally successful. Oftentimes genetically mediated host derived resistances are payed for by yield penalties. For all those reasons, the development of nematode resistant varieties focuses primarily on a limited number of plant species, leaving the overwhelming number of crops dependent on chemical and biological solutions. However, modern biotechnology develops extremely quick and generates several powerful techniques such as CRISPR/Cas, targeted usage of siRNA and genetic marker associated breeding. This has the potential to take plant derived nematode control to the next level.

2.5.3 Biological nematode control

The term biological nematode control mainly describes the application of endogenous plant metabolites and the targeted usage of living organisms with antagonistic potential against plant pathogens. This term primarily refers to nematophagous fungi, endophytic fungi and nematode antagonistic bacteria.

Nematophagous fungi separate into two major subgroups, obligate parasites and facultative parasites. In this, primarily the latter are of practical relevance. Facultative nematophagous fungal parasites have a nematode parasitic and a saprophytic phase. The saprophytic phase is a key trait, because it enables the fungus to establish in soil in the absence of nematodes

and additionally permits to grow larger populations for commercial use. Especially those species with rhizosphere competence have the potential to control plant-parasitic nematodes in the root zone. The most prominent facultative fungal parasite of nematodes might be *Purpureocilium lilacinus* strain 251, effectively controlling gall and cyst nematodes. Promising candidates for future solutions are *Pochinia* spp. and *Trichoderma* spp.

Among endophytic fungi primarily the so called arbuscular mycorrhizal fungi (AM) are of practical relevance. AM colonizes plant roots and facilitates mutual beneficial effects such as improved water access, altered rhizosphere interactions, improved systemic resistance and direct competition for nutrients and space with antagonists. In this way AM simultaneously improves the plant's capability to withstand invasion and colonization of a wide range of nematode species and other biotic and abiotic stresses.

Soil bacteria may affect nematodes by excretion of harmful antibiotics, enzymes or toxins such as fatty acids and various nitrogenous substances, or alternatively by colonizing the nematode itself. *Pasteuria* spp. are the most relevant and best studied nematode colonizing bacteria. Different plant growth promoting *Bacillus* spp., for example *B. velenensis* and *B. mojavensis*, reduced population densities of *H. glycines* under controlled and field conditions (Xiang *et al.*, 2017). Earlier studies already reported a suppressive potential of *B. methylotrophicus* and *L. antibioticus* against *M. incognita* under both, greenhouse and field conditions (Zhou *et al.*, 2016).

All living organisms for biological control must fit certain key requirements for potential commercial use: a dormant or resting stage that remains vital during storage with an appropriate shelf life, producibility in large volumes under *in vitro* conditions, rhizosphere competence, competitiveness and viability in different soils and different climatic conditions and most important an effective and reliable nematode control. Since it is extremely challenging to find organisms that match all of those requirements, the development of new biological solutions is very challenging and time consuming.

Plants synthesize various endogenous secondary metabolites with antagonistic potential against nematodes and additional other pests and diseases. In this, mainly nitrogen and sulfur containing compounds, phenolics and terpenes are of key relevance. The most prominent example might be extracts from *Azadirachta indica*, commonly known as neem. Aa are likewise native plant metabolites and for some aa a distinct nematicidal potential had been reported.

2.6 Effects of exogenously applied aa on nematodes

Starting in the 1960s, the intensive examining for nematicidal effects induced by exogenous aa applications is still ongoing. The vast majority of experimental approaches primarily aimed to identify substances that reduce the number of male and female nematodes, or cysts or galls per plant. Effects were observed on various life stages of multiple of nematode species under field, greenhouse and *in vitro* conditions, but the underlying effects remain unrevealed. Especially Met stood out to provide nematicidal potential by exogenous applications. Hereafter relevant effects by exogenous aa applications on nematodes will be introduced for all aa used in this study.

2.6.1 Effects reported for methionine

In 1962 a pioneer study revealed, that 16 mg DL-Met treatments per plant decreased the numbers of *M. incognita* and *Trichodorus christiei* extractable from the soil around tomato roots (Overman and Woltz, 1962). Driven by this, numerous studies on effects of Met followed over the next decades. *Heterodera avenae* females were successfully controlled by 150 mg DL-Met per plant in field experiments with *Triticum aestivum* (Prasad and Webster, 1967). In *in vitro* experiments on tomato, 5mg DL-Met and most effectively 5mg of the metabolically utilizable L-Met reduced the total number of *Heterodera rostochiensis* per plant. Additionally, it was reported that DL-Met-sulphoxide also impaired the number of males (Trudgill, 1974). Exogenous DL-Met, Lys and Trp applications using an *in vitro* system with *Brassica rapa* on agar, strongly lowered the rate of female development, concurrent with an increase in stagnated J2 and J3 nematodes on plants that were described as nematode “supportive” (Betka *et al.*, 1991). The assumption that D-isomers could act as so called “anti-metabolites” was investigated in a specific isoform focused study. Herein, DL-Met, D-Met and L-Met applications on *H. rostochiensis* infected potato plants at 3 and 28dpi, decreased the number of males and females per plant as well as number of hatched juveniles per cyst. Even though no isoform related differences could be detected, earlier treatments were generally more efficient (Evans and Trudgill, 1971).

A particular interest arose to utilize Met for nematode control strategies on golf course turf. In this, the applications of 224-448kg DL-Met per ha lowered the number of the ectoparasitic parasite *Belonolaimus longicaudatus* mixed life stages and the endoparasitic *M. incognita* J2s, revealing a positive dose–effect relationship. Interestingly, L-Thr and Lys did not induce effects on these species in the same experiment (Zhang *et al.*, 2010). In accordance with

these observations, the numbers of *B. longicaudatus* and *Mesocriconema ornata* extractable from soil were reduced by one rate of 1120kg per ha and also after two applications of 112kg per ha (Crow *et al.*, 2009). Despite these findings, Met had never been established as a nematode control agent for green keeping.

More detailed analysis aimed to examine the mechanisms provoking the observed symptoms. It was obvious to suppose a direct impairing effect by cuticle contact of the compound with the nematode cuticle. Direct contact with dissolved Met did not affect the activity of *H. rostochiensis* juveniles within 24h. This observation and also regarding other results, Evans and Trudgill postulated already in 1971 that DL-Met does not act as “a contact poison but a stomach poison”, requiring the preliminary uptake into the plant (Evens and Trudgill, 1971). In contrast to this, incubation and soil experiments on *M. incognita* Chitwood lowered the rate of egg hatching and subsequently the activity of these second-generation juveniles, positively correlated with increasing concentrations (Talavera and Mizukubo, 2005).

2.6.2 Effects reported for other aa

Apart from Met, various other aa also induced effects when applied on nematodes. Summarized, the expression of effects appears to be aa, nematode species and possibly also plant species dependent (Overman and Woltz, 1962; Prasad and Webster, 1967). A comprehensive screening analyzed the influence of Met, Lys, Thr, Trp, Ile and DL-amino butyric acid on the hatching of *H. schachtii* juveniles. In this, only L-Lys and L-Trp had a slightly stimulating effect, all other aa did not (Viglierchio and Yu, 1965).

Remarkable insights were repeatedly obtained from aa spray applications. In 1974, DL-Thr was applied on the above ground organs of tomato infected with *M. incognita*, but no effect on the nematodes could be observed suggesting no or low systematicity. Nevertheless, DL-Ala and DL-Ser significantly impaired the nematodes development and reproduction in the same study (Prasad and Setty, 1974). In a second study, among others tested aa L-Met successfully reduced *M. incognita* egg masses and galls per plant on tomato and sunflower, applied as spray treatments (Osman and Viglierchio, 1981 a,b). Accordingly, some aa can induce systemically effects of unknown modes of actions (MoA) when applied as foliar spray treatments on above ground plant organs.

Finally, three unique approaches generated additional interesting observations. Dipping *Bidens tripartita* roots into 1mM DL-Met for 3h prior to planting, subsequently increases the number of *Longidorus africanus* (Epstein, 1973). DL-Tyrosine shifted the sex ratio in favor of male *H. rostochiensis* on tomato, at 5mg per plant (Trudgill, 1974). On agar *C. elegans* avoids D-Trp at 0.1mM and higher, proving a repellent effect for this aa. Additional tested aa including Met had no effect (Dusenbery, 1975).

2.6.3 Summary on aa induced effects on nematodes

Apparently, aa can induce nematode species dependent effects on the hatching rate, male and female numbers, sex ratio, activity and many other more. This species dependency is explicitly visible in the studies of Overman and Woltz (1962) and Prasad and Webster (1967). Further on, a plant species dependent capability to induce effects may be given, regarding their associated nematode species. Despite these extensive investigations and possible due to magnitude of parameters involved, the mechanistic details for all observed effects remained elusive. To access this given, but so far unavailable potential of exogenous aa applications, it is fundamental to examine the underlying mechanisms.

3 MATERIALS

3.1 Biological materials

biological material	derived from
<i>A. thaliana</i> columbia (col-0)	Institute stock
<i>A. thaliana</i> mto1-1	The Nottingham Arabidopsis Stock Centre, Nottingham, UK
<i>A. thaliana</i> SALK_081563c	The Nottingham Arabidopsis Stock Centre, Nottingham, UK
<i>Caenorhabditis elegans</i> N2	Prof. Einhard Schierenberg, University Cologne
<i>Escherichia coli</i> OP50	Prof. Einhard Schierenberg, University Cologne
<i>Heterodera schachtii</i>	institute stock

3.2 Chemicals

chemical	company purchased from
2-Ketobutyric	Sigma-Aldrich Chemie GmbH, Hamburg, Germany
absolute Ethanol	Merck Chemicals GmbH, Darmstadt, Germany
absolute Ethanol	Sigma-Aldrich Chemie GmbH, Hamburg, Germany
Agar(SIGMA, St. Louis, USA)	Sigma-Aldrich Chemie GmbH, Hamburg, Germany
Bacto™-Tryptone	BD, Sparks Glencoe, USA
C ₂ H ₅ O ₂ NH ₄	Institute stock(MPM)
Ca(NO ₃) ₂ * 4 H ₂ O	Institute stock(MPM)
CaCl ₂	Institute stock(MPM)
Chloroform	Institute stock(MPM)
Cholesterol	Institute stock(MPM)
CoCl ₂ * 6 H ₂ O	Institute stock(MPM)
CuSO ₄ * 5H ₂ O	Institute stock(MPM)
Daichin agar	Institute stock(MPM)
DL-Met	Evonik Industries AG, Hanau, Germany
D-Lys	Sigma-Aldrich Chemie GmbH, Hamburg, Germany
DNase / RNase-free H ₂ O	Gibco®, Life Technologies Europe BV, Bleiswijk, Netherlands
DNase / RNase-free H ₂ O	Institute stock(MPM)
D-Thr	Sigma-Aldrich Chemie GmbH, Hamburg, Germany
D-Trp	Sigma-Aldrich Chemie GmbH, Hamburg, Germany
EDTA	Merck Chemicals GmbH, Darmstadt, Germany
EtOH	Institute stock(MPM)
FeNaEDTA	Institute stock(MPM)
FeSO ₄ * 7H ₂ O	Institute stock(MPM)
GAMBORG'S Vitamin SOLUTION 1000x	Sigma-Aldrich Chemie GmbH, Hamburg, Germany
Glycerol	Carl Roth GmbH & Co. KG, Karlsruhe, Germany

H ₂ MoO ₄	Institute stock (MPM)
H ₃ BO ₃	Institute stock (MPM)
HCl	Institute stock (MPM)
Hexadecyltrimethyl-ammoniumbromide (CTAB)	Institute stock (MPM)
HgCl ₂	Institute stock (MPM)
H-Met-Met-OH(MM)	Evonik Industries AG, Hanau, Germany
isoamylalcohol mixture	Institute stock (MPM)
K ₂ HPO ₄	Institute stock (MPM)
KH ₂ PO ₄	Institute stock (MPM)
KNO ₃	Institute stock (MPM)
KOH	Institute stock (MPM)
KPO ₄	Institute stock (MPM)
L-ethionine	Sigma-Aldrich Chemie GmbH, Hamburg, Germany
L-Hom	Sigma-Aldrich Chemie GmbH, Hamburg, Germany
L-Ile	Sigma-Aldrich Chemie GmbH, Hamburg, Germany
L-Lys	Sigma-Aldrich Chemie GmbH, Hamburg, Germany
LN ₂	Institute stock (MPM)
L-Thr	Sigma-Aldrich Chemie GmbH, Hamburg, Germany
L-Trp	Sigma-Aldrich Chemie GmbH, Hamburg, Germany
MgSO ₄	Institute stock (MPM)
MgSO ₄ * 7 H ₂ O	Institute stock (MPM)
MnCl ₂	Institute stock (MPM)
MnCl ₂ * 4H ₂ O	Institute stock (MPM)
Na ₂ EDTA	Institute stock (MPM)
Na ₂ HPO ₄ * 7H ₂ O	Institute stock (MPM)
NaCl	Institute stock (MPM)
NaOCl	Institute stock (MPM)
NaOH	Institute stock (MPM)
Peptone	Institute stock (MPM)

peqGold Universal Agarose	Peqlab Biotechnologie GmbH, Erlangen, Germany
peqGREEN	Peqlab Biotechnologie GmbH, Erlangen, Germany
Polyvinylpyrrolidone (PVP)	Institute stock (MPM)
Potassiumcitrate	Institute stock (MPM)
Rotiphorese® 50x TAEbuffer	Carl Roth GmbH & Co. KG, Karlsruhe, Germany
Sucrose	Netto Marken-Discount AG & Co, Maxhütte-Haidorf, Germany
Tris base	Institute stock (MPM)
YEAST EXTRACT	Institute stock (MPM)
ZnCl ₂	Institute stock (MPM)
ZnSO ₄ * 7 H ₂ O	Institute stock (MPM)

3.3 Plastic and glassware

item	company purchased from
96-well plate	Thermo SCIENTIFIC, Waltham, USA
1 L Erlenmeyer flask	DURAN Group GmbH, Wertheim/main, Germany
1 L pressure glass ⁺ glass bottle	DURAN Group GmbH, Wertheim/main, Germany
0.2 µM Acrodisc® Syringe Filters	Pall Corporation, Port Washington, USA
2 ml syringe	B. BRAUN, Melsungen, Germany
2 ml tube	Sarstedt AG & Co., Nümbrecht, Germany
0.5 ml tube	Sarstedt AG & Co., Nümbrecht, Germany
5 ml syringe	B. BRAUN, Melsungen, Germany
1.5 ml tube	Sarstedt AG & Co., Nümbrecht, Germany
3.5 cm in diameter Petri dish	Greiner Bio-One GmbH, Kremsmünster, Austria
9 cm glass Petri dish	DURAN Group GmbH, Wertheim/main, Germany
9.2 cm in diameter Petri dishes	Sarstedt AG & Co., Nümbrecht, Germany
20 ml syringe	B. BRAUN, Melsungen, Germany
24 well CELLSTAR® Cell Culture Multiwell Plates	Greiner Bio-One GmbH, Kremsmünster, Austria
25 ml serological pipette	Sarstedt AG & Co., Nümbrecht, Germany
50 ml screw cap tubes	Orange Scientific, Braine-l'Alleud, Belgium
11 & 100 µm mesh size PVC membrane sieve	Standard lab equipment
17 x 100 mm culture tubes with closures	VWR International, Radnor, USA
250 ml Erlenmeyer flask	DURAN Group GmbH, Wertheim/main, Germany
250 ml glass beaker	KAVALIERGLASS Co. Ltd, Sazava, Czech Republic
355 µm mesh size sieve	Retsch, Haan, Germany
10, 200 & 1000 µl pipet tips	Sarstedt AG & Co., Nümbrecht, Germany
aluminum foil	Netto Marken-Discount AG & Co, Maxhütte-Haidorf, Germany
common ruler	Möbius+Ruppert KG, Erlangen, Germany
filter paper circles 110 mm (cut in pieces)	Schleicher & Schuell GmbH, Dassel, Germany

forceps 5-Inox-H	DUMONT, Montignez, Swiss
glass funnel	DURAN Group GmbH, Wertheim/main, Germany
inoculation loop	Greiner Bio-One GmbH, Kremsmünster, Austria
Kimble™ Kontes™ Pellet Pestle™	Thermo SCIENTIFIC, Waltham, USA
metal beets	Standard lab equipment
metal clip (for funnel)	neoLab Migge Laborbedarf-Vertriebs GmbH; Heidelberg, Germany
optical adhesive film MicroAmp™	Applied Biosystems, Thermo SCIENTIFIC, Waltham, USA
PARAFILM® M sealing film	BRAND GMBH + CO KG, Wertheim, Germany
PCR 8-strip Multiply® lids	Sarstedt AG & Co., Nümbrecht, Germany
PCR 8-strip Multiply® tubes	Sarstedt AG & Co., Nümbrecht, Germany
transparent silicone tube Versilic®	Carl Roth GmbH & Co. KG, Karlsruhe, Germany

3.4 Instruments / machines

item	company purchased from
+20°C climate cabinet	Liebherr-International, Bulle, Swiss
+4°C fridge KS38R430IE	Siemens, Munich, Germany
0.5–10, 2–20, 20–200 & 100–1000 µl Research plus pipets	Eppendorf AG, Hamburg, Germany
-20°C fridge ARTIS CHAMPIONS LINE	AEG, Frankfurt a. M., Germany
accu-jet® pipette	BRAND GMBH + CO KG, Wertheim, Germany
balance NewClassic MF JP1603C	Mettler Toledo, Columbus, USA
Bioanalyzer 2100	Aglient Technologies, Santa Clara, USA
centrifuge 5424	Eppendorf AG, Hamburg, Germany
centrifuge 5810 R	Eppendorf AG, Hamburg, Germany
ddH ₂ O water filter PURELAB FLEX	ELGA LabWater, Celle, Germany
Gel Doc™ XR+ Molecular Imager®	Bio-Rad Laboratories GmbH, München, Germany
glass bead sterilizer	Hager & Werken GmbH & Co., Duisburg, Germany
hotplate stirrer CB 162	Bibby Scientific Limited, Stone, UK
incubator ICH 256	Memmert GmbH + Co.KG, Schwabach, Germany
LABOKLAV 55-195	SHP Sterieltechnik AG, Magdeburg, Germany
Leica Application suite v.4.3.0	Leica Camera AG, Wetzlar, Germany
Leica M165 C stereo microscope, 12:1 zoom	Leica Camera AG, Solms, Germany
Leica S8APO binocular	Leica Camera AG, Wetzlar, Germany
Microwave	Siemens, Munich, Germany
NanoDrop 2000c™	Thermo SCIENTIFIC, Waltham, USA
nutator POLYMAX 1040	Heidolph Instruments, Schwabach, Germany
PCR-strip centrifuge Mini Star	VWR International GmbH, Darmstadt, Germany
pH-meter	WTW Inolab, Ingolstadt, Germany
PowerPac Basic™ power supply	Bio-Rad Laboratories GmbH, München, Germany
qPCR vortexer MS 3	IKA®, Staufen, Germany

sample grinder Mixer Mill MM 400	Rentsch, Haan, Germany
Sanyo MDF-U74V(-80°C)	SANYO, Moriguchi, Japan
shaker KS-15	Edmund Bühler GmbH, Hechingen, Germany
StepOnePlus™ Real-Time PCR System Thermal Cycling Block	Life Technologies Europe BV, Bleiswijk, Netherlands
sterile bench Mars Safety Class 2	LaboGene ApS, Lyngé, Denmark
Sub-Cell® GT Agarose Gel Electrophoresis Systems	Bio-Rad Laboratories GmbH, München, Germany
thermal cycler C1000™	Bio-Rad Laboratories GmbH, München, Germany
thermal cycler S1000™	Bio-Rad Laboratories GmbH, München, Germany
Thermomix comfort	Eppendorf AG, Hamburg, Germany
Vortex-Genie 2 G560 E	Scientific Industries Inc, Bohemia, USA
water bath WNB 22	Memmert GmbH + Co.KG, Schwabach, Germany

3.5 Purchased kits

kit	company purchased from
1 kb DNA ladders	Promega GmbH, Mannheim, Germany
100 bp DNA ladders	Promega GmbH, Mannheim, Germany
Agilent RNA 6000 Nano Reagents Part I	Agilent Technologies, Waldbronn, Germany
dNTPs Mix 10 mM	Promega GmbH, Mannheim, Germany
Fast SYBR® Green Master Mix	Applied Biosystems, Thermo SCIENTIFIC, Waltham, USA
GoTaq® G2 DNA polymerase	Promega GmbH, Mannheim, Germany
High-Capacity cDNA Reverse Transcription Kit	Invitrogen, Thermo Fisher Scientific, Waltham, Massachusetts, USA
NucleoSpin® RNA kit	MACHEREY-NAGEL GmbH & Co. KG, Düren, Germany
PCR primer	Invitrogen, Thermo Fisher Scientific, Waltham, Massachusetts, USA
RNeasy® Plant Mini Kit	QIAGEN, Hilden, Germany
RQ1 RNase-free DNase	Promega GmbH, Mannheim, Germany

3.6 Software

software	company purchased from
Agilent Technologies 2100 Bioanalyzer 2100 Expert v.B.02.08.SI6-48 (SR2)	Agilent Technologies, Santa Clara, USA
CFX Manager™ v.2.1	Bio-Rad Laboratories GmbH, München, Germany
Image Lab™ v.3.0.1 (Beta 2)	Bio-Rad Laboratories GmbH, München, Germany
Microsoft Excel	Microsoft Corporation, Redmond, USA
Nematode-Arabidopsis Transcriptomic Interaction Compendium(NEMATIC spreadsheet)	Cabrera <i>et al.</i> , 2014
Primer3 web v.4.0.0	Untergrasser <i>et al.</i> , 2012
SigmaPlot v.12.5	Systat Software Inc, San Jose, USA
StepOne™ v.2.2.2	Life Technologies Europe BV, Bleiswijk, Netherlands

4 METHODS

The following general statements apply for all experimental procedures described hereafter. All aseptic procedures were conducted under a sterile bench Mars Safety Class 2. All materials were purchased sterile or sterilized by autoclaving using a LABOKLAV 55-195. In case other sterilization techniques were used, the method is mentioned and described in the respective chapter. All protocols for nutritional mediums, solutions, buffers, and standard reagents are listed in the appendix. Statistical differences were analyzed by running one-tailed t-Test ($P \leq 0.05$) using SigmaPlot v.12.5 on the absolute mean values of $n \geq 3$ biological repetitions. In this, the exact numbers of biological and technical repetitions are stated individually for each experiment. The results are indicated in figures with average values \pm standard error calculated on the means.

4.1 Preparation of test compound solutions

The test compounds L-Ile, L-Hom, Ket, L-Lys, D-Lys, L-Trp, D-Trp, L-Thr and D-Thr were purchased from Sigma-Aldrich. H-Met-Met-OH (MM) and DL-Met lab grade were provided by Evonik. Substance volumes were weighed using a NewClassic MF JP1603C balance and dissolved in ddH₂O at room temperature under constant shaking at 300rpm using a Thermomix comfort. ddH₂O was purified by a PURELAB FLEX water filter system. To promote dissolving, MM, L-Trp, and D-Trp were additionally heated to 88°C, DL-Met to 45°C by Thermomix comfort. All solutions were filter sterilized with 0.2µM Acrodisc® Syringe filters before usage in experiments. All stock solutions were prepared fresh prior to each experiment and used within 24 h.

4.2 Experiments with *C. elegans*

The *C. elegans* strain N2 stock culture was maintained on nematode growth medium (NGM) carrying an *E. coli* OP50 bacterial lawn as bacterial food source. Culture maintenances and experimental procedures were conducted as described in “Maintenance of *C. elegans*” (Stiernagle, 2006) with only minor adaptations. Aseptic conditions were maintained at all time.

4.2.1 Culture establishment and maintenance of *C. elegans*

4.2.1.1 Establishment and maintenance of *E. coli* OP50

E. coli OP50 were used as food source for the bacteriophage nematode *C. elegans*. Bacteria stocks were initially grown in liquid medium and finally on NGM plates together with the *C. elegans* stock culture population. As a first step to prepare fresh *E. coli* cultures, 10µl *E. coli* OP50 -80°C glycerol stock was transferred into a 17 x 100mm culture tube with closures, filled with 5ml lysogeny broth (LB) liquid medium, cf. 8.1.2. *E. coli* was allowed to multiply at 37°C over night, using an ICH 256 incubator. After this growth period, 50µl of the *E. coli* containing liquid LB medium were streaked out on a LB-medium plate, cf. 8.1.2, by using an inoculation loop. All prepared plates were sealed with PARAFILM® and stored at 37°C over night. Afterwards, a single colony was selected and transferred with a 200µl pipette tip into 50ml LB liquid medium in a 250ml Erlenmeyer flask covered with aluminium foil and again incubated overnight at 37°C. Finally, the obtained *E. coli* liquid culture grown from a single colony was aliquoted into 2ml tubes and stored at +4°C in a KS38R430IE fridge until further usage.

Concentrated *E. coli* pellets are required to prepare the liquid medium “S-Basal complete”, cf. 8.1.5. To grow the needed larger volumes of bacteria, 250ml LB liquid medium were inoculated with 1ml *E. coli* liquid LB stock culture in a 1l Erlenmeyer flask covered with aluminum foil. The culture was allowed to grow at 37°C overnight, before aliquoting it into 50ml screw cap tubes. Afterwards, the bacteria were pelleted at the bottom of the tubes by centrifugation at 4000rpm for 5min. The supernatant was discarded and the concentrated *E. coli* pellets were stored at -80°C in a Sanyo MDF-U74V ultra deep freezer.

4.2.1.2 Preparation of NGM plates

The *C. elegans* stock culture was maintained on NGM agar plates carrying an *E. coli* OP50 bacterial lawn. To prepare NGM plates, the autoclaved liquid medium, prepared as described in chapter 8.1.1, was dispensed into 9.2cm Petri dishes. After cooling and solidification, 50µl *E. coli* stock culture solution was applied to each plate and distributed equally over the whole surface area with an inoculation loop. All plates were sealed with PARAFILM®. The bacterial lawn was allowed to grow for at least 24h at room temperature before usage. All prepared NGM culture plates were stored in sealed containers at room temperature.

4.2.1.3 Establishment and maintenance of *C. elegans*

In order to maintain the bacterial food source and to avoid contaminations, the nematode stock population was transferred onto fresh plates every three days. For this purpose, a 1x1cm piece of nematode carrying agar was cut loose with a fire sterilized scalpel and transferred onto a fresh NGM + *E. coli* plate. The same procedure was used to multiply the *C. elegans* population for experiments. To obtain large populations, eight NGM *E. coli* plates were infected at once from a single stock culture plate. The *C. elegans* stock cultures on the NGM *E. coli* plates were kept constant in a +20°C climate cabinet.

4.2.1.4 Synchronization

C. elegans stock culture plates always carry mix stages including adults, juveniles and eggs. A homogenous L2 population was required for the experiments. For that reason, a synchronization process was implemented as follows: Initially, eight NGM plates were inoculated with *C. elegans* and stored at +20°C for population multiplication. After approx. 3-4 days a large proportion of hermaphrodites containing clearly visible eggs could be identified using a Leica S8APO binocular. At this population stage, the plates were harvested. The plates were flooded with ddH₂O, carefully swiveled, and positioned slightly slanted. All nematodes, now freely swimming in ddH₂O, were transferred within the supernatant by pipetting it into a 50ml screw cap tube, using an accu-jet® pipette equipped with a 25ml serological pipette. Afterwards, the tube was placed vertically on ice for the nematodes to settle at the bottom by precipitation. The supernatant was discarded using the accu-jet®, keeping the concentrated *C. elegans* pellet. Next, 5ml bleach solution, cf. 8.1.4, was added per tube and put horizontally and slowly turned and slanted for ≤ 10min of incubation. Additionally, the mixture was vortexed every 150sec. using a Vortex-Genie 2 G560 E on full speed. The applied bleach solution degrades the nematode cuticle and finally releasing the containing eggs from the hermaphrodite body into the solution. After max. 10min the bleach treatment was immediately stopped by filling up the tube to a total remaining volume of 45ml with M9, cf. 8.1.3. The tube was immediately vortexed for 5sec and centrifuged for 3min at 1400rpm with minimal deceleration speed using a centrifuge 5810R. The supernatant was discarded by using an accu-jet® automatic pipet before fresh M9 buffer was added to a total volume of 45ml. This procedure was repeated four times until ultimately 15ml M9 were added. At this point, the eggs are located freely in the buffer. The L1 were allowed to hatch from those eggs overnight in the absence of food on a POLYMAX

1040 nutator, running on 2 mots/1min at +20 °C. The obtained synchronized L1 population was eventually ready for experimental use.

4.2.2 Tests for effects on the activity of *C. elegans*

To test for direct effects on the activity of *C. elegans*, the nematodes were exposed to aa in S-Basal complete liquid medium, cf. 8.1.5. The applied aa concentrations are listed in table 1. This experiment was set up in 24 well CELLSTAR® Cell Culture Multiwell plates. Each well contained 400µl S-Basal complete and 50 freshly hatched L1 *C. elegans* in 50µl M9 buffer, prepared and synchronized as described in chapter 4.2.1. Additionally, 50µl test compound solution or ddH₂O as control were added to each well. The plates were sealed with PARAFILM® and stored at +20°C in a climate cabinet with constant shaking at 30mot /1min using a KS-15 shaker. This experiment was set up as n=4 biological repetitions (three for L-Trp), each with n=4 wells per treatment. To assess effects on the activity, the numbers of active and inactive nematodes per well were counted under a Leica S8APO binocular every 24h for three days. Before counting, the nematode activity was stimulated by shock moving the plate, inducing an intense kinetic impulse on the nematodes resulting in hyperactive motions.

Table 1 aa concentrations applied in *C. elegans* activity test experiments

compound	concentration (mM)
DL-Met	20
MM	1
L-Lys	10
D-Lys	10
L-Thr	10
D-Thr	10
L-Trp	10
D-Trp	10

4.2.3 Effects on the development of *C. elegans*

This experiment aimed to identify effects induced by exogenously applied aa on the development of *C. elegans*. It was set up as described in chapter 4.2.2, applying the aa at concentrations indicated in table 2. Additionally, OP50 bacteria were added as bacterial food source to stimulate swallowing of solution and by this uptake of aa into the nematode. In order to identify developmental effects, the needed timespan between incubation of the L1 nematodes in aa solutions until the following events was measured:

- 1) Egg laying = first eggs were visible in solution, laid by hermaphrodites that meanwhile developed from the 1st L1 generation.
- 2) Hatch of the 2nd L1 generation = first free swimming 2nd generation L1 were visible after egg laying took place. Accordingly, the lifecycle of the 1st generation was completed.

The development was monitored for those events in a 24h interval using a Leica S8APO binocular. The experiment continued until the lifecycle was completed. In case the 1st generation was unable to complete the lifecycle, thus the development was inhibited, the experiment was canceled after a maximum of 6 days. This event was finally marked in the table by: ∞ . Timespans are given in days from the day of inoculation, defined as day 0. For example, 3-4 days until egg laying describes that eggs were not visible at day 3 but present at day four. The experiment was repeated two times. Three biological repetitions were accomplished, each with n=4 wells per treatment.

Table 2 Aa concentrations applied in *C. elegans* development experiments

compound	concentrations (mM)
DL-Met	20
MM	1
L-Lys	10; 1; 0.1
D-Lys	10; 1; 0.1
L-Thr	10
D-Thr	10
L-Trp	10; 1; 0.1
D-Trp	10

4.3 Experiments with *Heterodera schachtii*

4.3.1 Maintenance and preparation

In order to obtain the needed nematode material for experiments a *H. schachtii* stock culture was established and maintained. Separate nematode batches were extracted from this stock culture to be further processed for experiments. This involved the collection of egg containing cysts, the hatch of J2 nematodes from those cysts in a “funnel system” followed by surface sterilization of nematodes, and specific preparation as needed for the very experiment type as described in detail hereafter. Aseptic conditions were ensured at all times if not stated differently.

4.3.1.1 *H. schachtii* stock culture

The *H. schachtii* stock culture was maintained on mustard grown on Knops'-medium in 9.2cm in diameter / Petri dishes under aseptic conditions, cf. 8.1.6 for the Knops'-medium protocol. All stock culture plates were sealed with PARAFILM® and stored in the dark at constant 25°C. In order to prepare *H. schachtii* populations for experiments, mature cysts of brownish color were picked from the stock culture plates with forceps and transferred into the so called ‘funnel system’ to hatch J2 nematodes for experimental use, as illustrated in figure 14. The basic setup of a funnel is a 250ml glass beaker containing a glass funnel. Inside of this glass funnel, a 100µm mesh size PVC membrane sieve melted to a cut part of a 20ml syringe is placed. Its orifice leads into a 3-4cm transparent Versilic® silicone tube, closed by a metal clip. The constructed vessel consisting of the glass funnel, sieve element, clip, and tube was filled with 3mM ZnCl₂ covered with aluminum foil. Prior to further usage, the construction was heat sterilized as a whole by autoclaving, before it was sealed with PARAFILM® for storage.

The sterile funnel was equipped with *H. schachtii* cysts, transferred into the ZnCl₂ filled sieve element. All cysts were handpicked with 5-Inox-H forceps that where heat sterilized in a glass bead sterilizer. The 100µm mesh size PVC sieve functions as a barrier for cysts but can easily be traversed by the smaller J2s, which emerge from the cysts. After passing the membrane, the nematodes sink to the lowest point and accumulate in the silicone tube above the metal clip. The accumulated juveniles were extracted after a maximum of 7 days.

The cyst filled funnels were stored at 25°C in the absence of light. All described procedures were processed under aseptic conditions.

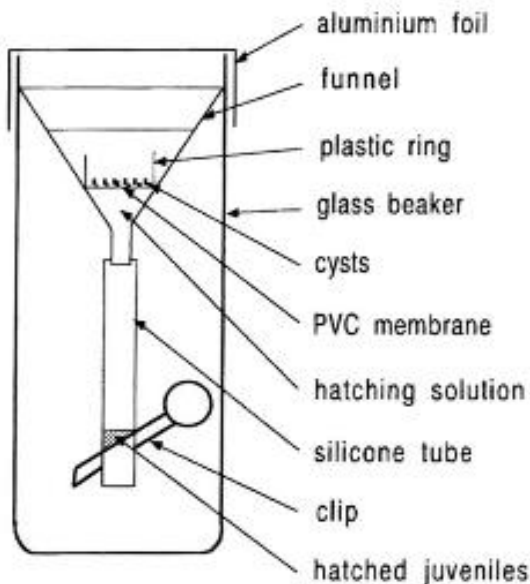


Figure 14 Schematic diagram of a funnel
Construction sketch of a funnel used to hatch and collect J2 *H. schachtii* from cysts

3.3.1.2 Sterilization of *H. schachtii* J2s

Post extraction and prior to experimental usage, the collected *H. schachtii* J2s were surface sterilized in HgCl_2 . By briefly opening of the metal clip, the J2s were flushed out of the tube onto a 10 μm mesh size sieve melted to a 1.5cm long syringe piece. The 10 μm mesh size membrane retains nematodes but is permeable for solutions. For sterilization, the nematode containing sieve element was placed into a 3.5cm in diameter Petri dish filled with 4ml 0.02% HgCl_2 for 2min. In the same way, they were washed another 4 times in 4ml sterile dd H_2O , provided in separate Petri dishes. Hereafter, 1.5ml dd H_2O was added into the sieve element. After it was slanted the nematodes were stirred up before they were finally transferred into a 2ml tube by pipetting.

3.3.1.3 Evaluation of nematode number per volume

Before equipping the individual experiments with prepared *H. schachtii* J2s, the exact number of individuals/volume had to be determined. For this purpose, the solution was mixed by inverting the tube multiple times before placing it vertically oriented for the

nematodes to descend and form a pellet. The supernatant was taken off and the pellet was resuspended in 1ml ddH₂O. Finally, the number of active (moving) nematodes was counted in six aliquots of 5µl and the average was calculated.

4.3.2 Maintenance and preparation of *A. thaliana*

4.3.2.1 Surface sterilization of *A. thaliana* seeds

Prior to experimental applications all *A. thaliana* seeds were surface sterilized under aseptic conditions. In this, a batch of seeds was transferred into a 1.5ml tube before 1.1ml of 70% EtOH was added and the tube placed on a Thermomix comfort at 1400mots/min for 60sec. Next, the seeds were immediately spun down by centrifugation and the supernatant was discarded. 1.1ml of 0.5% NaOCl was added and the probe was incubated for 10min on a Thermomix comfort at 1400mots/min. Subsequently, the probe was briefly centrifuged and the supernatant discarded. Afterwards, it was washed a second time with 70% EtOH as described above. To clean the seeds, 1.1ml ddH₂O was added and the tube was vortexed for 5sec before it was briefly centrifuged and the supernatant was discarded. This procedure was repeated five times. Finally, the seed containing ddH₂O solution was sprinkled onto filter paper placed in a 9cm glass Petri dish. The filter paper and seeds were allowed to dry for 60min with opened lids before the plate was sealed with PARAFILM® and stored at +4°C in a KS38R430IE fridge.

4.3.2.2 Multiplication of *A. thaliana* seed material

For multiplication, sterilized *A. thaliana* wildtype and mutant seeds were initially germinated on Knops'-medium under sterile conditions. For this purpose, nine seeds were positioned per plate and grown for ten days under controlled conditions, as described in chapter 4.3.2.3. In parallel, a 1:2 soil /sand mixture was prepared in a 1l pressure glass bottle and sterilized by autoclaving in a LABOKLAV 55-195. Subsequently, the pots were prepared with 180ml sterilized substrate each and pre-moistened by sterile ddH₂O spray application. The 10-day old seedlings were carefully lifted from the agar with 5-Inox-H forceps and transferred onto the prepared substrate which was sprayed a second time with ddH₂O. Afterwards, all pots were transferred into a growth chamber with constant 24°C with a 16h light/8h darkness day length. To avoid cross contamination, all pots were kept covered with a top closed translucent plastic tube at all time. Once the siliques were completely dry, the plants were harvested and the seeds were extracted.

To extract the seeds, a plant was placed inside a folded DinA4 paper sheet and crushed by carefully rolling this “envelope”. Loose seeds were separated from the dry remains by sieving, using a 355µm mesh size sieve. Finally, all obtained seeds were stored in 1.5ml tubes at +4°C in a KS38R430IE fridge for surface sterilization and follow-up use in experiments.

4.3.2.3 Preparation of *A. thaliana* on Knops'-medium plates

A. thaliana was cultured as previously described by Sijmons *et al.* (1991) with the hereafter described adaptations. For *in vitro* studies, two plants per plate were grown on Knops'-media in 9.2cm Petri dishes. Both seeds were located in the upper third of the plates, leaving equal space between the plate border and each other. Seeds were transferred by using a dissection needle, sterilized in a glass bead sterilizer. All plates were sealed with PARAFILM® and grown under controlled light and temperature conditions at 25°C with a 15h light/11h darkness day length. The plates were kept vertically for four days before they were shifted into an upright position with an angle of approximately 60°. This positioning promotes a gravity driven straight vertical root growth flush against the Petri dish bottom plate.

4.3.3 Infection assay analyses

The infection assays analyses were performed as previously described (Siddique *et al.*, 2014). All plants were grown on Knops'-medium and inoculated at ten days past seeding (dps) with 60 surface sterilized and active *H. schachtii* J2s, applied as two drops of 30 individuals. To ensure a homogenous distribution of nematodes in solution, the tube was closed and inverted after the inoculation of every four plates. All inoculated plates were sealed with PARAFILM® and stored slanted as described in chapter 4.3.2.3.

The number of male and female nematodes per root were counted at 12 days past infection (dpi) using a Leica S8APO binocular. For this purpose, the whole root was systematically searched for attached nematodes and their position was marked on the Petri dish. Male and female nematodes were visually differentiated based on their characteristic body shape, size, color, and eventually visible vermiform shape, as shown in figure 15.

Female and syncytium sizes were measured at 14dpi (additionally 28 dpi for the experiment in chapter 4.3.6). For this purpose, pictures of syncytia and females were taken by using a 12:1 zoom Leica M165 C stereo microscope. Afterwards, software-based size measurements

were conducted on the taken pictures using the Leica Application suite v.4.3.0. The syncytium and female outlines were manually marked, as indicated in figure 15, and the hereby enclosed area software based calculated, equating to the female and syncytium sizes. The values given in the results are means, calculated on the averages of at least three biological repetitions. The individual number of conducted measurements per biological repetition is indicated separately for each experiment.



Figure 15 Female and male *H. schachtii* body shape
Characteristic body shape of *H. schachtii* females (left) and males (right). The female outline was manually marked, as indicated by the red line, for software-based size calculation. The resulting female size is defined as the total area inside this line.

4.3.4 Activity test in solution

The experiment aimed to identify effects induced by test compounds on the activity of *H. schachtii* J2s. It was set up in 24 well CELLSTAR® Cell Culture Multiwell plates, each well containing 900µl ddH₂O, 40 sterile *H. schachtii* J2s, and 100µl test compound stock solution or ddH₂O as control. The final test compound concentrations of the incubation solutions are reported in table 3. After preparation, all plates were sealed with PARAFILM® and kept in the dark at 24°C. The number of active (moving) and inactive (not moving) juveniles was counted at seven days after incubation, using a Leica S8APO binocular. Prior to counting, the nematode activity was stimulated by shock moving the 24-well plate multiple times, inducing an intense kinetic impulse resulting in hyperactive movement of the juveniles. A nematode was considered as ‘inactive’ when no movement was observed during the period of counting the respective well. The experiment was set up as four biological replications (three for L-Ile, L-Hom and Ket) with n=4 wells per treatment each.

Table 3 Final test compound concentration in the wells of the *H. schachtii* activity and 24h incubation analysis experiments

compound	concentration (mM)
DL-Met	20
MM	1
L-Lys	10
D-Lys	10
L-Thr	10
D-Thr	10
L-Trp	10
D-Trp	10
L-Hom	10
L-Ile	10
Ket	0.1

4.3.5 24h incubation of nematodes prior to inoculation

The applied test compound concentrations and the experimental setup in 24 well CELLSTAR® Cell Culture Multiwell plates were done as described in chapter 4.3.4. with the following adaptations. To allow to surface clean the nematode batches after 24h of incubation by multiple washing steps, all nematodes were located in 'incubation tubes' with solution permeable bottoms fitted into the incubation wells. An incubation tube was constructed of a 1.5cm long piece cut of a 2ml syringe with a 11µm mesh size PVC membrane melted to the bottom. One incubation tube was used per treatment, whereas all tubes contained an equal number of nematodes. Initially, the nematode containing tube was placed into the 1st test compound solution filled well. After 1min it was lifted out of this 1st well and the solution was allowed to leak out, before it was placed into a 2nd well, filled with fresh test compound incubation solution. In the same manner, the tube was subsequently transferred into a 3rd well, in which the nematodes remained exposed to the treatment solutions for 24h of incubation. During incubation, the PARAFILM® sealed plates were stored at 25°C in the absence of light. Hereafter, the nematodes were washed four times with

ddH₂O before they were transferred into 2ml tubes. Finally, the infection assay was conducted as described in chapter 4.3.3.

4.3.5.1 Analysis of incubation treatment effects in the absence of ZnCl₂ and HgCl₂

To analyze the putative occurrence of a ZnCl₂ or HgCl₂ complex formation with Lys, the experiment was repeated for this aa using a slightly modified protocol where all nematodes were hatched in ddH₂O filled funnels, and the HgCl₂ sterilization step was skipped. All other steps remained unchanged. The number of male and female nematodes per plant at 12dpi was analyzed as described in chapter 4.3.3. The experiment was conducted in three biological replications with n≥8 plants each.

4.3.6 Knops'-medium supplemented with test compounds

For this experiment, the Knops'-medium was supplemented with the set of test compounds. The Knops'-medium was prepared as described under 8.1.6. In this experiment, the test compound stock solutions were supplemented to the liquid agar medium together with Vitamin B in volumes of 1 -10ml/l medium under aseptic conditions, once the medium was brought down to 55°C after autoclaving. After adding of Vitamin B, the medium was immediately homogenized by stirring for 3min on a CB 162 for hot plate stirrer. The pH level of the medium was measured in aliquots by pH-meter and adjusted to pH 6.4 by adding KOH or HCl. Finally, the enriched medium was poured into 9.2cm in diameter Petri dishes and left in the lamina flow to solify overnight. Hereafter, the prepared plates were directly used for the following experiments. Knops'-medium with supplemented test compounds was always prepared fresh for every experiment in order to avoid degradation of active substances during storage. The final test compounds concentrations in the medium are reported in table 4. *A. thaliana* was seeded and cultured as described in chapter 4.3.2.3. The standard infection assay was conducted as described in chapter 4.3.3. In addition to the included parameters, the invasion rate, main root lengths, female size at 28dpi, and eggs per cyst at 35dpi were analyzed as described hereafter. All plates were sealed with PARAFILM® and stored at 25°C with a 15h light/11h darkness day length until 35dpi. The experiment was conducted in n≥3 biological replications, each with n≥10 plants.

Table 4 Final test compound concentrations in Knops'-medium as used for *A. thaliana* cultivation

compound concentrations (mM)

DL-Met	0.2
MM	0.1
L-Ile	0.1
Ket	0.1
L-Lys	0.001
D-Lys	0.1
L-Thr	0.1
D-Thr	0.1
L-Trp	0.1
D-Trp	0.1
L-Hom	0.1

4.3.6.1 Main root length measurement of *A. thaliana*

The main root lengths *A. thaliana* were measured at 10dps by using a common ruler. The translucent agar in combination with the mostly straight root growth, induced by the vertically positioning of the plates, enabled full access for measurements of the main roots. Only main roots that were located flush to Petri dish bottom were evaluated. The given root lengths are the means values of $n \geq 16$ plants per treatment, relative to the average control root length.

4.3.6.2 Nematode invasion rate analysis

The invasion rate analysis of the nematodes was performed as previously described by Siddique *et al.* (2014) using a Leica S8APO binocular. Pure Knops'-medium with no additional enrichment was used to grow the control plants. At 2dpi the position of every nematode that invaded the plant successfully was marked on the Petri dish. In this, the invasion was considered as successfully when the nematode head was located inside the root (close to the vascular cylinder) and remained motionless during the time of observation. In

this way, the number of invaded nematodes per plant was ascertained for three biological replications, each with $n \geq 9$ plants per treatment.

4.3.6.3 Number of eggs per female nematode on *A. thaliana*

The number of eggs per female, feeding on treated *A. thaliana* was ascertained at 35dpi. The hereafter described method was developed by Bredenbruch *et al.*, (unpublished data). Female nematodes were picked from the roots using 5-Inox-H forceps transferred into 1.5ml tubes filled with 50 μ l ddH₂O and stored at +4°C in a KS38R430IE fridge. To crush the surface and to release the eggs into solution, the females were squeezed with a Kimble™ Kontes™ Pellet Pestle™. Afterwards, the eggs were washed out of the opened females pipetting 10 times, followed by a brief centrifugation step at ≥ 1000 rpm in a 5424 centrifuge. Next, the suspension was mixed again by another three times pipetting. Finally, the number of eggs was counted in three aliquots of 5 μ l and the obtained average was used to extrapolate to number of eggs in the total volume of 50ml. The experiment was set up as three biological replications, each with $n \geq 17$ females per treatment.

4.3.7 Detailed analysis of the infection and development of *H. schachtii*

Here we examined the infection and development of *H. schachtii* on aa treated *A. thaliana* roots in detail on a daily basis between 1-14dpi. The main focus of this experiment was to determine if a certain event / parameter / developmental step can be identified to restrict the development of females upon aa treatments. In this, plants were cultured on 0.1mM L-Thr, 0.1mM L-Ile and 0.2mM DL-Met enriched Knops'-medium which was prepared and stored as described in chapter 4.3.6 and inoculated according to the infection assay protocol given in chapter 4.3.3. Three biological replications were conducted, each with $n=19$ daily monitored nematodes per treatment. Initially, the locations of these 19 successfully invaded nematodes per treatment were marked on the plates in consecutive numbers. Each of these nematodes was then photographed at 1-8, 10, 12 and 14dpi with a Leica M165 C stereo 12:1 zoom microscope. Based on the pictures available, the infection and development progress of each nematode was evaluated and categorized as follows:

- 1) the invaded nematode fully develops into an adult male or female
- 2) the nematode leaves the infection site at a certain dpi

3) the development stops = no size increases after a certain dpi. The nematode remains in the root. Evaluated by size measurements.

4) continuous root and leave growth cover the nematode, restricting further observations

In this, the nematode body diameter expansion was used to determine the integrity of development. As long as the nematodes body diameter expands between two consecutive measurements, the development of the nematode continuous. To analyze this, the lateral-ventral diameter was measured at three different positions (at least two), leaving an appropriate distance to the head and tail. The average diameter was calculated and compared to the ascertained size of the previous dpi. In case the value was unchanged, the last dpi with size increase was defined as the dpi of developmental stop.

Example: In case the diameter expanded between 2 - 3dpi but not between 3 - 4dpi, the development stopped at 3dpi.

All result values for the categories ‘developmental stop’, ‘exit infection site’, ‘female’, ‘male’ and ‘undetectable’ are the total aggregated numbers from the three biological replications. In contrast to this, the result values for ‘dpi developmental stop’ and ‘dpi exit infection site’ are means, calculated on the average values of the three biological replications.

4.3.8 Infection assays with SALK_081563c and mto1-1 mutant lines

The seed material of SALK_081563c and mto1-1 mutant lines was purchased from the Nottingham Arabidopsis Stock Centre (NASC). To multiply the purchased seeds, both mutants were grown on soil and the seeds were extracted and stored as described in 3.3.2.2. The presence of the described mutation and homozygosity were determined before conducting infection assays, as described in chapter 4.3.3.

Both studies did not reveal any significant effects on the number of adult nematodes per plant or female and syncytium sizes. For this reason, the results of mto-1 and SALK_081563c experiments were included as supplementary data, see chapter 8.2.2.8.

4.3.8.1 SALK_081563c homozygosity confirmation

DNA was extracted from leafs of 10-days old SALK_081563c and col-0 (control) seedlings, cultured as described in chapter 4.3.2.3. The sample material was placed into a 2ml tube

together with two metal beets and frozen in LN₂. These prepared samples were then crushed analogous to the procedure described for RNA extraction, chapter 4.3.10.2. Afterwards, 500µl CTAB buffer were added before incubating for 15min at 55°C using a Thermomix comfort. Next, the probe was centrifuged at 12000g for 5min using a 5424 centrifuge and the supernatant was transferred into a sterile 1.5ml tube. 250µl previously prepared chloroform:isoamyl alcohol mixture (ratio 24:1) were added under a fume hood and subsequently mixed by inverting. The mixture was centrifuged at 13000rpm for 1min before the upper aqueous phase was transferred into a clean 1.5ml tube. 50µl of 9.5M ammonium acetate together with 500µl of -20°C cold absolute ethanol were added and the probe was inverted multiple times before incubating it at -20°C for 1h in an ARTIS CHAMPIONS LINE fridge. After incubation, the probe was centrifuged at 13000rpm for 1min and the supernatant was subtracted. The now present DNA pellet was washed two times by adding and removing 1ml of 70% ethanol. After washing, the tube was centrifuged at 13000rpm for 1min and the supernatant was removed by pipetting before the pellet was air dried for 15min at room temperature. Next, 100µl DNase/RNase-free H₂O was added and the probe was incubated at 65°C for 20min using a Thermomix comfort. Finally, the nucleic acid concentration was measured by NanoDrop 2000c™ according to chapter 4.3.10.3 and the probe was stored at -20°C in an ARTIS CHAMPIONS LINE fridge. Adapted from: http://www.cilr.uq.edu.au/UserImages/File/Plant%20Genomic%20DNA%20Extraction%20by%20CTAB%20_2__Fiona.pdf

To confirm the insertion-based knockout of the *A. thaliana* TS (AT4G29840.1) in SLAK_081563c, the insertion specific primers given in table 5 were used. The forward and reverse primer sequences were derived from <http://signal.salk.edu/tdnprimers.2.html> and purchased from Invitrogen (Thermo Fisher Scientific, Waltham, Massachusetts, USA). The PCR was performed as described in chapter 4.3.10.6 applying the thermocycler protocol described in table 9 (60°C primer). The prepared SALK and col-0 templated DNA was added in volumes of 0.5µl per reaction in combination with the SALK_081563c LP and RP to confirm the insertion, and additionally together with ACT as positive control. Moreover, ACT was used as reference primer with DNase/RNase-free H₂O as negative control.

Table 5 Primer sequences used for SALK_081563c homozygosity determination

primer name	Sequence 5'-3'
SALK_081563c LP	CCCGGTTCAAATTGATATTG
SALK_081563c RP	GAACCCACTCTTCTTCGACC
ACT F	ACAGCAGAGCGGGAAATTGT
ACT R	AGCA GCTTCCA TTCCCACAA

4.3.8.2 mto1-1 homozygosity confirmation

As demonstrated by Inaba *et al.* (1994), mto1-1 is unaffected by ethionine, a toxic analog of methionine. This lack of sensitivity to ethionine was utilized to confirm the homozygosity. The method described by Inaba and colleagues was conducted with minor adaptations: *A. thaliana* mto1-1 and the wild type *A. thaliana* col-0 were grown on a selective Knops'-medium enriched with 0.1mM L-ethionine. In parallel a col-0 control batch was grown on Knops'-medium without of supplements, to demonstrate the integrity of the tested seeds stocks. Initially, the seeds were sterilized as described in chapter 4.3.2.1. Twenty seeds were used per plate in a symmetrical arrangement to ensure equal distances between all plants. All plates were seeded under aseptic conditions, sealed with PARAFILM® and stored as described in chapter 4.3.2.3.

4.3.9 Gene expression analysis by NEMATIC

The data-mining spreadsheet Nematode-Arabidopsis Transcriptomic Interaction Compendium (NEMATIC) (Cabrera *et al.*, 2014) was used to mine published transcriptomic data from experiments with *H. schachtii* in *A. thaliana*. This spreadsheet allows a comparison of the gene expression in un-infected control root segments with the expression in microaspirated syncytia tissue, combined for 5 and 15dpi (Szakasits *et al.*, 2009) and at 3dpi (Puthoff *et al.*, 2003). In this way, we generated a 5 - 15dpi syncytium specific gene expression profile of aspartate pathway related enzymes, cf. appendix 6.1.8. The NEMATIC spreadsheet was used in Microsoft Excel (Microsoft, Redmond, USA).

4.3.10 Gene expression analysis by qRT-PCR

4.3.10.1 Culturing and sampling of *A. thaliana*

The quantitative real time polymerase chain reaction (qRT-PCR) was used to analyze the expression of aspartate family marker genes in:

- 1) un-infected and aa treated *A. thaliana*
- 2) *H. schachtii* infected and aa treated *A. thaliana*

Plants for qRT-PCR analysis were grown on Knop's-medium supplemented with 0.1mM L-Thr, 0.1mM MM and 0.2mM DL-Met as described chapter 4.3.6. All root tissue samples of un-infected and aa treated *A. thaliana* were collected at 10dps. *H. schachtii* infected and aa treated root tissue samples were inoculated with *H. schachtii* J2s as described in chapter 4.3.3 and sampled at 3dpi. For sampling, the shoots were dissected by using a scalpel and discarded before the roots were extracted from the agar by using forceps and immediately transferred into liquid nitrogen (LN_2) cooled 2ml tubes. Special attention was paid to minimize the carryover of attached agar remains. Multiple roots were combined per 2ml tube to obtain a total roots sample of ~70mg per tube, as weight checked on a NewClassic MF JP1603C balance. All prepared root samples were immediately stored at -80°C in a Sanyo MDF-U74V ultra deep freezer until further usage.

4.3.10.2 RNA extraction

Initially, two metal beats were added per root sample tube before transferring it into LN_2 . To break down the tissue, the frozen samples were crushed in a Mixer Mill MM 400 sample grinder at a frequency of 25motions/sec for 60sec. The machine specific adapter container for samples was cooled in LN_2 prior to loading the samples and running the grinding process. Right after all sample tubes were immediately returned into LN_2 .

RNA was extracted from the processed samples by using the RNeasy® Plant Mini Kit according to the provided manufacturers protocol. The following adaptations were implemented: RLT buffer was selected and the sample was incubated for 2min at 56°C using a Thermomix comfort, before proceeding with protocol step 4. The RNA was eluted in 35 μl DNase / RNase-free H₂O before the tube was directly placed on ice. Finally, the RNA concentration was measured by NanoDrop, as described hereafter (chapter 4.3.10.3). The samples were directly processed or alternatively stored at -80°C in a Sanyo MDF-U74V ultra deep freezer.

4.3.10.3 Nucleic acid quantification

Nucleic acid quality and concentration were determined by NanoDrop 2000cTM. For all measurements, the samples were vortexed for 4sec on a Vortex-Genie 2 G560 E apparatus, before applying a sample volume of 1 μ l per measurement. Each sample was measured in three aliquots and the reported average concentrations were calculated.

4.3.10.4 DNase digestion in RNA samples

RQ1 RNase-free DNase was used to digest remaining genomic DNA in all RNA samples, according to the manufactures protocol. The herein used component specific volumes were applied as indicated in table 6. After genomic DNA digestion, RNA concentrations were measured once more by NanoDrop, as described in chapter 4.3.10.3. All treated samples were afterwards stored at -80°C in a Sanyo MDF-U74V ultra deep freezer.

Table 6 Reagents and volumes used in the DNase digestion reaction using RQ1 RNase-free DNase

reagents	volume (μ l)
RNA in ddH ₂ O	≤ 14 (4 μ g RNA)
RQ1 10x reaction buffer	2
RQ1 RNase-free DNase	4
DNase / RNase-free H ₂ O	add to Σ 20
Σ	20

After DNase digestion, the integrity and purification grades of aa treated and un-infected *A. thaliana* root RNA probes were ascertained by Bioanalyzer 2100 equipped with Aglient Technologies 2100 Bioanalyzer 2100 Expert v.B.02.08.SI6-48 (SR2). The kit Aglient RNA 6000 Nano Reagents Part I was used with the provided chemicals and according to the manufacturers protocol.

All RNA samples proofed to provide very high integrity and purification grades. Due to this high reliability of the used extraction and purification kits, all other RNA probes were only tested for DNA contaminations by PCR with subsequent analysis by gel electrophoresis described in chapter 4.3.10.6 and 4.3.10.7. Actin primers (ACT) where used to perform the

PCR reactions and *A. thaliana* col-0 complementary deoxyribonucleic acid (cDNA) was used as positive control. RNA probes were considered to be free of genomic DNA contaminations, when no amplification occurred, i.e. no specific band was visible.

4.3.10.5 cDNA preparation

The prepared RNA probe set was reverse transcribed into cDNA by using the High-Capacity cDNA Reverse Transcription Kit according to the manufacturers protocol. All steps described hereafter were performed on ice. Initially, a common 2 x RT (reverse transcriptase) master mix was prepared in a 1.5ml tube, at 25µl for each RNA sample to be transcribed. Afterwards, 25µl of the master mix were added to 25µl DNase/RNase-free H₂O containing 2.5µg RNA, in PCR 8-strip Multiply® tubes with PCR 8-strip Multiply® lids. Finally, all prepared 50µl reactions were gently mixed by pipetting before running the reverse transcription in a C1000™ thermal cycler combined with the CFX Manager™ v.2.1 as described in table 7. After cDNA synthesis, 50µl DNase/RNase-free H₂O was added to each reaction, before they were mixed by vortexing on a Vortex-Genie 2 G560 E. All cDNA samples were stored at -20°C.

Table 7 Thermo cycler protocol for cDNA synthesis

step	temperature (°C)	time (min)
1	25	10
2	37	120
3	85	5
4	4	∞

4.3.10.6 Polymerase chain reaction

The polymerase chain reaction (PCR) reagent mixes were set up in PCR 8-strip Multiply® tubes with PCR 8-strip Multiply® lids on ice, vortexed by Vortex-Genie 2 G560 E and spun down in a table top PCR-strip centrifuge Mini Star. Each reaction was prepared at a total volume of 25µl, applying the proportion of ingredients as listed in table 8. DNase/RNase-free H₂O replaced the DNA template for the negative control. The C1000™ or S1000™ thermal cyclers were used together with the CFX Manager™ v.2.1. The individual thermocycler protocols are listed in their respective chapters and the standard PCR reaction mix is listed in table 8.

Table 8 standard PCR reaction mix

Reagents	volume (μ l)
5 x Green GoTaq® Reaction Buffer	5
dNTPs (10mM)	0.5
DNA template	0.5
Go Taq® DNA Polymerase (5u/ μ l)	0.15
Primer forward	1.25
Primer reverse	1.25
ddH ₂ O	16.35
Σ	25

4.3.10.7 Gel electrophoresis

For preparation of 1% agarose gels, 98ml purified ddH₂O, 2 ml of Rotiphorese® 50x TAE buffer and 1g of peqGold Universal Agarose were mixed and melted into solution in a common microwave. The solution was allowed to cool down to 45°C, before 4 μ l peqGREEN per 100ml agar were added under constant stirring on a CB 162 hotplate stirrer. Finally, the liquid agar was poured into a casting mold and left 30min at room temperature for setting.

The 1 kilo base (kb) and 100 base pair (bp) DNA ladders were prepared according to the manufacturer's protocols. 6 μ l DNA ladder marker mix or 10 μ l PCR product were applied per gel pocket. The DNA fragments were separated in a Sub-Cell® GT Agarose Gel Electrophoresis equipped with PowerPac Basic™ power supply at 80V for 80min. For imaging, a Gel Doc™ XR was used together with the Image Lab™ v.3.0.1 (Beta 2) analysis software.

4.3.10.8 Establishment of the aspartate pathway primer set

A set of marker genes was established, containing enzymes relevant for the synthesis and degradation of key metabolites of the aspartate family pathway. Accordingly, the expression analysis of this gene compilation may enable to identify alternated regulations between and in the Thr, Met and Ile pathways. The qRT-PCR primer set is listed in table 10. All primers were designed by Primer3 web v.4.0.0 (Untergasser *et al.*, 2012) for the respective coding sequences (cds) as referred to by accession numbers in table 10. All cds were obtained from The Arabidopsis Information Resource (TAIR), on www.arabidopsis.org (year 2015). In this, the default settings listed in chapter 8.1.9 were used, aiming for a primer Tm of minimum 59°C, optimal 60°C and maximum 61°C. All primers were purchased from Invitrogen (Thermo Fisher Scientific, Waltham, Massachusetts, USA). Before experimental

usage, they were diluted to a working concentration of 0,01nmol/µl by adding DNase/RNase-free H₂O on ice. Afterwards they were vortexed on a Vortex-Genie 2 G560 E and stored at -20°C in an ARTIS CHAMPIONS LINE fridge.

4.3.10.8.1 Primer specificity and functionality analysis

The primer specificity and functionality were separately tested for both organisms, *A. thaliana* and *H. schachtii*. The latter cDNA was prepared from the extracted RNA of ~ 3000 J2, using the NucleoSpin® RNA kit following the provided protocol. The obtained nematode RNA was reverse transcribed into cDNA by High-Capacity cDNA Reverse Transcription Kit using the equipped random primers, according to the manufacturers protocol. *H. schachtii* cDNA was kindly prepared and provided by Samer Habash (unpublished).

Initially, the *A. thaliana* and *H. schachtii* cDNAs were diluted 1:10 after synthesis and before usage as template in the following PCR reactions. All primers listed in table 10 were tested for specificity and functionality by standard PCR reactions, cf. 4.3.10.6. The applied thermal cycle protocol is given in table 9, followed by gel electrophoresis as described in chapter 4.3.10.7, using a 100bp ladder. Primers were considered to be specific, when one single band was visible per reaction.

Table 9 Thermocycler protocol for qRT-PCR primer specificity and functionality analysis

no.	step	temperature (°C)	time (min)	cycles
1	initialization	94	00:30	
2	denaturation	94	00:30	
3	Annealing	60	00:30	35x
4	elongation	72	01:00	
5	final elongation	72	05:00	
6	cooling	4	∞	

4.3.10.8.2 Primer efficiency analysis

The primer efficiency was ascertained by qRT-PCR, using the materials listed in 4.3.10.9. For each primer to be tested, the master mix was prepared at a total volume of 216µl, vortexed and aliquoted into the wells of the 96-well plate as described. Serial dilutions of uninfected *A. thaliana* (col-0) control cDNA were set up with DNase/RNase-free H₂O (1:1, 1:10, 1:100, 1:1000 for ACT, MGL, CGS, OMR, TS 1 and THA 1; 1:5, 1:25, 1:125, 1:625 for SAM 1-4, TS 2, THA 2) and added to the master mix containing wells at volumes of 2µl/well. All primers were tested at each cDNA concentration in 3 technical replications.

After loading all wells, the plate was sealed, centrifuged and the machine-based analysis was started. Finally, the primer efficiency was calculated based on the mathematical model established by Pfaffl (2001), which is based on the CT means of the single dilution steps. The hereby ascertained primer efficiencies are reported in table 10, below.

Table 10 Aspartate gene family targeted set of primers used for qRT-PCR experiments

gene family	EC:	accession	primer name	Sequence 5'-3'	efficiency
ACT	-	AT3G18780.2	ACT F	ACAGCAGAGCGGGAAATTGT	1,92
			ACT R	AGCAGCTTCCATTCCCACAA	
SAMS 1	2.5.6.1	AT1G02500	SAMS 1 F	GCCACTGATGAAACCCCTGA	1,95
			SAMS 1 R	TCCTTGA TGCCTGCCTTGAG	
SAMS 2	2.5.6.1	AT4G01850	SAMS 2 F	GCCACTGATGAAACCCCTGA	1,93
			SAMS 2 R	GGGTTGAGATCAGGACGGTG	
SAMS 3	2.5.6.1	AT2G36880	SAMS 3 F	GCTCAGGGTGTCA TGGTCA	1,89
			SAMS 3 R	CCTCAACCATGGGCAA GTCT	
SAMS 4	2.5.6.1	AT3G17390	SAMS 4 F	CTCATGGAGATGCAGGGCTT	1,99
			SAMS 4 R	ACACAGACAATGGCTCAGGG	
MGL	4.4.1.11	AT1G64660	MGL F	TACAGCCGACACTTCAACCC	1,95
			MGL R	TGAGAGAGCAAAGCGTGTGT	
CGS	2.5.1.48	AT3G01120	CGS F	CACGCTTAATCCGAACGCTG	2,36
			CGS R	CCAGTCATTTGTCGCTTGGC	
TS 1	4.2.3.1	AT4G29840	TS 1 F	GAGATGAGGCTCGTCGTAATCG	2,03
			TS 1 F	GCCTCCAATCGTGTTCGACATC	
TS 2	4.2.3.1	AT4G29810	TS 2 F 1	AGAGCTGTGTATGCGTTGAAGA	1,98
			TS 2 R 1	AGTCCGATCAATCGCTCCA	
OMR	4.3.1.19	AT3G10050	OMR F	GGAGACGAGGTCTATGCCG	2,20
			OMR R	CCATTCTTGCTCGGGGACT	
THA 1	4.1.2.5	AT1G08630	THA 1 F	GGAGGCCATTGAAGCAGCTA	1,98
			THA 1 R	GCATTGAAAAGACGGGCTCC	
THA 2	4.1.2.5	AT3G04520	THA 2 F	TCTGTGGCACTTGGAGTTCC	1,94
			THA 2 R	TGGCGACGTTTCA TGGAGA	

4.3.10.9 qRT-PCR protocol

The qRT-PCR based gene expression between aa treated and untreated *A. thaliana* roots was separately compared for two scenarios, 1) infected and 2) un-infected with *H. schachtii*. The expression of each gene was analyzed in n=3 biological replications per treatment, with n=3 technical repetitions. Herein, a biological replicate was defined as the RNA extracted from one sample of ~70mg plant root material, as combined from the roots of multiple plants of the same plant batch and treatment. Both probe sets, nematode infected and un-infected were

processed and analyzed separately and successive, commencing with the infected probe set. All biological and technical replicates of the same gene were simultaneously analyzed in one plate, i.e. during one thermocycler run.

For master mix preparation, the Fast SYBR® Green Master Mix was used according to the manufacturer's protocol. A separate batch was prepared for each gene in a 1.5ml tube on ice. The total volume of 324 μ l per tube was distributed between the needed 18 single reactions of 18 μ l/gene: 9 individual reactions for the untreated control plus 9 reactions for the aa treated plant probes = 18 reactions/gene.

The Fast SYBR® Green Master Mix was first thawed on ice and briefly vortexed, before 180 μ l were aliquoted per 1.5ml tube, containing 126 μ l DNase/RNase-free H₂O. Afterwards, the 18 μ l primer solution was added and the mix was thoroughly vortexed with a Vortex-Genie 2 G560 E. Next, the master mix was aliquoted in volumes of 18 μ l/well into a 96-well plate. To each well, 2 μ l of the respective templated cDNA were added before the plate was sealed with an optical adhesive film MicroAmp™, paying special attention not to damage or smear the translucent cover slide. After preparation, the plate was centrifuged at 3500rpm in a 5810 R centrifuge for 3sec and then visually checked. The gene expression was automatically analyzed with an Applied Biosystems StepOnePlus™ Real-Time PCR System Thermal Cycling Block equipped with the StepOne™ v.2.2.2 software. The protocol of the applied qRT-PCR cycling conditions is listed in table 11.

Table 11 qRT-PCR thermocycler protocol used for gene expression and primer efficiency analysis

stage	step	temperature (°C)	time (sec)	rate %
holding stage	1	95	20	100
	1	95	3	100
cycling stage	2	60	30	100
	1	95	15	100
	2	60	60	100
melt curve stage	3	95	15	100

As the first step of result evaluation, all obtained melting curves were checked for unspecific amplification. Afterwards, the conformity of all three amplification plots per technical replicate for each gene were compared and maximum one outlier with divergent conformity was excluded. In case the grade of conformity for at least 2 of 3 amplification plots was inconsistent, the gene expression analysis was repeated. After this data quality check, the raw data was exported as .xls format to be processed with a Microsoft Excel based

spreadsheet, based on the mathematical model for relative quantification of gene expressions measured by RT-PCRs (Pfaffl, 2001). Differences in gene expression between treated and untreated plants are given as fold changes with standard error bars, both calculated on the average CT mean value triplet of the biological replications taking into account the determined primer efficiency. Statistically significant differences were calculated by t-Test comparisons of the ΔCT means.

Table 12 qRT-PCR master mix protocol 1x and 18x for gene expression analysis and primer efficiency analysis

reagents	1 x	18 x
	volume (μl)	volume (μl)
Fast SYBR® Green Master Mix	10	180
primer F	0.5	9
primer R	0.5	9
DNase / RNase -free H ₂ O	7	126
Template cDNA	2	36
Σ	20	360

5 RESULTS

The simplest mode of action of nematicidal substances is to directly affect the target organism by cuticle contact alone or after uptake. Active compounds of this functional category would primarily lower or interrupt the nematode activity and development. In this, the biology of *C. elegans* allows to screen for effects with and without compound uptake. The first set of experiments assessed, if those direct toxic effects can be detected on the free-living nematode *C. elegans* and/or on the plant-parasitic species *H. schachtii*. All raw data underlying the herein presented results are provided as supplementary data in the appendix.

5.1 *C. elegans* experiments

5.1.1 Effects on the activity

This experiment aimed to identify effects on the activity of *C. elegans* occurring from the contact between exogenously applied aa and the nematode cuticle without uptake (= swallowing) by the nematode. For this purpose, juveniles were incubated in aa solutions for 3 days and the numbers of active and inactive individuals were counted. Compounds with direct toxicity would reduce the rate of active nematodes in relation to the untreated control.

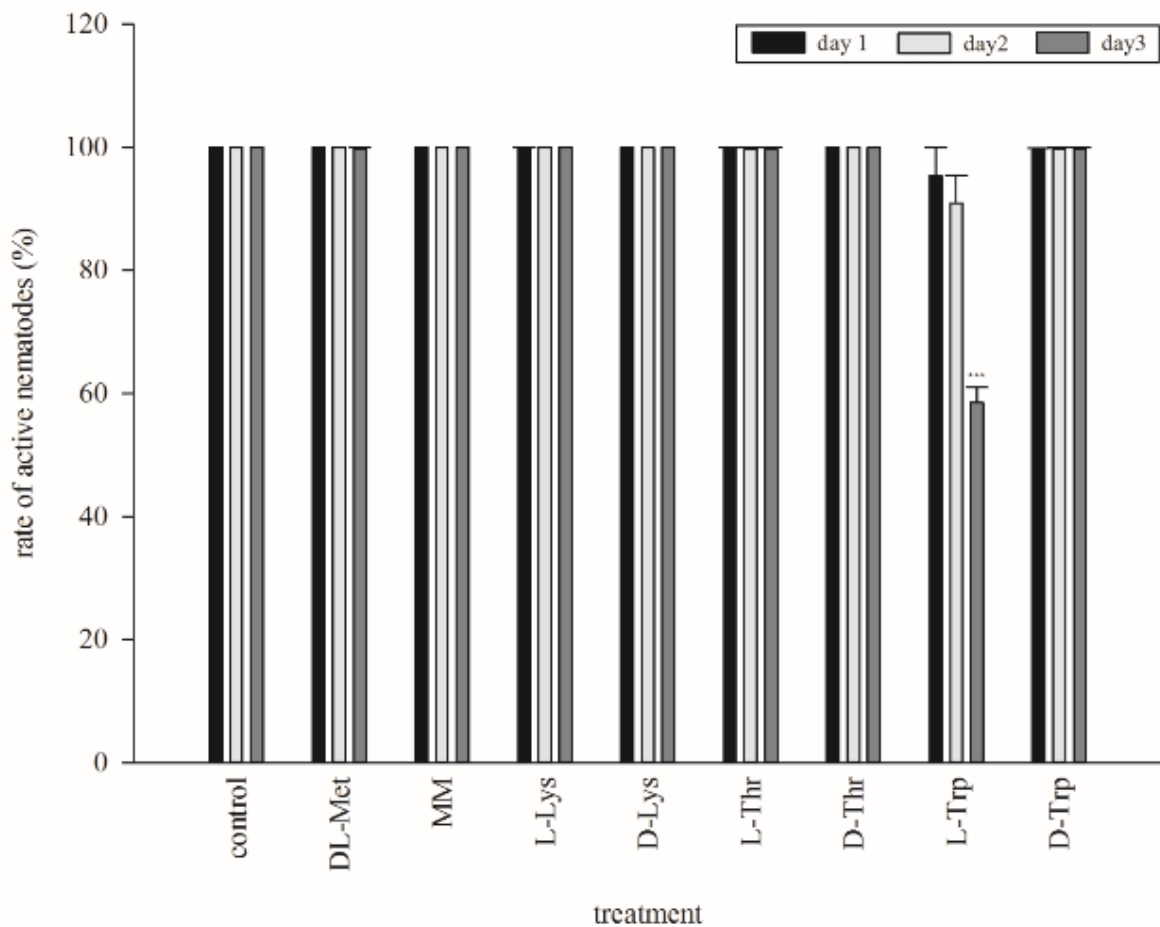


Figure 16 *C. elegans* activity test *C. elegans* larvae were incubated for three days in aa enriched S-Basal complete solutions at following concentrations in mM: DL-Met 20, MM 1, L-Lys 10, D-Lys 10, L-Thr 10, D-Thr 10, L-Trp 10 and D-Trp 10mM. The rate of active =moving nematodes was counted daily, given as % rate of active nematodes. Indicated are averages, calculated on the means of three biological replications \pm standard error. The asterisks (***) refers to a significant difference, according to t-Test of $P \geq 0.001$.

As apparent from figure 16, only 10mM L-Trp reduced the activity of *C. elegans* by cuticle contact alone. The rate of active *C. elegans* decreased continuously from 95.3% after 1 day, to 90.9% after 2 days and significantly and finally 58.6% after 3 days. Accordingly, all other aa did not induce negative effects on the activity of *C. elegans* by cuticle contact alone and are therefore not directly toxic to this species.

5.1.2 Effects on the development

After screening for influences on the activity the identification of effects with impact on the development of *C. elegans* was targeted. Substances with development interfering potential might prolong the different lifecycle intervals between L1, L2, L3, L4, reproductive adults

and possibly the time span between egg laying and hatching of 2nd generation juveniles. Very active substances might even interrupt the development completely.

Table 13 To screen for developmental effects, *C. elegans* L1 were incubated in aa enriched S-Basal complete solutions with added OP50 bacteria for 6 days. The time span between incubation of larvae until: a) first eggs were laid and b) 2nd generation L1 hatched from those eggs was measured.

Compound	Concentration(mM)	eggs (days)	L1 hatch (days)
Control	-	3-4	4
DL-Met	20	3-4	4
MM	1	3-4	4
	10	∞	∞
L-Lys	1	3-4	4
	0.1	3-4	4
	10	∞	∞
D-Lys	1	3-4	4
	0.1	3-4	4
	10	∞	∞
L-Trp	1	4-5	6
	0.1	3-4	4
D-Trp	10	3-4	4
∞ = development interrupted			

For this purpose, synchronized *C. elegans* juveniles were incubated in aa solutions with at concentrations. Daily assessments determine the period until:

- 1) larvae developed into adults and first eggs were laid = “eggs”
- 2) the first 2nd generation L1 hatched from those eggs = “L1 hatch”

In untreated control batches egg laying occurred after 3-4 days and the first 2nd generation L1 hatched after 4 days. Incubations in the highest concentrated solutions with 10mM L-Lys, D-Lys and L-Trp interrupted the nematode development, the life cycle was uncompleted until the experiment was stopped after 6 days. Even though the development was disrupted, all larvae remained active until day 6.

Upon the incubation with L-Lys and D-Lys, the vast majority of juveniles did not develop from the L1 to L2 stage and no individual developed into a reproductive adult. Remarkably, the 10 times lower 1mM Lys treatments induced no significant effect on the development.

Upon 10mM L-Trp all larvae arrested in the L1 stage. At the 10-fold lower concentration of 1mM a one-day delay was observed for both analyzed parameters. For 0.1mM the period until egg laying and hatch of L1 did not differ from the control, indicating a dose rate

response relationship for L-Trp. Summarized L-Lys, D-Lys and L-Trp negatively affect the development of *C. elegans*, whereas all other tested aa did not.

5.2 *H. schachtii* experiments

After focusing on the free-living nematode *C. elegans*, effects induced by exogenous application of aa on the plant-parasitic nematode *H. schachtii* were studied. In contrast to *C. elegans*, *H. schachtii* does not actively take up solutions outside of the plant root. Moreover, *H. schachtii* only develops from the J2 stage onwards after entering the sedentary stage inside the host plant root. For this reason, only direct toxic effects on the activity, resulting from direct contact between test compound and nematode cuticle, were studied in incubation experiments. A second trial series investigated those effects on *H. schachtii* that involve the treatment of their host plant *A. thaliana*.

5.2.1 Effects on the activity

Comparable to the method used for *C. elegans*, the incubation of *H. schachtii* J2s in test compound solutions over 7 days aimed to detect direct effects on the nematode activity as induced by sole nematode cuticle-compound contact. Those compounds with direct toxicity should show a reduced rate of active nematodes compared to the untreated control.

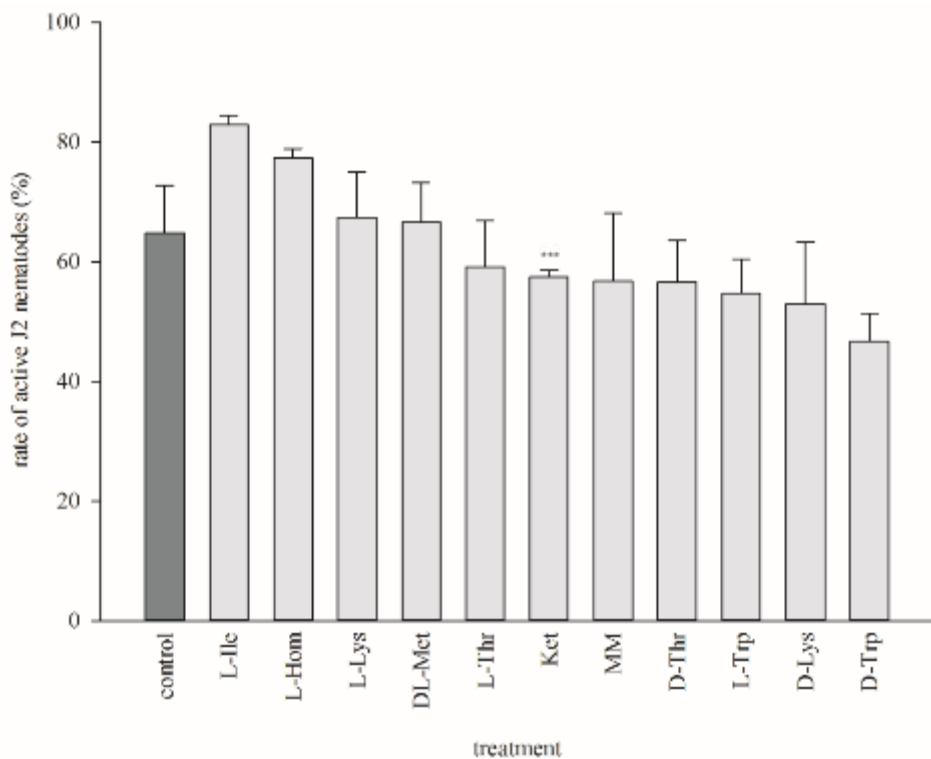


Figure 17 *H. schachtii* activity test 40 *H. schachtii* J2 per well were incubated in compound enriched ddH₂O (concentrations in mM: DL-Met 20, MM 1, Ket 0.1, L-Lys, D-Lys, L-Thr, D-Thr, L-Trp, D-Trp, L-Hom, L-Ile each at 10) over 7 days under the absence of light in 24 well plates. The number of active (moving) and inactive (not moving) juveniles was counted after 7 days of incubation. Indicated are averages, calculated on the means of three biological replications ± standard error

After 7 days of incubation 64.8% of the total J2s remained active in the H₂O control. Only 0.1mM Ket treatments reduced the rate of active nematodes significantly to 57.4%. All other aa did not affect the activity of *H. schachtii* J2 significantly within 7 days at the applied concentrations.

5.2.2 24h incubations of *H. schachtii*

Even though the activity level of *H. schachtii* was only reduced by Ket, it could not be excluded, that effects on parasitism and/or on the development during the sedentary stage might occur. A screening with *H. schachtii* J2s incubated in aa solutions for 24h followed by cuticle cleaning and finally infection of *A. thaliana* roots focused on those possible effects. For these trials, J2s were only exposed to test compounds during the 24h of incubation and not during infection and parasitism of the roots.

5.2.2.1 Count of adult nematodes per plant

At first, the numbers of male and female nematodes per plant were counted. Harmful effects on parasitism or development would reduce the number of adult nematodes per plant or change the sex ratio.

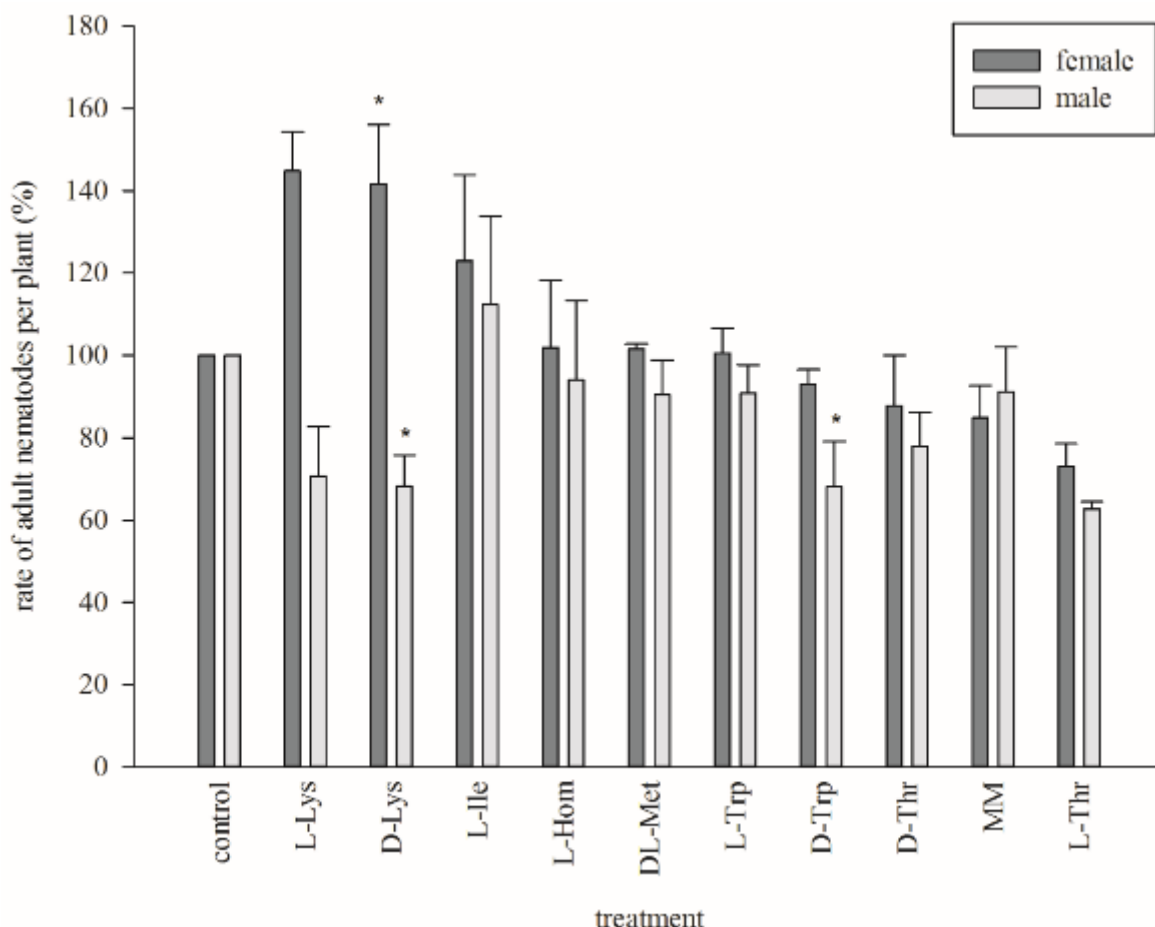


Figure 18 24h incubation: adult nematodes per plant *H. schachtii* J2s were incubated for 24h under the absence of light in 24 well plates in test compound enriched ddH₂O at following concentrations (mM): DL-Met 20, MM 1, Ket 0.1, L-Lys, D-Lys, L-Thr, D-Thr, L-Trp, D-Trp, L-Hom, L-Ile each at 10. Subsequently, 60 treated and surface cleaned juveniles were inoculated per 10 days old *A. thaliana* (col-0), cultured on Knops medium. The number of adult nematodes per root was counted at 12dpi. Indicated are averages \pm standard errors calculated on the means of three biological replications. Asterisks (*) refer to significant differences according to t-Tests ($P \geq 0.05$).

Effects were detected for D-Lys, L-Lys and L-Trp. Incubations in 10mM D-Lys shifted the sex ratio per plant by +41.6% females and -31.9% males. For 10mM L-Lys treatments the rate of females increased by +44.7% whereas males were reduced by -29.4%. In total: +5.7 (L-Lys) and +5.6 (D-Lys) females in relation to -3.9 (L-Lys) and -4.2 (D-Lys) male nematodes per plant. This equates to a shift of ~0.84 to ~0.39 males per female per plant.

Additionally, 10mM D-Trp treatments reduced the number of males by -27.1%, whereas female numbers were unaffected, cf. figure 18. All other tested substances had no significant influence.

Table 14 *H. schachtii* J2s were incubated in 10mM L-Lys and D-Lys for 24h under the absence of light in 24 well plates. Afterwards, 60 treated and surface cleaned juveniles were inoculated per 10 days old *A. thaliana* (col-0), cultured on Knops'-medium. Indicated are average male and female numbers per root ascertained at 12dpi.

treatment	control	treatment	control	treatment	+/-	+/-
	females	females	Males	males	females	males
L-Lys	13.6	19.3	11.6	7.6	+5.7	-3.9
D-Lys	14.7	20.3	12.3	8.1	+5.6	-4.2

Summarized, cuticle contact with L-Lys and D-Lys shifted the male per female ratio per plant at an unchanged total number of adult nematodes per plant. Additionally, D-Trp reduced the number of male nematodes per plant significantly.

5.2.2.2 Female and syncytium size measurements

Female and syncytium size measurements were performed next. Since sedentary *H. schachtii* feeds exclusively from their syncytium, its volume determines the available food quantity. Even though female sizes undergo natural variations, it is likely that strong impairing conditions should reduce female sizes significantly. Possibly the pronounced development of females upon L-Lys and D-Lys treatments is the result of an improved nutritional situation = increased syncytium and female sizes.

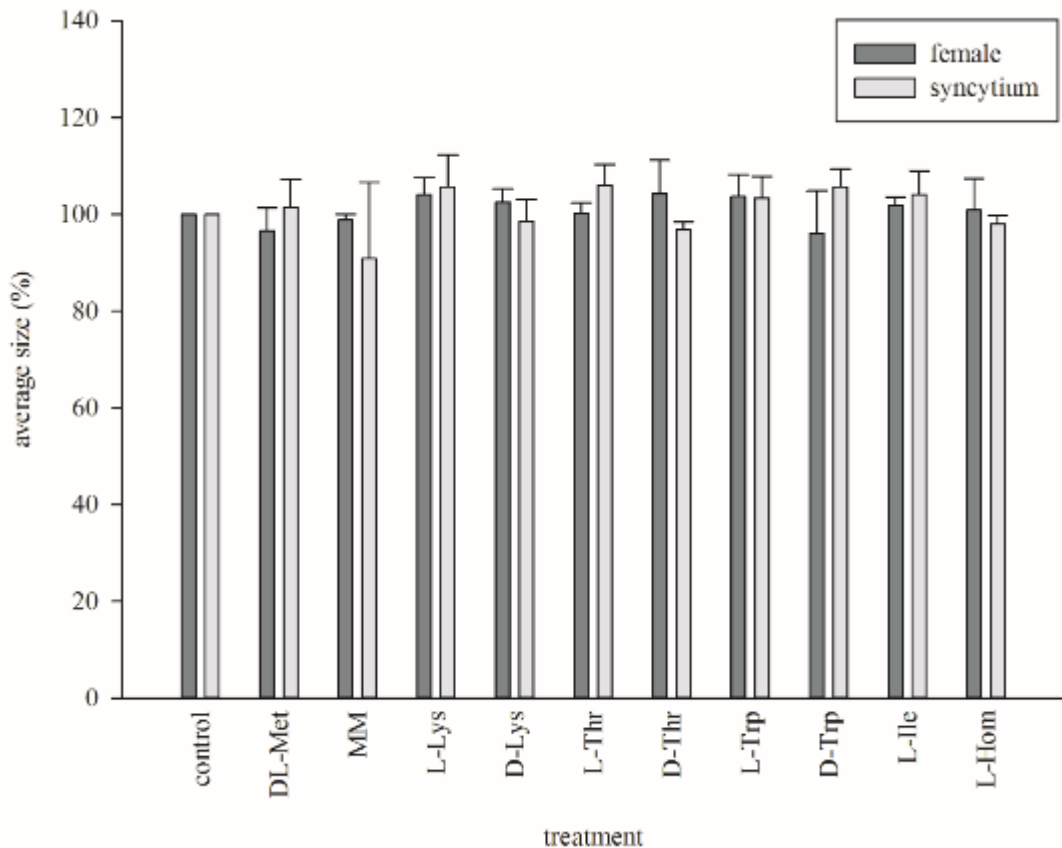


Figure 19 24h incubation: syncytium and female sizes *H. schachtii* J2s were incubated in compound enriched ddH₂O (concentrations in mM: DL-Met 20, MM 1, Ket 0.1, L-Lys, D-Lys, L-Thr, D-Thr, L-Trp, D-Trp, L-Hom, L-Ile each at 10) for 24h under the absence of light in 24 well plates. 60 treated and surface cleaned juveniles were inoculated per 10 days old *A. thaliana* (col-0), cultured on Knops'-medium. *H. schachtii* female and syncytium sizes were measured at 14dpi. Relative average sizes were calculated in relation to the control. Indicated are averages \pm standard errors, calculated on the means of three biological replications.

As visualized in Fig. 19, 24h incubation treatments did not increase or decrease female or syncytium sizes for any of the tested compounds at 14dpi.

5.2.2.3 Count of adult nematodes per plant in the absence of ZnCl₂ and HgCl₂

Lys tends to form complexes with ZnCl₂, added for hatching in the funnel system, and HgCl₂ used for surface sterilization of juvenile nematodes. In order to exclude an influence of ZnCl₂ and HgCl₂, the prior experiment 5.2.2.1 was repeated in the absence of both substances.

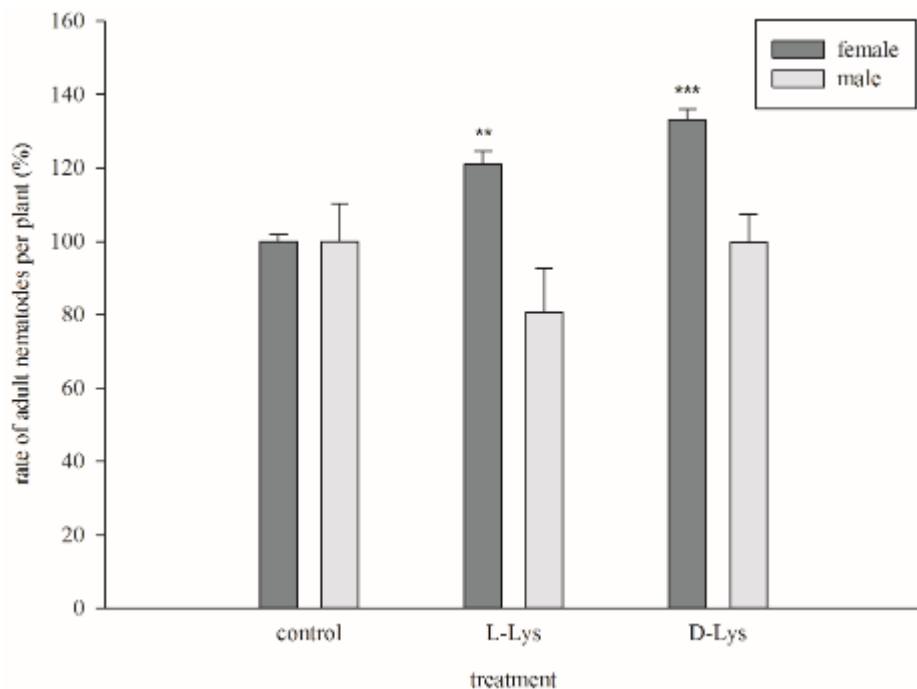


Figure 20 24h incubation in the absence of ZnCl₂ and HgCl₂ *H. schachtii* J2s were incubated for 24h in 10mM L-Lys and D-Lys enriched. The 24 well plates were kept under the absence of light. 60 treated and surface cleaned juveniles were inoculated per 10 days old *A. thaliana* (col-0), cultured on Knops'-medium. In contrast to the standard procedure, ZnCl₂ and HgCl₂ were not used for nematode sterilization and hatching. Given are the average rates of male and female nematodes per *A. thaliana* (col-0) at 14dpi. The averages \pm standard errors were calculated on the means of three biological replications. Asterisks (**; ***) refer to significant differences according to t-Tests (** = P \geq 0.01; *** = P \geq 0.001).

L-Lys induced a significant increase of +21% females and a decrease of -19.4% males per plant. D-Lys incubations significantly increased the number of females by +33% at an unchanged number of male nematodes. Accordingly, the results reconfirm that the observed sex ration change was provoked by the 24h treatments with L-Lys and D-Lys prior to infection of untreated roots. Moreover, an influence of ZnCl₂ and HgCl₂ can be herewith excluded.

5.2.3 Treatment of *A. thaliana*

Aiming to provoke effects on *H. schachtii* that require the involvement of the host plant, *A. thaliana* was grown on test compound enriched Knops'-medium and infected with untreated J2s. Hereby, it was possible to screen for effects on parasitism and development processes of the nematode. At first the impact of compound supplementation to Knops'-medium on the plant root development was determined by measuring the main root length at 10dps.

Additionally, effects on *H. schachtii* induced by treatment of the host plant were screened by examining the nematode invasion rates, the rate of adult nematodes per plant and measuring female and syncytium sizes.

5.2.3.1 Main root length measurement

Table 15 Analysis on effects of agar enrichment with test compounds on the main root length of *A. thaliana* (Col-0). Plants were cultured on Knops'-medium supplemented with test compounds under aseptic conditions. Measures were taken at 10dps. Indicated are average main root lengths and length differences of treated roots (treated) compared to untreated roots (control).

compound	concentration (mM)	average root length (cm)		
		Control	treated	difference
DL-Met	0.2	4.8	3.2	-1.6
MM	0.1	5.2	3.8	-1.4
L-Lys	0.001	6.2	5.2	-1
D-Lys	0.1	4.5	5.1	+0.6
L-Thr	0.1	4.5	3.5	-1
D-Thr	0.1	4.8	3.4	-1.4
L-Trp	0.1	4.4	2.3	-2.1
D-Trp	0.1	4.5	1.5	-3
L-Hom	0.1	5.1	3.3	-1.8
L-Ile	0.1	6.1	4.7	-1.4
Ket	0.1	5.8	5.1	-0.7

For all test compounds *A. thaliana* responded towards the enrichments of the Knops'-medium by root length increases or decreases. In this, a margin from +0.6cm for D-Lys to -3cm for D-Trp treatments was measured. Upon D-Trp enrichment *A. thaliana* developed a dense multibranched root phenotype that rendered visual assessments of nematode numbers and size measurements impossible. For this reason, D-Trp was excluded from further experiments and analysis.

5.2.3.2 Invasion rate analysis

The process of invading involves the localization of the host root, the migration towards the roots and finally the penetration of the epidermis. Hypothetically, supplementing aa to the plant growth medium could impact all of those steps. If the process of invasion is unaffected,

the same number of nematodes should be finally present in treated and untreated roots. To test this, the %-rate of invaded nematodes per plant root was counted at 2dpi.

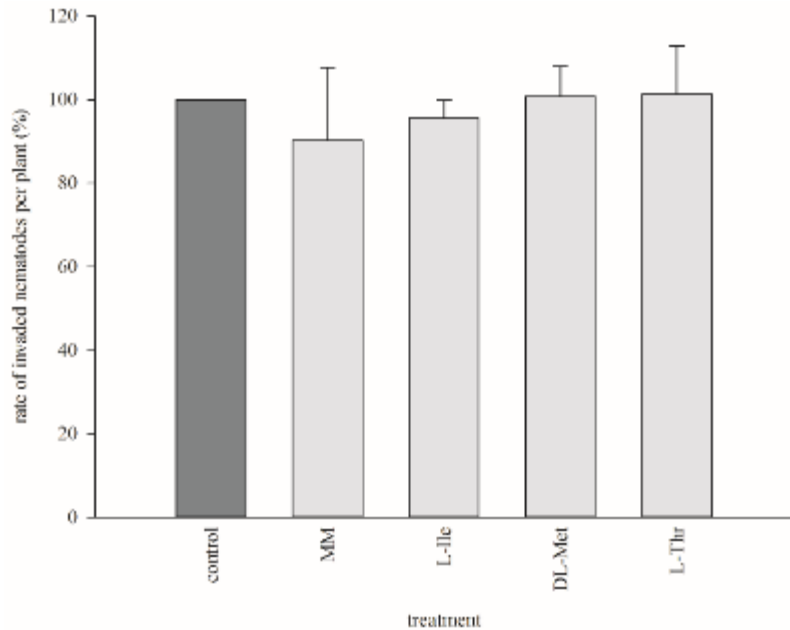


Figure 21 Aa treated *A. thaliana*: invasion rate analysis 60 sterile *H. schachtii* J2s were inoculated per 10 days old *A. thaliana* (col-0) under aseptic conditions. Plants were cultured on Knops'-medium supplemented with aa at following concentrations (mM): DL-Met 0.2, MM, L-Thr, L-Ile each at 0.1. The number of invaded juveniles was assessed at 2dpi. Indicated are means \pm standard errors calculated on the average numbers of three biological replications.

Supplementing 0.1mM MM, 0.2mM DL-Met, 0.1mM L-Ile and 0.1mM L-Thr to the medium did not affect the nematode invasion, the same number of nematodes were present in treated and untreated roots. Hence, the hereafter discussed decrease of males and females per plant must occur after successful invasion at 2dpi and before adult nematodes were counted at 12dpi.

5.2.3.3 Adult nematodes per plant

After invasion of the host plant roots juvenile nematodes establish and maintain a functional syncytium and molt multiple times before they finally develop into adult males or females. Effects induced by exogenously applied substances on these processes might increase or decrease the number of adult nematodes per plant, the female or syncytium sizes or change

the sex ratio as observed upon incubation treatments. As a first step, the number of males and females per root was examined.

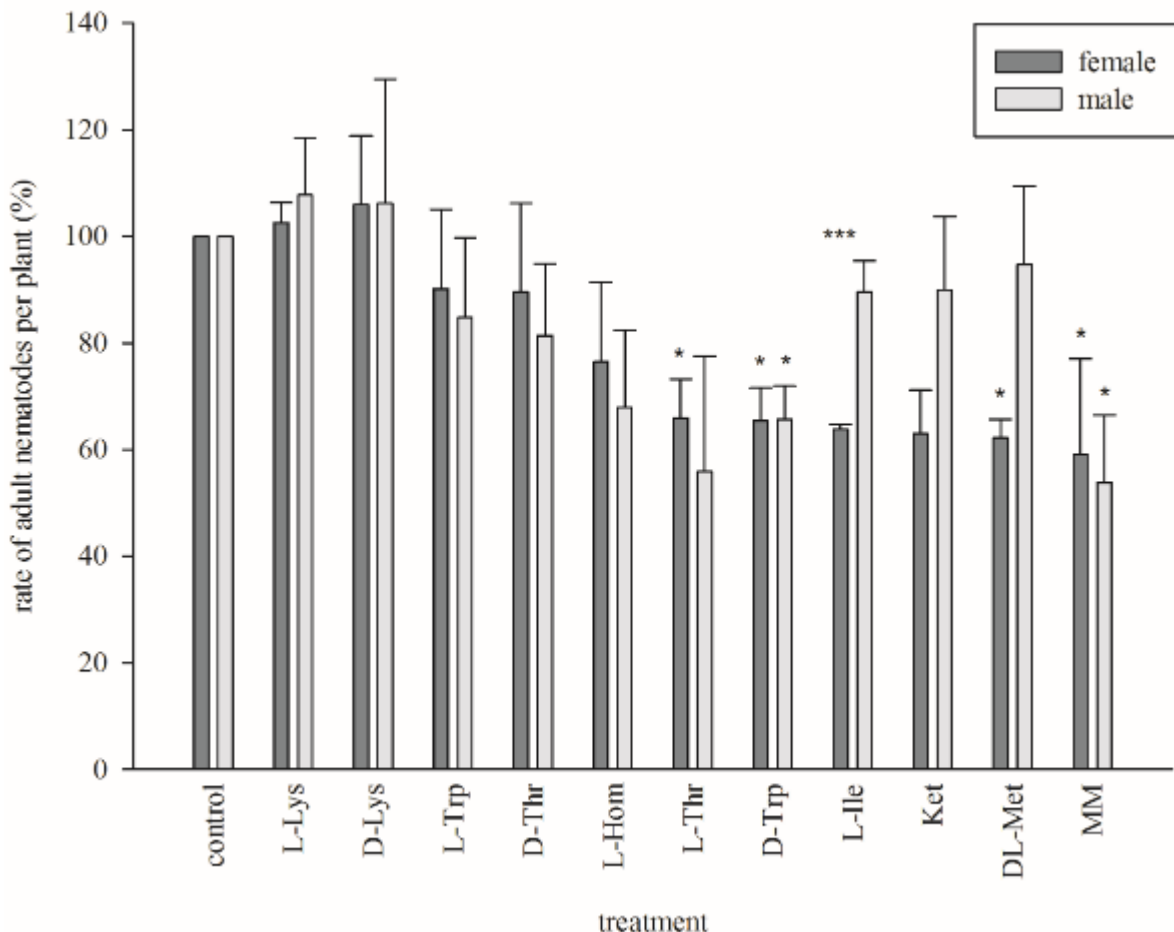


Figure 22 Aa treated *A. thaliana*: adult nematodes per plant 60 sterile *H. schachtii* J2s were inoculated per 10 days old *A. thaliana* (col-0) under aseptic conditions. Plants were cultured on Knops'-medium supplemented with test compounds at following concentrations (mM): DL-Met 0.2, L-Lys 0.001, MM, D-Lys, L-Thr, D-Thr, L-Trp, D-Trp, L-Hom, L-Ile, Ket each at 0.1. The number of male and female per root was counted at 12dpi. The indicated averages \pm standard errors were calculated on the means of \geq three biological replications with $n \geq 8$ plants. Asterisks (*, ***) refer to significant differences according to t-Test ($* = P \geq 0.05$; $*** = P \geq 0.001$).

The number of male and female nematodes per plant was significantly lower upon L-Thr, D-Trp, L-Ile, DL-Met and MM treatments of *A. thaliana*, cf. figure 22. Remarkably, all of these aa treatments decreased the number of females equally strong: -34% L-Thr, -34.6% by D-Trp, -36.2% L-Ile, -37.8% DL-Met and -40.9% MM. Additionally, the number of males was significantly reduced by -34.3% for D-Trp and -46.2% for MM treatments. Not significant but remarkably strong decreases of males were observed by -32.1% for L-Hom and -44.2% for L-Thr treatments.

5.2.3.4 Measurement of female and syncytium sizes

The reported decrease of adult nematodes might result from treatment induced functional problems in syncytium establishment and maintenance processes. To determine if the decreased numbers are paired with female and syncytium size reductions, measurements were conducted at 14 and 28dpi.

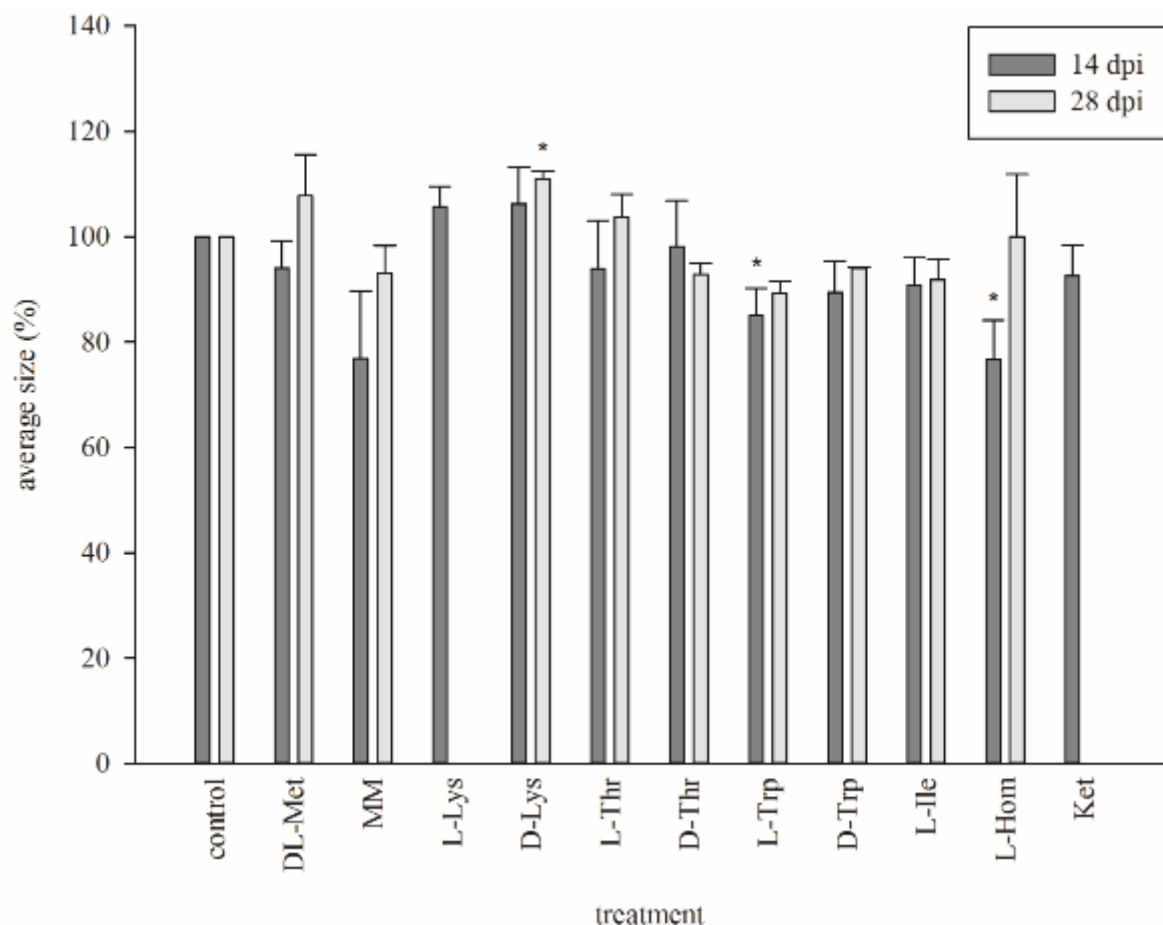


Figure 23 Aa treated *A. thaliana*: measurement of female sizes 60 s sterile *H. schachtii* J2s were inoculated per 10 days old *A. thaliana* (col-0) under aseptic conditions. Plants were cultured on Knops'-medium supplemented with compounds at following concentrations (mM): DL-Met 0.2, L-Lys 0.001, MM, D-Lys, L-Thr, D-Thr, L-Trp, D-Trp, L-Hom, L-Ile, Ket each at 0.1. Sizes were measured at 14 and 28dpi on *A. thaliana*. Indicated are relative averages \pm standard errors, calculated on the means of three biological replications. Asterisks (*) refer to significant differences according to t-Test ($P \geq 0.05$).

Significantly smaller sizes were observed upon treatments with L-Trp (-15%) and L-Hom (-23.3%) at 14dpi but not at 28dpi. In contrast to this, female sizes upon 0.1mM D-Lys treatments did not differ at 14dpi but were significantly bigger by +10.9% at 28dpi. Interestingly, this observation adds on to the described female development promoting

effects of Lys induced by 24h incubation treatments. According to the statistics, all other treatments did not affect the female sizes at 14 and 28dpi.

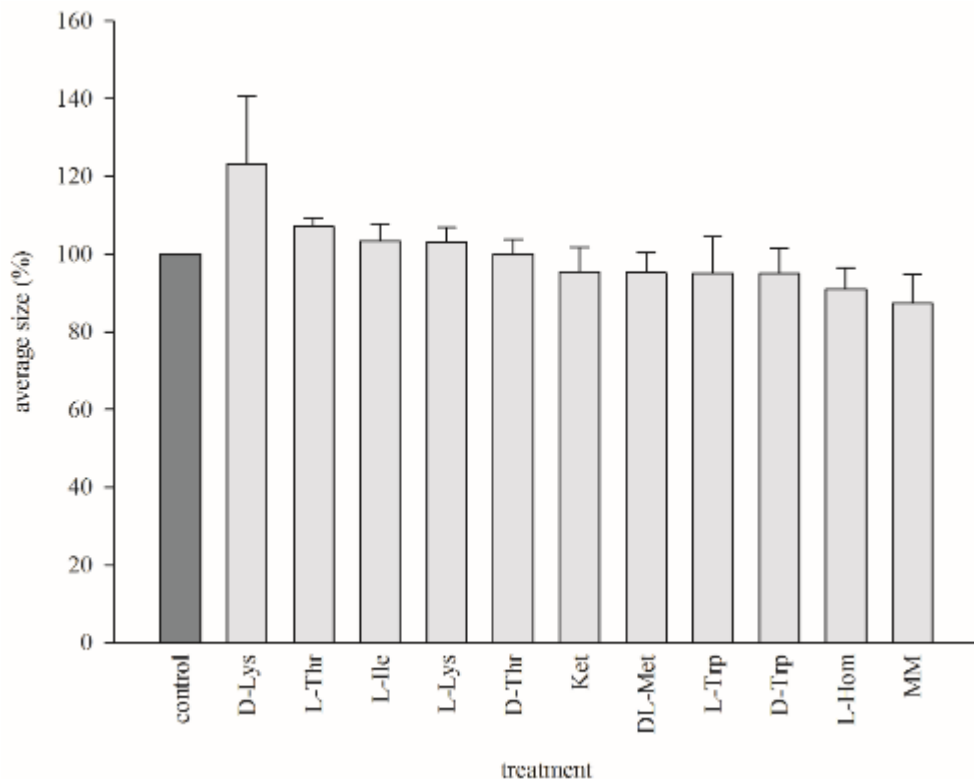


Figure 24 Aa treated *A. thaliana*: measurement of syncytium sizes 60 sterile *H. schachtti* J2s were inoculated per 10 days old *A. thaliana* (col-0) under aseptic conditions. Plants were cultured on Knops medium supplemented with test compounds at following concentrations (mM): DL-Met 0.2, L-Lys 0.001, MM, D-Lys, L-Thr, D-Thr, L-Trp, D-Trp, L-Hom, L-Ile, Ket each at 0.1. Syncytium sizes were measured at 14dpi. All indicated averages \pm standard errors were calculated on the means of three biological replications.

No treatment of *A. thaliana* affected the syncytium sizes in relation to the sizes measured in the untreated control plants at 14dpi.

5.2.3.5 Number of eggs per female

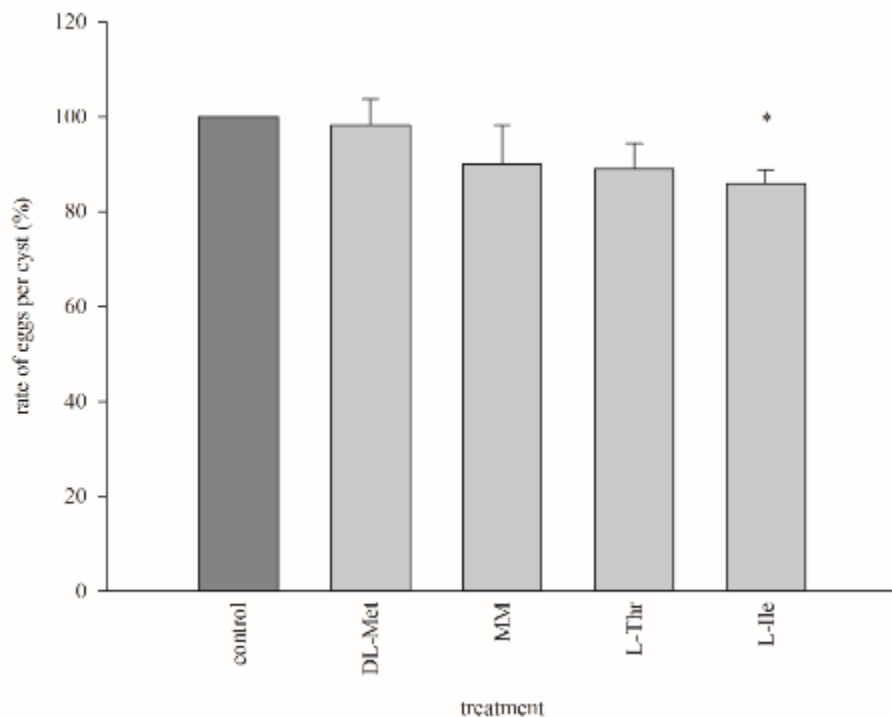


Figure 25 Aa treated *A. thaliana*: no. of eggs per cyst 60 sterile *H. schachtii* J2s were inoculated per 10 days old *A. thaliana* (col-0) under aseptic conditions. Plants were cultured on Knops'-medium supplemented with compounds at following concentrations (mM): DL-Met 0.2, MM, L-Thr, L-Ile 0.1. The number of eggs per female was counted for $n \geq 17$ per treatment per repetition at 35dpi. The indicated averages \pm standard error, were calculated on the means of three biological replications. The asterisk (*) refers to a significant difference according to t-Test ($P \geq 0.05$).

Only the treatments with 0.1mM L-Ile reduced the number of eggs per cyst significantly by -14.08% compared to the control. All other compounds did not influence this parameter.

5.2.3.6 Key conclusions from infection assays with treated *A. thaliana*

The most important finding was, that treating *A. thaliana* with L-Thr, L-Trp, D-Trp, L-Ile, DL-Met and MM decreased the rate of females per plant equally strong by approx. -37%. Except for D-Trp all of these effective aa are inherent and closely related metabolites of the so-called aspartate pathway. Even though effects on female sizes and egg numbers were detected they did correspond to the female reductions. The critical period was determined to

be between 2dpi and 12dpi. To narrow down the exact timepoint and critical event in this period, the invasion and development was assessed in detail on a daily basis between 1-14dpi.

5.2.4 Detailed infection and development analysis

The critical period between 2-12dpi involves key syncytia establishment and maintenance processes, nutrient uptake, growth and finally sex determination. To understand when and why a subgroup of individuals arrests in development, the nematode infection and development was monitored in detail. It was assumed that those individuals that do not develop into a male or female an individual might exit the infection site or alternatively arrest in development.

Table 16 Daily close up analysis of individual *H. schachtii* during infection and early development: 57 sterile J2s were inoculated per 10 days old *A. thaliana* (col-0). The plants were cultured on Knops'-medium supplemented with DL-Met, L-Ile and L-Thr under aseptic conditions. Juveniles were monitored between 1-14dpi to assess if they were arrested in development, left the infection site or successfully developed into adult males or females. For the categories “developmental stop”, “exit infection site”, “male”, “female” and “undetectable” the total numbers of nematodes summed up from all three biological repetitions is indicated. For the categories “dpi dev. stop” and “dpi exit infection site”, averages were calculated on the means of three biological replications. n=19 nematodes were monitored per repetition and treatment.

treatment	concentration (mM)	developmental stop	dpi dev. stop	exit infec- tion site	dpi exit infec- tion site	male	female	undetect- able
control	-	12	3.3	8	1.4	16	16	5
DL-Met	0.2	12	3.3	12	1.5	11	14	8
L-Ile	0.1	11	4.4	7	1.3	11	20	8
L-Thr	0.1	14	3.0	8	1.3	15	14	6

As apparent from table 16, no treatment increased or decreased the number of individuals that arrested in development (“development stop”) or left the infection site (“exit infection site”). Upon DL-Met and L-Thr treatments and in the control consistently 11-14 out of 57 nematodes arrested in development between 3-4dpi. Only L-Ile treatments delayed the event of “developmental stop” by 1 day to 4.4dpi. In average 8 individuals left the infection site between 1-2dpi, except for DL-Met treatments. Slightly more females developed on 10mM L-Ile treated plants than in control, L-Ile and DL-Met treated batches.

None of the assessed parameters could be doubtlessly identified as the decisive event behind the decreased number of females per plant. Likewise, the results do not disprove that the effect may be caused by a developmental arrest at a certain stage or that individuals simply

leave their infection sites. It cannot be excluded that such events occurred, but couldn't be captured due to inevitable limitations of the experimental procedure, see also discussion in chapter 6.2.3.

5.2.5 Gene expression analysis by NEMATIC

All effective aa, namely L-Thr, L-Trp, L-Ile, DL-Met and MM, are closely related metabolites of the so-called aspartate pathway, see figure 13 and 26. Possibly *H. schachtii* regulates the aspartate pathway in the syncytium tissue according to the nutritional stage specific need by secretion of effector proteins through their stylet. One explanation could be that successfully establishing a certain regulation is crucial for the nematode to facilitate its parasitism. This assumption was approached by studying the *H. schachtii* syncytium specific gene expression of a selected set of marker genes compared to uninfected root tissue. For this purpose, the NEMATIC spreadsheet was used, a database that comprises published data of transcriptomic studies on *H. schachtii* in *A. thaliana* roots.

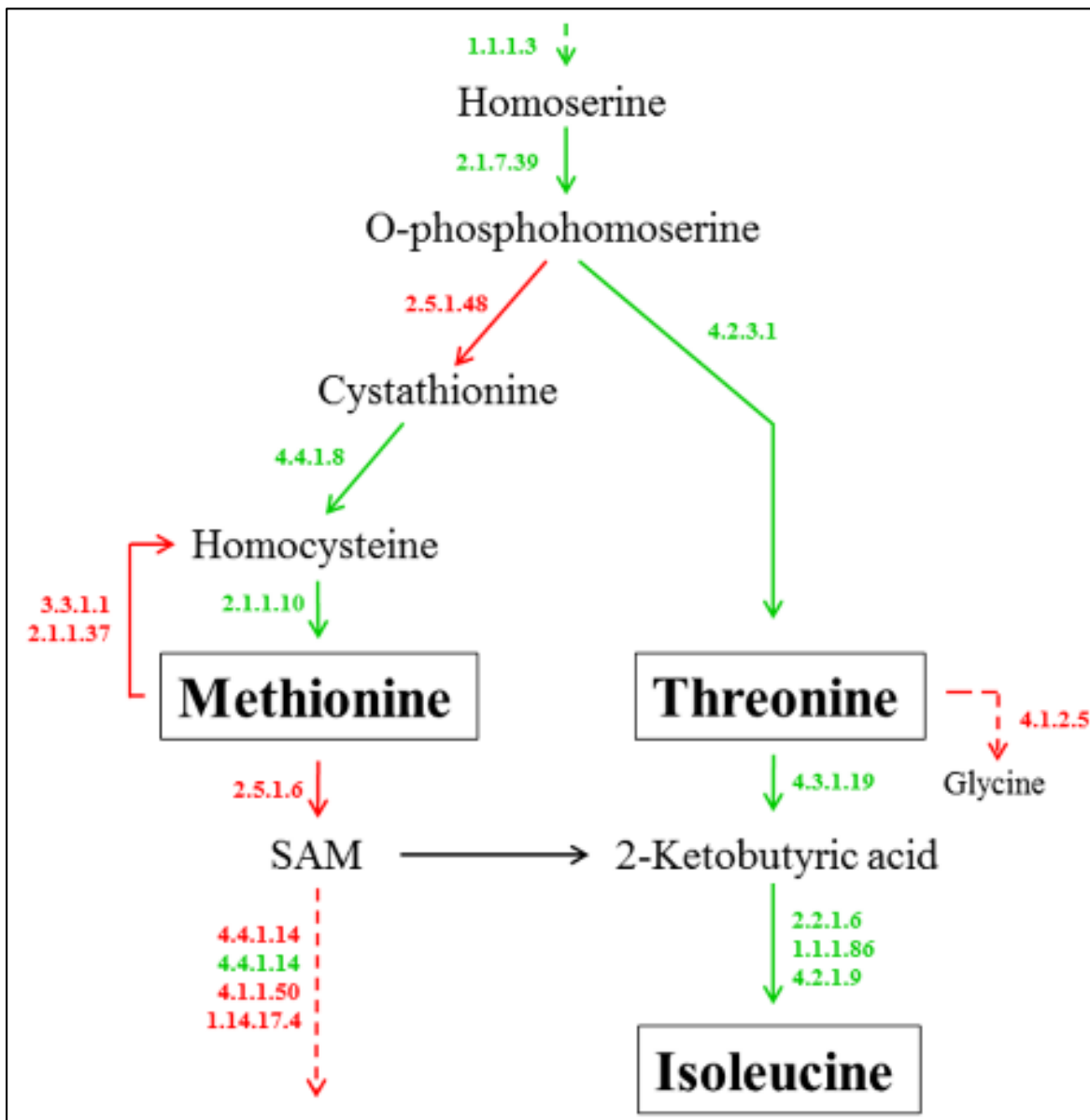


Figure 26 NEMATIC analysis: syncytia specific aspartate pathway marker gene expression Differential expression of aspartate marker genes in *H. schachtii* syncytia tissue in *A. thaliana* roots at 5 and 15dpi. Indicated are gene family ECs with down regulated expression in red and up regulated expression in green, compared to control root segments. Gene specific accession numbers together with exact fold change values are listed in table 17 in detail. The presented data was derived from the NEMATIC database.

Table 17 Differential expressions of aspartate family pathway genes in *H. schachtii* syncytia at 5 & 15 dpi in *A. thaliana* roots in comparison to control root segments, as extracted from NEMATIC.

metabolite	process	gene (family)	EC	accession no.	fold change
Hom	synthesis	homoserine kinase	2.1.7.39	AT2G17265	2.2
		homoserine dehydrogenase	1.1.1.3	AT1G31230 AT4G19710	3.7 4.5
	synthesis	cystathione gamma-synthase	2.5.1.48	AT1G33320	-3.1
Met	synthesis	cystathione beta-lyase	4.4.1.8	AT3G57050	1.3
		homocysteine S-methyltransferase	2.1.1.10	AT3G63250	2.3
		S-adenosylmethionine synthetase	2.5.1.6	AT1G02500 AT4G01850 AT2G36880	-3.1 -1.3 -2.6
	degradation	adenosyl homocysteinase	3.3.1.1	AT4G13940	-2.4
		1-amino cyclopropane-1-carboxylate synthase	4.4.1.14	AT4G08040 AT4G26200	-1 1.2
		S-adenosylmethionine decarboxylase	4.1.1.50	AT3G02470 AT3G25570	-0.6 -1.4
		DNA (cytosine-5)-methyltransferase	2.1.1.37	AT3G05430	0.5
		1-amino cyclopropane-1-carboxylate oxidase	1.14.17.4	AT1G05010 AT1G62380 AT2G19590	-4 -3.3 -2.4
		threonine synthase	4.2.3.1	AT4G29840	3.1
	degradation	threonine aldolase	4.1.2.5	AT3G04520	-1.7
		threonine dehydratase	4.3.1.19	AT3G10050	2.9
		acetolactate synthase	2.2.1.6	AT3G48560 AT5G16290	2.3 2.6
		ketol-acid reductase	1.1.1.86	AT3G58610	2.2
		dihydroxy-acid dehydratase	4.2.1.9	AT3G23940	4
		threonine dehydratase	4.3.1.19	AT3G10050	2.9
Ile	synthesis	acetolactate synthase	2.2.1.6	AT3G48560 AT5G16290	2.3 2.6
		ketol-acid reductase	1.1.1.86	AT3G58610	2.2
		dihydroxy-acid dehydratase	4.2.1.9	AT3G23940	4

This gene expression pattern reveals the *H. schachtii* syncytium tissue specific regulation compared to control root tissue segments of *A. thaliana*. The strongest fold change increases were identified by +4.5 x for AT4G19710, +4 x AT3G23940 and +4 x AT3G23940. The strongest down regulations appeared with -3.3 x for AT1G62380, -3.1 x AT1G33320 and -3.1 x AT1G02500. The expression of another 30 genes was unchanged, cf. 8.2.2.6.

A distinct pattern clearly became apparent, as schematically outlined in figure 26. The transcription of all enzymes located upstream of OPH, the last common precursor substrate

of Thr, Met and Ile, is increased. Additionally, the expression of all Thr→Ile pathway branch enzymes is upregulated. In contrast to this, the transcription of crucial bottleneck enzymes of the Cystathionine→Met→ Sam pathway branch were downregulated. In particular the expression of the first enzyme unique to the Met pathway, CGS (AT1G33320), is lowered by -3.1-fold, possibly reducing the substrate intake. Additionally, the expression fold change of all Met salvage cycle and subsequent degradation steps related enzymes is reduced, except for AT4G26200. Only AT3G57050 and AT3G63250 were found to be upregulated in the Met branch.

5.2.6 qRT-PCR

The NEMATIC analysis revealed that cyst nematodes regulate the aspartate pathway gene expression in syncytium associated tissue. This might be crucial for the parasitism process. Treating host plants with exogenous aa, that are likewise native metabolites of the plant, might modify the overall aspartate pathway regulation in the root and as a consequence in the embedded *H. schachtii* feeding sites. To study if and how exogenous DL-Met, MM and L-Thr applications affect the gene expression of aspartate pathway enzymes, qRT-PCR gene expression studies were conducted on nematode infected and uninfected *A. thaliana* root samples. All marker gens listed in table 10 were included, covering all enzyme families of the Thr, Met and Ile pathways.

First of all, the gene expression in MM, DL-Met and L-Thr treated but uninfected *A. thaliana* roots was analyzed. Subsequently, the expression was also measured MM, DL-Met and L-Thr treated and additionally *H. schachtii* J2 infected *A. thaliana* root samples. For this purpose, RNA was extracted from the plant roots, purified and quality checked before it was transcribed into cDNA. Finally, the specificity and efficiency of the generated aspartate family marker gene set was tested and confirmed.

5.2.6.1 RNA integrity, quantity and purification examination

RNA was extracted from *A. thaliana* roots grown on Knop's-medium supplemented with 0.1mM MM, 0.1mM L-Thr, and 0.2mM DL-Met respectively. To guarantee the appropriate

quality of all samples, the RNA integrity, quantity and purification was confirmed by Bioanalyzer and PCR in combination with gel electrophoresis.

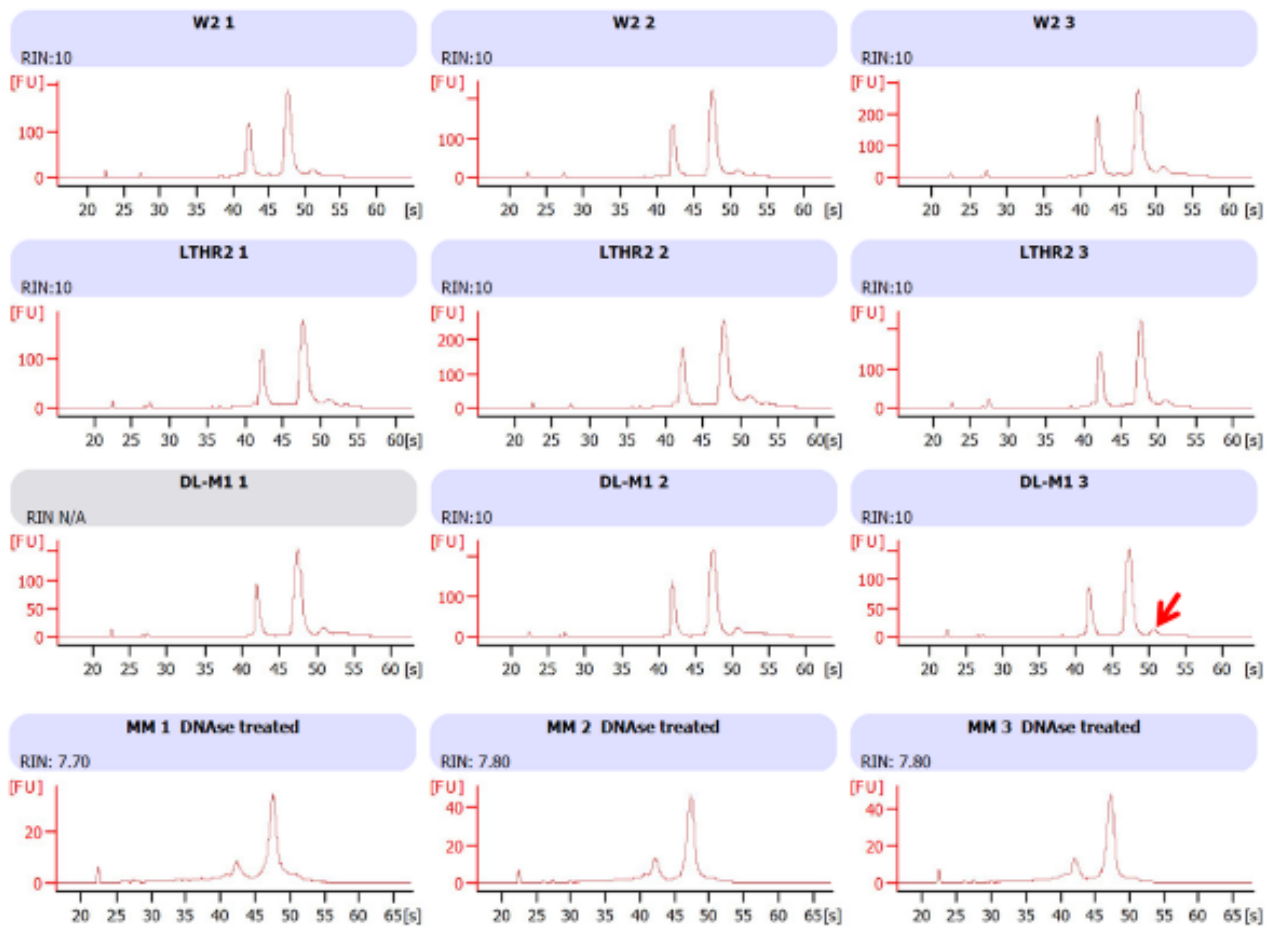


Figure 27 RNA integrity, quantity and purification test RNA integrity, quantity and DNA clean up analysis by Bioanalyzer. RNA was extracted from not nematode infected *A. thaliana* (col-0) roots cultured under aseptic conditions on Knops'-medium supplemented with 0.1mM L-Thr (LTHR), 0.2mM DL-Met (DL-M), 0.1mM MM (MM) or no compound (W=control). The arrow exemplarily indicates a low putative genomic DNA contamination.

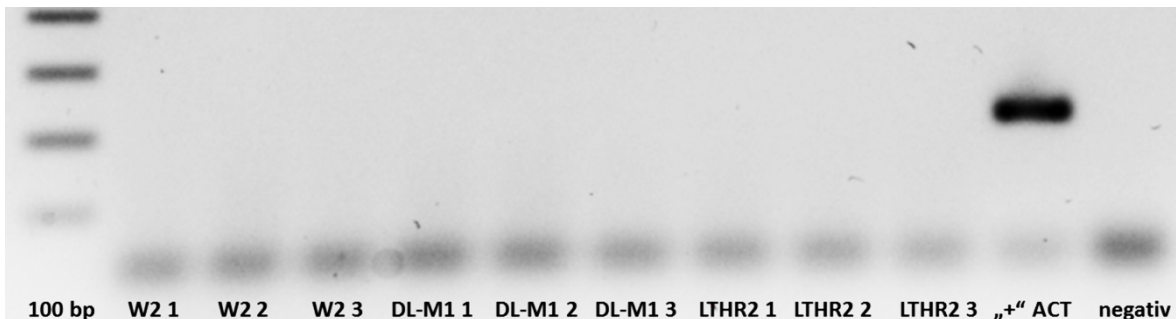


Figure 28 DNA digestion confirmation in RNA samples 1/3 by completeness check on genomic DNA cleanup by RQ1 RNase-free DNase in RNA samples from treated roots. RNA was extracted from *A. thaliana* (Col-0) roots cultured under aseptic conditions on Knops'-medium supplemented with 0.1mM L-Thr (LTHR), 0.2mM DL-Met (DL-M1) and untreated (W) *A. thaliana* roots without of nematode infections. Samples were taken at 10dps. PCR was set to 35 cycles using Actin primers ("+" ACT) on all probes followed by gel electrophoresis.

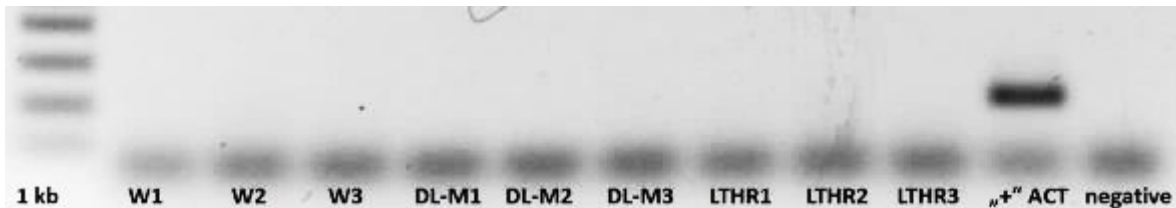


Figure 29 DNA digestion confirmation in RNA samples 2/3 RNA was extracted from *H. schachtii* infected *A. thaliana* (Col-0) roots cultured under aseptic conditions on Knops'-medium supplemented with 0.1mM L-Thr (LTHR), 0.2mM DL-Met (DL-M1) and untreated (W) *A. thaliana* roots at 3dpi. Roots were infected with 60 *H. schachtii* per plant at 10dps. PCR was set to 35 cycles using Actin primers ("+" ACT) on all probes followed by gel electrophoresis.

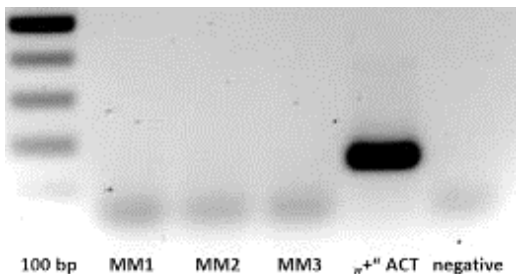


Figure 30 DNA digestion confirmation in RNA samples 3/3 RNA was extracted from *A. thaliana* (Col-0) roots cultured under aseptic conditions on Knops'-medium supplemented with 0.1mM MM and untreated (W) *A. thaliana* roots at 3dpi. Roots were infected with 60 *H. schachtii* per plant at 10dps. PCR was set to 35 cycles using Actin primers ("+" ACT) on all probes followed by Gel electrophoresis.

According to figure 27, the RIN value of 10 proofs, that all RNAs extracted from L-Thr, DL-Met and control roots had an excellent integrity level. Reduced but still sufficiently high RIN values between 7.7 to 7.8 were obtained for the MM RNA probe set. Given that the

curve of DLM1 1 matches to the one of DLM1 3 it can be assumed that the quality is also corresponding. Minor undigested genomic DNA remains were detected between 50-51 seconds for all DL-M, L-Thr and the control RNAs. As confirmed by PCR no amplification on genomic DNA remains were detected in any RNA probe. The positive control generated a single 250bp amplicon. No amplification occurred in the negative control cf. figure 28, 29, 30. Summarized all 24 individual DNA removal treatments provided a sufficient to optimal RNA integrity level and grade of DNA digestion.

5.2.6.2 Primer specificity

It was demonstrated in this experiment, that all marker gene primers amplify on plant DNA but not on nematode cDNA, Fig. 31 and 32. For this purpose, a first set of PCRs was conducted by using cDNA generated from *H. schachtii* infected *A. thaliana* root samples. Afterwards, a second series with pure *H. schachtii* cDNA was generated. A functional specific primer should amplify on plant, but not on nematode cDNA.

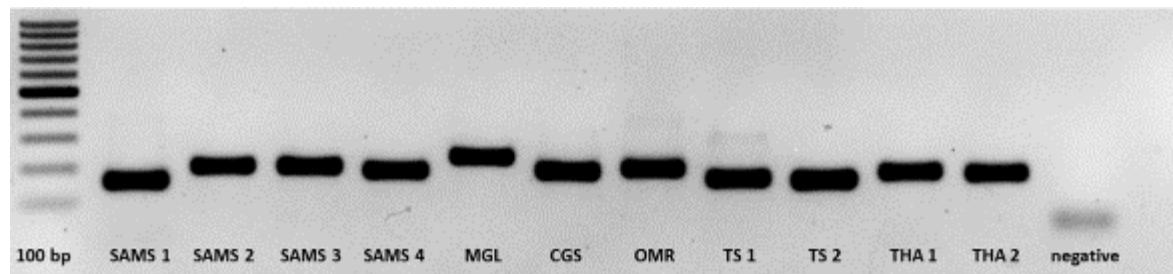


Figure 31 PCR on *H. schachtii* infected *A. thaliana* cDNA Gel electrophoresis picture of the PCR based primer specificity test of the qRT-PCR primer set using *H. schachtii* infected *A. thaliana* (col-0) cDNA. All sampled roots were infected with 60 *H. schachtii* per plant.

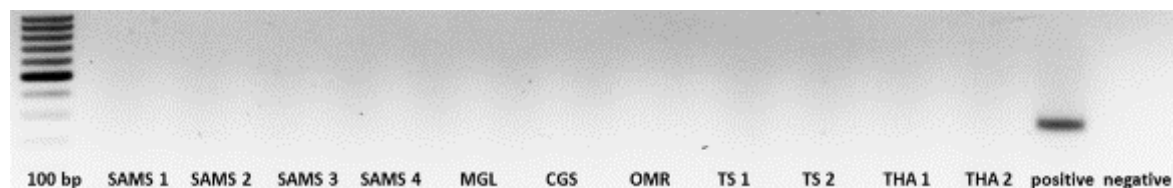


Figure 32 PCR on *H. schachtii* cDNA Gel electrophoresis picture of the PCR based primer specificity test of *A. thaliana* marker gene using *H. schachtii* col-0 cDNA.

All aspartate family marker gene primers generated strong specific single amplifications when used on infected *A. thaliana* cDNA, cf. figure 31. Neglectable minor amplifications were only detected for TS 1 at ~250bp and additionally at ~300bp length for OMR. Artifacts

were not visible for any other marker. Finally, the negative control clearly confirms the reaction's integrity.

In a second step it was demonstrated, that the primer set is specific for *A. thaliana* as no amplification was generated when used on *H. schachtii* cDNA, cf. figure 32. Moreover, the positive control demonstrates the integrity of the reagents, and the negative control the absence of contaminations.

5.2.6.3 Gene expression analysis in uninfected *A. thaliana* roots

The quantitative real time polymerase chain reaction (qRT-PCR) was used to analyze the expression of aspartate family synthesis and degradation marker genes in *A. thaliana* root samples for two scenarios, 1) uninfected roots and 2) *H. schachtii* infected roots. Comparing the gene expression profile in DL-Met, MM and L-Thr treated with control roots samples in the absence of nematodes allowed to study the general response upon treatment with those compounds.

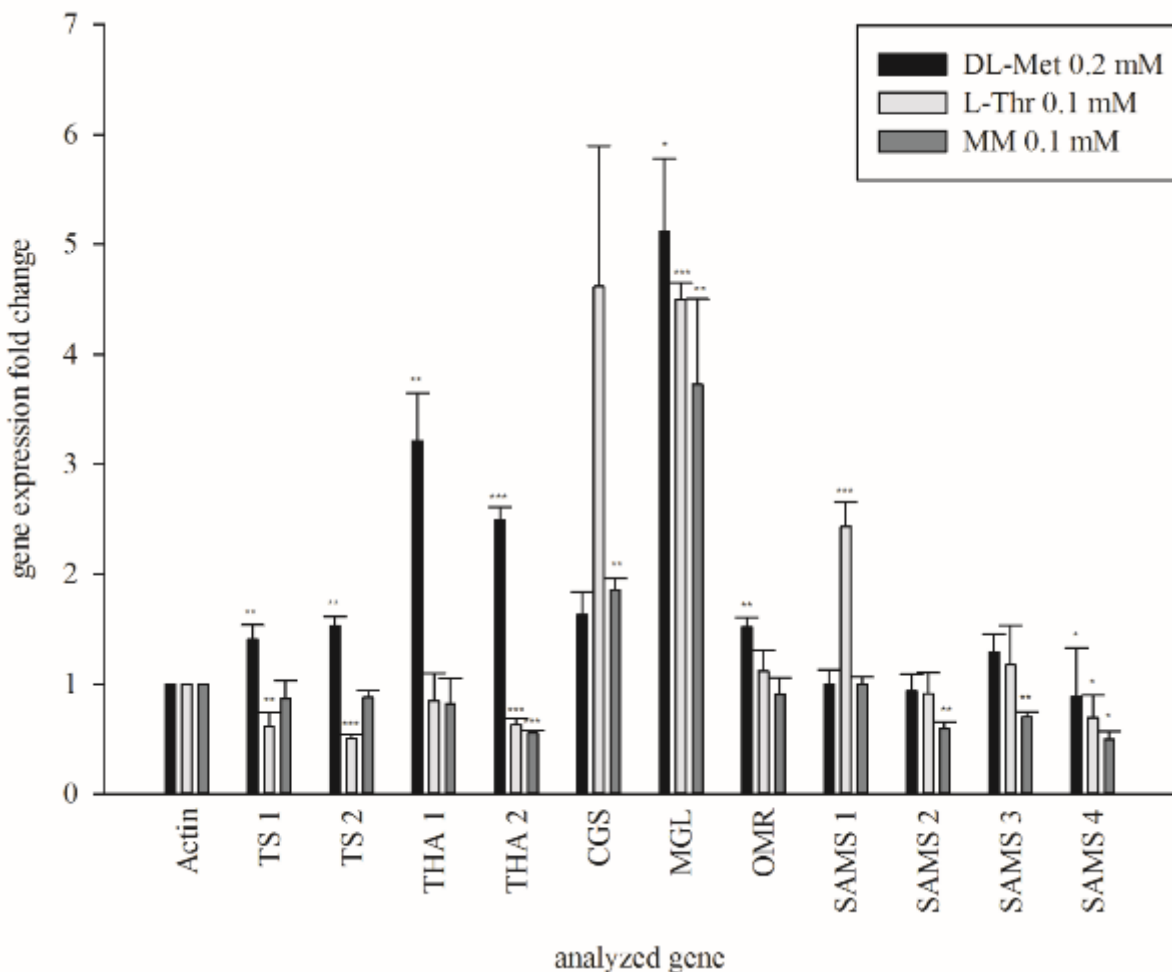


Figure 33 qRT-PCR: Gene expression in aa treated uninfected *A. thaliana* roots Gene expression analysis by qRT-PCR on aspartate family pathway genes in aa treated *A. thaliana* (Col-0) roots. Roots were sampled at 10dps from plants cultured on Knops'-medium supplemented with DL-Met, MM and L-Thr grown under aseptic conditions. Indicated are expression fold changes with standard error bars, both calculated on the average CT mean value triplet of three biological replications taking in account the determined primer efficiencies. Fold changes were calculated in relation to Actin. Asterisks refer to significant differences according to t-Test using the ΔC_t values ($*=\text{P}\geq 0.05$; $**=\text{P}\geq 0.01$; $***=\text{P}\geq 0.001$).

Supplementing the Knops'-medium of uninfected *A. thaliana* with DL-M, MM and L-Thr changed the expression pattern of the selected set of marker genes as follows:

treatments with 0.1mM L-Thr increased the gene expression fold change significantly to 4.5 x for MGL and 2.4 x for SAMS 1. Contrary to this, the expression was significantly decreased to 0.6 x for TS 1, 0.5 x TS 2, 0.6 x THA 2 and 0.7 x SAMS 4. Upon 0.2mM DL-Met treatments it was determined 1.4 x for TS 1, 1.5 x TS 2, 3.2 x THA 1, 2.5 x THA 2, 5.1 x MGL and 1.5 x OMR. Exclusively the expression of SAMS 4 was reduced to 0.9 x. Finally, 0.1 MM treatments significantly increased the expression to 1.9 x for CGS and 3.7 x for MGL, whereas the expression was decreased to 0.6 x for THA 2, 0.6 x SAMS 2, 0.7 x SAMS

3 and 0.5 x SAMS 4. Remarkably, only MGL was consistently and remarkably strong overexpressed in response to DL-Met, MM and L-Thr.

5.2.6.4 Gene expression analysis in *H. schachtii* infected *A. thaliana* roots

In this experiment, the gene expression in DL-Met, MM and L-Thr treated *A. thaliana* roots infected with *H. schachtii* was examined. Comparing the different gene expression profiles of a) *A. thaliana* roots infected with *H. schachtii* and b) uninfected *A. thaliana* roots reveals how the global aspartate pathway regulation in aa treated roots changes upon infection with *H. schachtii*.

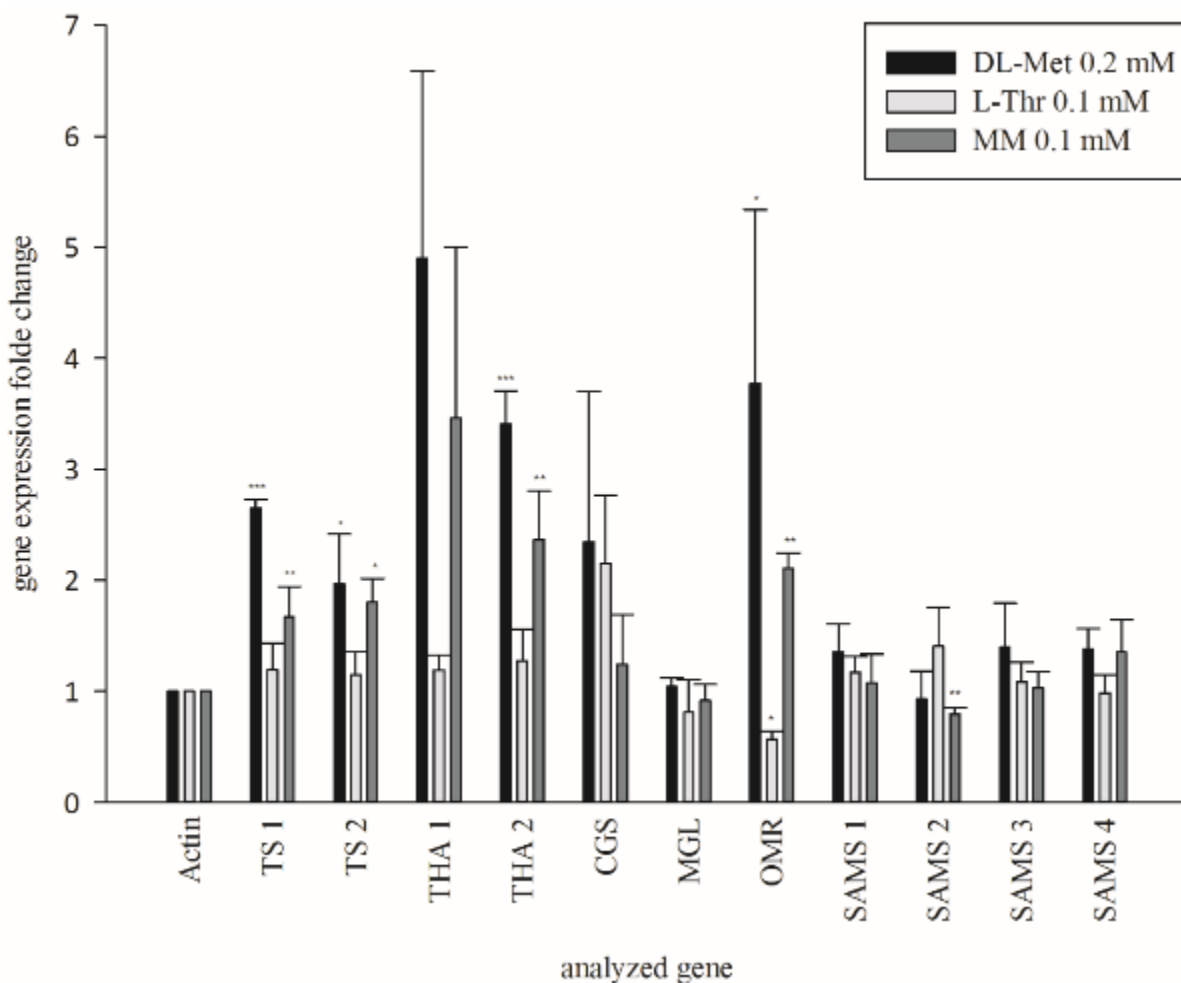


Figure 34 qRT-PCR: Gene expression in aa treated infected *A. thaliana* roots Gene expression analysis by qRT-PCR, studying the regulation of aspartate family pathway gens in *H. schachtii* infected and aa treated *A. thaliana* roots. Roots were sampled at 3dpi from plants cultured on Knops'-mediums supplemented with DL-Met, MM and L-Thr grown under aseptic conditions. Indicated are expression fold changes with standard error bars, both calculated on the average CT mean value triplet of three biological replications taking in account the determined primer efficiencies. Fold changes were calculated in relation to Actin. Asterisks refer to significant differences according to t-Test using the ΔCt values ($^*=P\geq 0.05$; $^{**}=P\geq 0.01$; $^{***}=P\geq 0.001$).

The expression of aspartate family marker genes in *H. schachtii* infected *A. thaliana* roots treated with L-THR, MM and DL-Met is given in figure 34. Treatments with 0.1mM L-Thr treatments decreased the gene expression only for OMR to 0.6 x. Supplementing 0.2mM DL-Met to the medium increased the gene expressions by 2.6 x. for TS 1, 2 x TS 2, 3.4 x THA 2, and 3.8 x OMR. Comparable effects were detected in response to 0.1mM MM treatments. Herein, the expression increased by 1.7 x for TS 1, 1.8 x TS 2, 2.4 x THA 2, 2.1 x OMR and was reduced by 0.8 x for SAMS 2. It has to be highlighted that no aa treatment altered the expression level of MGL in those aa treated *A. thaliana* roots that were additionally infected with *H. schachtii* in contrast to the consistent upregulation observed in uninfected roots, compare figure 33 and 34.

6 DISCUSSION

Plant-parasitic nematodes are major yield reducing pathogens, damaging above and below ground plant organs of all relevant agricultural crops worldwide. For instance, the annual economic losses in the North American soy production induced by *Heterodera* sp. were estimated to exceed 1 billion \$ (Koenning and Wrather, 2010). Indeed, the importance of cyst forming nematode species for instance in soy, potato, small grain and sugar beet production is tremendous and continuously increasing with expanding production areas.

The combination of high multiplication rates with long retention times in soil makes plant-parasitic nematode populations extremely competitive to withstand biotic and abiotic stresses. A single root maybe invaded by numerous individuals leaving open wound that function as entrance gates for secondary fungal and bacterial infections. Subsequent inner root migration of the invaded nematodes may induce additional tissue damage. Finally, the feeding sites are established by fusing of adjacent root cells. This impairs or even blocks the transport of water and nutrients through the central cylinder. Nematode infested and damaged plants are less competitive to withstand biotic and abiotic stresses, especially under draught conditions on light sandy soils. Ultimately, high nematode pressure can result in growth depression, plant losses and ultimately heavy yield drags.

Various chemical substances, biological agents and nematode tolerant/resistant varieties are used to prevent nematode induced yield losses. However, none of the available nematode control tools offers 100% reliable and efficient protection against all relevant nematode species in all crops over the whole cropping season. Additionally, extensively used traits slowly decrease in efficacy as recently described for *H. glycines* resistant PI88788 soy varieties (McCarville *et al.*, 2017). All in all, the overall control remains insufficient and is in need of improvement (Chitwood, 2003). Additional efficient tools, at best with new modes of action, are required. This demand might be addressed by different aa that were already described to induce diverse harmful effects on the different plant-parasitic nematode species. The most promising aa candidates were selected based on a literature review and tested in *in vitro* experiments for nematicidal effects as induced by their exogenous application.

The studies demonstrated that the aa D-Lys, L-Lys, L-Thr, L-Ile, D-Trp, DL-Met, Ket and MM treatments induced effects on *C. elegans* and *H. schachtii* under *in vitro* and *in vivo*

conditions. Those effects affected the sex ratio, rate of adult nematodes per plant, activity, reproduction and female sizes.

A first set of incubation experiments aimed at identifying effects resulting from direct cuticle-compound contact on *C. elegans* and *H. schachtii*. In this, nematode activity, development and parasitism related parameters were evaluated.

In the second set of experiments, the model host plant *A. thaliana* was grown on Knops'-medium supplemented with test compounds and infected with untreated *H. schachtii*. The objective was to reveal and describe those effects, that require the involvement of the host plant. An equally strong reduction of female nematodes per root was observed on L-Thr, DL-Met, MM, L-Ile and Ket treated *A. thaliana* roots. Afterwards, the underlying mechanisms were studied in detail by *in silico*, microscopic and molecular techniques.

6.1 Effects induced by direct contact

6.1.1 Implications of the nematode biology for compound exposures

An active ingredient may interact with substances in or on the nematode cuticle or alternatively after active uptake or passive diffusion into the nematode. To clearly differentiate between those causal mechanisms, at first those effects that result from compound-cuticle contact without uptake into the nematode were examined. This was done for *C. elegans* and *H. schachtii*. Subsequently, those effects resulting from compound-cuticle contact with simultaneous compound uptake (only for *C. elegans*) were studied.

The nematode species dependent divergent feeding styles build the base for in detail evaluations: Whereas *C. elegans* swallow bacteria from solution through the mouth opening, *H. schachtii* must invade roots and establish a syncytium before they take up cells sap through their stylet. It is currently the common assumption, that *H. schachtii* does not actively take up solution outside of the plant roots. Accordingly, they are not able to take up dissolved test compounds during incubation experiments and as a consequence only the cuticle can get in contact with it. In contrast, adding a bacterial food source to the incubation solution triggers *C. elegans* to swallow liquid through the mouth opening. This allows to screen for those effects that require the preliminary uptake into the digestive system.

6.1.2 Effects on the activity of *C. elegans* and *H. schachtii*

Impairing effects that arise exclusively from the direct cuticle-compound contact were assessed in the first experiment. This explicitly excludes the active uptake into the nematode by swallowing. A general loss of activity was observed throughout the experiment: For all treatments and the control in average 38% of the *H. schachtii* J2s were inactive after 72h. Considering that the nematodes were exposed to ZnCl₂ over seven days in the glass funnel system, followed by another week of incubation in 24 well plastic plates, a loss of 38% appears as an inevitable natural mortality rate under adverse artificial conditions.

Whereas the metabolically relevant L-Trp isomer reduced the activity of *C. elegans* significantly at 10mM, the metabolically unsuitable D-Trp did not. This suggests a direct functional involvement of the exogenously applied L-Trp on the nematode metabolism induced by cuticle contact. Despite L-Trp was harmful for *C. elegans*, no effect was observed on *H. schachtii* over seven days of exposure. Ket was the only treatment that reduced the activity of *H. schachtii* significantly in comparison to the H₂O treated control. Ket was added to the set of testing substances at an advanced late stage of the project, it was decided to skip an additional testing against *C. elegans* in order to focus primarily on examining the aspartate pathway related effects discussed later on.

The observation that Met did not affect *H. schachtii* corresponds to the published results of *G. rostochiensis* incubation experiments: nematodes were treated with 100mM Met for 24h at a 5-fold higher concentration than tested in this study, not inducing any harmful effects (Evans and Trudgill, 1971). The underlying mechanisms of the Ket and L-Trp induced treatments remain unknown and should be determined in follow-up studies.

All test compounds were applied close to their maximum dissolubility in order to emphasize the significance of effects. Summarized, only high rates of L-Trp and Ket induced effects on the activity by cuticle contact. All compounds of relevance for later experiments, namely L-Thr, DL-Met, MM and L-Ile, did not generate any measurable or visible effects. Accordingly, those effects on *H. schachtii* that were observed in later experiments did not result from direct compound-cuticle contact, except for Ket and L-Trp.

6.1.3 Effects on the development of *C. elegans*

To examine effects on the development of *C. elegans* the uptake of the test compounds into the digestive system was provoked by adding the bacterial food source *E. coli* into the incubation solution. Herein, D-Lys, L-Lys and L-Trp induced impairing effects.

At 10mM L-Trp arrested the development and additionally reduced the activity. At a 10-fold dilution the development continued, but was delayed by 1 day, compared to the control. At a 100-fold dilution no effects were detected. Even though the studies are of limited comparability, it should be mentioned that the observations do not correspond to the reported finding that *C. elegans* selectively avoids D-Trp \geq 0.1mM (Dusenbery, 1975). In this experiment juveniles were kept in 24 well plates and would have only been able to avoid the incubation exposure by leaving the well onto the dry plastic plate. This event was not observed at any time. Even though both studies indicate that L-Trp is harmful for the bacterivore nematode *C. elegans*, the results prove that it is harmless for the plant-parasitic nematode *H. schachtii*.

Whereas the sole cuticle contact with both Lys isomers was harmless, the additional oral uptake consistently arrested the development of *C. elegans*. Accordingly, the uptake into the nematode body is crucial to induced effects. Even though the development was arrested, all treated juveniles remained active and might have entered the so called “dauer stage”, an alternative intermediate live stage of developmental arrest. It enables *C. elegans* to endure unfavorable environmental conditions (Cassada and Russell, 1975).

Lys is an essential aa for the closely related nematode species *Caenorhabditis briggsae* and also for vertebrates in general (Balasubramanian and Myers, 1971; Vanfleteren, 1973). For this reason, it is possible but rather unlikely that the uptake of Lys would be harmful for nematodes. It might well be, the observed effects at 10mM might result from extreme overdosing, especially as *C. elegans* was indifferent to 1mM and 0.1mM L-Lys and D-Lys.

D-Lys, L-Lys and L-Trp did not induce corresponding effects when tested on *H. schachtii* in experiments that involved active feeding, as described later. For this reason, it was concluded, that the described effects of L-Trp, D-Lys and L-Lys are nematode species dependent. Indeed, such species dependency of effects induced by exogenous aa treatments is well reported in literature (Overman and Woltz, 1962; Prasad and Webster, 1967; Talavera and Mizukubo, 2005). For instance, DL-Met reduced the activity of *M. incognita* Chitwood

juveniles, but not the activity of *G. rostochiensis* juveniles within 24h (Talavera and Mizukubo, 2005).

6.1.4 Effects on the parasitism of *H. schachtii*

To assess for cuticle-compound contact induced effects on the subsequent parasitism process of *H. schachtii* in plant roots, 24h incubation experiments were combined with detailed infection assays. In this, J2s were initially incubated in treatment solutions for 24h. Afterwards, all treated juveniles were thoroughly washed in order to remove remaining active ingredient from the cuticle. Finally, the treated and cleaned nematode batches were used to infect the roots of untreated *A. thaliana*. Whereas host plants did not get into contact with test compounds, the nematodes were exposed to them during incubation but not during infection and parasitism. Accordingly, all detected effects can only result from the compound-cuticle contact without of uptake into the nematode's body over a period of 24h. Effects occurred in response to 10mM D-Lys, 10mM L-Lys and additionally to 10mM D-Trp treatments, as described below.

Both Lys isomers consistently changed the sex ratio in favor of female development. The relative average increase of females per root corresponded in its magnitude to the relative decrease of males. In this, the average total number of nematodes per root was unchanged compared to the control. It was reported earlier, that 5mg DL-Tyrosine per plant clearly promoted the development of *G. rostochiensis* males (Trudgill, 1974). Repeating the experiment in the absence of ZnCl₂ and HgCl₂, added for hatching and sterilization, allowed to exclude a modifying impact of the two reagents, see figure 20.

Since the sex development of *H. schachtii* is not entirely understood, an unambiguous explanation for the L-Lys and D-Lys induced effects cannot be given. Even though more females per root were present, the female or syncytium sizes were unchanged. One hypothesis is, that the smell of the potentially essential aa Lys indicates a high-quality food source. This might “prime” the J2s prior to invasion for instance via increasing the effector protein synthesis. Primed J2s might have a more efficient infection process subsequently resulting in an improved nutritional situation. It is the current assumption that a beneficial nutritional situation favors the development of females over males (Grundler, 1989; Grundler *et al.*, 1991).

Lys is essential for *Caenorhabditis briggsae* and *Aphelenchoides* sp. (Balasubramanian and Myers, 1971; Vanfleteren, 1973) and this might also apply to *H. schachtii*. It is not unlikely that J2s would take up essential Lys from solution even though a selective oral uptake outside of the plant root has not been observed for *H. schachtii* so far. Additional follow up experiments could be of interest in order to examine if Lys enters the nematode during incubation by active uptake or passive diffusion. One approach could be to radioactively label L-Lys and D-Lys or alternatively to use fluorescing dyes. Until now, effects on the sex ratio by exogenous application had only been reported for Tyr.

6.2 Effects on *H. schachtii* induced by treatments of the host plant *A. thaliana*

It had first been postulated in 1971 that Met needs to be preliminary taken up into the host plant before impairing effect on nematodes are induced (Evans and Trudgill, 1971). In fact, the results of the infection studies in aa treated *A. thaliana* roots fully correspond to this statement.

6.2.1 Effects induced by supplementing aa to Knops'-medium on *A. thaliana*

Supplementing aa to Knops'-medium allows the model host plant *A. thaliana* to take up the active ingredients from germination onwards. The uptake of aa from the medium into the roots and the following translocation towards the sink and source organs of the plant is facilitated by a complex aa transporter system (Liu and Bush, 2006; Tegeder and Rentsch 2010; Tegeder, 2012; Pratelli and Pilot, 2014; Tegeder, 2014). For the specific set of applied aa and under the experimental conditions chosen it had not been determined which quantities were imported, translocated and further metabolized by the plant. Follow-up experiments with isotopic labeled compounds are needed to clarify compound uptake and flux.

After passing the epidermis, aa may be transported within the roots or into above ground plant organs. Since all exogenously applied aa are also native metabolites of the plant, they might yield as substrates for their associated local and global metabolic processes, cf. 2.3.1. In fact, the qRT-PCR results revealed that MM, DL-Met and L-Thr treatments all induce gene expression changes of related enzymes of the aspartate pathway within *A. thaliana* roots, as discussed under 6.3.3.

6.2.2 Effects on the parasitism of *H. schachtii*

The strongest effects on *H. schachtii* were observed after supplementing the test compounds into the nutrient agar of *A. thaliana*. Even though the same number of nematodes initially invaded the root, the rate of females per root was equally strong reduced by approx. -37% at 12dpi upon L-Thr, D-Trp, DL-Met, L-Ile and MM treatments. In contrast, the number of males was only lowered in response to L-Trp and MM. Whereas L-Trp and L-Hom decreased the female sizes at 14dpi all reductions were compensated at 28dpi.

6.2.3 Detailed infection and development analysis

The results proof that the same number of nematodes successfully invaded DL-Met, MM, L-Ile, L-Thr treated and untreated roots at 2dpi. Accordingly, supplementing aa to the plant growth medium did not affect the ability to localize and invade the host roots. Even though the same number of *H. schachtii* invaded at 2dpi, the number of females per plant was consistently strong decreased at 12dpi upon L-Thr, D-Trp, DL-Met, L-Ile and MM treatments. Hence, the impairing event must occur between 2-12dpi. This very period involves major syncytia establishment processes, uptake of nutrients from the feeding site, progressive nematode development and sex determination (Sijmons *et al.*, 1991). Each of these parameters could be affected alone or in combinations. Only a minor fraction of invaded nematodes fails to develop whereas the majority continues. This suggests that not all individuals are affected equally and critically strong or that most individuals successfully overcome the impacting stress factor. Aiming to identify the crucial event between 2–12dpi, selected parameters infection and developmental processes were monitored daily. It was determined, that for all treatments the number of nematodes that left the infection site or arrested in development did not differ from the untreated control. A previous study showed that upon Met treated “supportive” *Brassica* varieties, the reduction of females was accompanied by an increased number of arrested J2 and J3 nematodes (Betka *et al.*, 1991). This observation did not match with the results of this work.

Even though none of the examined parameters was clearly correlated to the actual event behind the reduced female numbers, their involvement could also not be unambiguously excluded. This is the consequence of inevitable limitations of the selected experimental design: living and therefore moving nematodes were pictured daily, at 1-8, 10, 12 and 14dpi, on continuously growing roots. Living roots changed their orientation and may have overlapped during the experiment. Since all pictures were taken by microscope at a 90° angel

from above, only those nematodes could be pictured and afterwards measured which were laterally attached to the growing root with a horizontal body orientation. Since this applied only to very few nematodes per plates, the total number of 19 nematodes per repetition per treatment had to be combined from multiple plates. Nevertheless, if one distinct parameter or event between 2-12 dpi was selective, the experiment should have revealed it, despite of the above described limitations. In case of repeating this experiment, the fate of all invaded nematodes per plate should be analyzed in order to identify at what time and why the described approx. -37% female reduction takes place. Summarized, this experiment did not yield additional insights.

6.2.4 Effects on the quantitative and qualitative nutritional situation

As described in chapter 2.1.1 the quantitative and qualitative nutritional conditions within the syncytium may affect the sex determination, wherein a beneficial nutritional situation is supportive for the development of females (Grundler, 1989; Betka *et al.*, 1991; Grundler *et al.*, 1991). Aa treatments of host plants might impair the nutritional quality or quantity in the nematode feeding sites. In this regard, three key observations are meaningful:

- 1) every treatment that reduced the number of females per plant also showed slightly decreased female sizes at 14dpi (only significant for L-Hom and L-Trp). However, those size reductions were less pronounced at 28dpi.
- 2) syncytium sizes were not reduced.
- 3) only the number of females per plant was markedly reduced. In contrast to this, the number of males was overall unchanged.

A quantitative nutritional problem can be excluded since syncytium sizes were unchanged. Therefore, a qualitative deterioration within the feeding site should be considered. In fact, it had already been postulated before that rather the quality than the quantity of the aa pool might be decisive (Grundler *et al.*, 1991; Betka *et al.*, 1991). For instance, *Brassica rapa* varieties were manipulated in *in vitro* experiments, generating plants, which were supportive or impairing for female development. In this, impairing varieties had elevated Met, Lys, and Trp levels whereas supportive ones had increased glutamine levels (Betka *et al.*, 1991). The later on discussed qRT-PCR studies revealed significant gene expression changes of Met, Thr and Ile pathways related enzymes in response to aa treatments. It is possible that those regulatory changes might as a consequence change the aa levels in the host root and the

embedded syncytium to the disadvantage of female development. The NEMATIC analysis proved, that the individual Met, Thr and Ile pathway branches clearly show an overall up or respectively down regulated profile in syncytium tissue. For this reason, it was concluded that *H. schachtii* systematically manipulates aa synthesis related pathways in the syncytium according to its needs. This might be disturbed by treating the host plant. Aa treatments of host plants prior to nematode invasion might modify the gene expression of pathways that are important for parasitism. This might render it more difficult or even impossible for the invading nematode to induce the essential adaptations and generate a disadvantageous nutritional situation, impairing the development of females. Measurements of aa levels in roots and syncytia with and without aa treatments should be conducted to draw further conclusions.

6.3 Analysis with regard to the aspartate pathway

6.3.1 The involvement of the aspartate pathway

L-Thr, DL-Met, MM, L-Ile and Ket decreased the number of females per plant consistently strong by approximately approx. -37%. It is striking that these substances are all native metabolites within the aspartate pathway. They are closely interlinked by molecular pathway regulation mechanisms, as described in detail in the chapters 2.3.1 and 2.3.2. The finding, that closely related treatments consistently induce a comparable distinct negative effect on the female population is remarkable and points towards a functional involvement of this very metabolic region.

The gene expression and enzymatic activity within the global aspartate pathway is connected and tightly regulated by multiple feedback mechanisms, influencing the syntheses and degradation processes of each other (Amir, 2010; Amir *et al.*, 2002; Bartlem *et al.*, 2000; Chiba *et al.*, 2003; Joshi and Jander, 2009). Downstream of O-phosphohomoserine, the pathway splits into two main branches competing for one common substrate, cf. figure 13:

- 1) OPH → Thr → Ket → Ile
- 2) OPH → Met → Ket → Ile

Both branches are interconnected by one pathway that originates from the Met branch and channels into the synthesis of α-ketobutyrate, the first metabolite that is also a derivative of

Thr. Further downstream the derivatives of α -ketobutyrate feed into Ile synthesis (Joshi and Jander, 2009).

To further elaborate a possible functional involvement of these pathways, molecular and *in silico* in depth studies were conducted on this under three focus aspects:

- 1) The syncytium tissue specific gene expression of aspartate pathway associated genes was studied by mining the open source spreadsheet NEMATIC.
- 2) The expression of aspartate pathway genes in response to treatments of *A. thaliana* with DL-Met, MM and L-Thr was determined by qRT-PCR studies.
- 3) The expression of aspartate pathway genes in response to treatments of *A. thaliana* with DL-Met, MM and L-Thr and additional infection with *H. schachtii* were also investigated by qRT-PCR studies.

6.3.2 Regulation of the aspartate pathway in the syncytium

The expression analysis of aspartate family genes in *H. schachtii* syncytia at 5 and 15dpi was studied by mining the open source spreadsheet NEMATIC (Cabrera *et al.*, 2014; Szakasits *et al.*, 2009). Nematodes actively induce, establish, keep up and control the syncytium by secretion of effector proteins, *i.e.* highly specific small molecules that facilitate host colonization (Grundler *et al.*, 1998; Hogenhout *et al.*, 2009). To establish optimal conditions for their survival and reproduction, *H. schachtii* manipulates and optimizes the host cell metabolism in syncytium associated tissue according to its requirements. The results of this study proof that this also involves regulating the expression of aspartate pathway genes inside the feeding sites. Three differential regulative patterns of whole branches became clearly apparent, cf. figure 26:

- 1) at the pathway “entrance”, downstream of Aspartate semialdehyde and upstream of O-Phosphohomoserine, the expression of both enzyme families catalyzing the synthesis of L-Hom and OPH was upregulated. This might increase the substrate influx towards OPH, the unique precursor metabolite of Thr and Met. Downstream of OPH the Met and Thr branches separate and their overall gene expression was inversely regulated.
- 2) the expression rate of all OPH \rightarrow Thr \rightarrow Ile branch specific gene families were up regulated or remained unchanged. Additionally, transcripts of enzymes related to Thr \rightarrow Gly catabolism were significantly reduced, suggesting a promotion of the Thr \rightarrow Ile route.

3) CGS, the first enzyme unique to the Met branch, showed the second strongest downregulation of all pathway related enzymes. This might function as a bottleneck for the substrate influx at the very beginning of the Met branch. Additionally, the expression of all downstream located enzymes was upregulated or at least unaffected up to Met. Further on, the expression of the SAMS family, a key bottleneck of the Met degradation, as well as the genes involved in Met salvation towards homocysteine were reduced.

Given that Met is the principal methyl group donor for protein biosynthesis and also taking into account that the syncytium is metabolically highly active, high Met levels would be expected to be beneficial and desirable for the nematode. In this context the overall downregulated expression of relevant Met branch enzymes is remarkable (Sauter *et al.*, 2013). Anyway, the actual impact of the determined differential gene expression on the actual quantitative metabolite flux and consequently on the aa levels in root and syncytium tissue under *in vivo* conditions remains to be determined.

The OPH branch point, hosting the TS (Thr branch) and CGS (Met branch), is allocating the overall metabolic flux between the competing Met and Thr branches. Regulatory changes of OPH, TS and CGS trigger comprehensive adaptations, as apparent from literature. For instance, a constitutive TS-antisense expression in potatoes increased the Met level by 239-fold (Zeh *et al.*, 2001) and TS deficient *A. thaliana* mutant *mt02-1* had 22-fold increased Met levels (Bartlem *et al.*, 2000). In an inverted approach using a constitutional expression of a CGS antisense construct in *A. thaliana* resulted in 20 times accumulated OPH levels and 20 times decreased CGS activity with a 35% decreased Met level at a 4-fold increased Thr content (Gakiere *et al.*, 2009). Follow up research should at first quantify the actual metabolically available levels of selected aspartate pathway metabolites in treated and untreated roots, with and without of *H. schachtii* infection, to reveal the actual impact of the described gene expression changes.

6.3.3 Transcriptional changes in aa treated *A. thaliana* roots

As apparent from figure 33, *A. thaliana* responds towards L-Thr, DL-Met and MM treatments by adapting the expression of associated aspartate pathway genes. Those changes will be discussed in detail hereafter.

6.3.3.1 Transcriptional changes in L-Thr treated *A. thaliana* roots

Treating *A. thaliana* with L-Thr decreased the expression of exactly those enzymes that catalyze the synthesis of Thr, namely TS1 and TS2. In parallel, transcripts of the Met branch related enzymes SAMS1 and CGS were more abundant. This pattern fully corresponds to the natural response of the plant metabolism upon elevated Thr levels, as described in literature: a decreased enzymatic activity in the Thr branch accompanied by an increased flux through the Met branch and the downstream located side pathways, c.f. 1.3.2.1(Amir, 2010).

6.3.3.2 Transcriptional changes in DL-Met and MM treated *A. thaliana* roots

DL-Met is composed of two isomers, L-Met and D-Met. Since the majority of metabolic processes only works with L-isomeric aa, it is likely that only L-Met is metabolically useable, whereas D-Met is not or to a very limited extend. Since MM is the dipeptide of Met, it must be detached to become metabolically accessible. For this reason, MM might be available relatively slower than DL-Met but induce effects might last for a longer duration of time. Anyhow, DL-Met and MM can be considered as L-Met treatments of host plants with possibly differing accessibilities over time.

The common reaction of plants towards increased metabolic levels of Met would be the downregulation of Met branch enzymes and *vice versa* the upregulation of Thr branch enzymes. Running qRT-PCR studies on MM and DL-Met treated *A. thaliana* root samples revealed the following key observations:

Whereas DL-Met treatments induce an upregulation of TS1 and TS2, MM treatments did not. Interestingly DL-Met treatments did not affect CGS or SAMS, the key regulatory enzymes of the Met branch. MM reduced the abundance of SAMS2-4. The strongest transcription increase was detected for MGL for both compounds, also corresponding to Thr treatments. Overall, the qRT-PCR results of MM and DL-Met treatments did not fully correspond to one another, but they are also not contradictory.

The determined gene expression changes upon L-Thr, MM and DL-Met overall corresponded to those regulatory adaptations in response to elevated aa concentrations in plant cells described in literature (Amir, 2010). Accordingly, it can be assumed that at least a fraction of the supplemented aa entered and altered the metabolism in the root. As a next

step it should be quantified, which amounts of the applied aa are imported into the root, remain in the roots cells and are translocated towards sink organs.

6.3.3.3 Transcriptional changes in aa treated and *H. schachtii* infected *A. thaliana* roots

All primers specifically amplify their target sequences on *A. thaliana* cDNA but not on *H. schachtii* cDNA. Accordingly, it was possible to measure the expression of *A. thaliana* marker genes on mixed cDNA samples generated from *H. schachtii* infected *A. thaliana* root tissue. At 3dpi, the time of sampling, all syncytia were just at the initial stage of their formation. For this reason, the relative amount of syncytium tissue per root in relation to uninfected root tissue per root was vanishingly low.

The expression of multiple marker genes clearly differed between aa treated infected *A. thaliana* roots and aa treated uninfected roots, as described in detail in chapter 5.2.6. Accordingly, aa treated roots clearly responded towards the nematode infection by changing the expression of certain aspartate pathway marker genes. An earlier study determined the expression of the same marker genes in *H. schachtii* infected, but not aa treated *A. thaliana* at 3dpi. In this, the expression did not change in response to the nematode infection alone (Puthoff *et al.*, 2003). Accordingly, treating *A. thaliana* with aa was a functional precondition for the reported gene expression changes in response to *H. schachtii* infections.

Overall, the qRT-PCR results of aa treated infected whole root samples revealed a general upregulated expression of Thr branch associated genes together with a rather unchanged regulation of Met branch genes, cf. figure 34. It is remarkable, that this overall expression pattern measured in whole root samples corresponded to the expression pattern in syncytium specific tissue at 5 and 15dpi (Szakasits *et al.*, 2009). Nematodes established and maintain syncytia by secretion of effector proteins. Possibly, those effectors do not only target and control the metabolism in syncytium related tissue, but also in morphologically unchanged plant root tissue beyond their feeding sites. Indeed, tissue samples taken in a few cm distance from syncytium tissue showed different levels of free aa than tissue samples from absolutely uninfected roots in oil radish and rape roots (Krauthausen and Wyss, 1982). For a single nematode it might be impossible to manipulate the global root metabolism by secretion of effector proteins, but the joint secretion of multiple nematodes per root might be capable to even manipulate the global root metabolism according to their needs. Mining the nematodes'

secretome for effectors with sequence similarities towards the aspartate family enzymes of interest would proof if they are actually targeted by nematode effectors or not.

Among all studied marker genes MGL became of particular interest. It might be of key functional relevance as discussed hereafter in detail.

6.3.4 Examining the influence of MGL

MGL is positioned on the interconnecting pathway between the Met and Thr branches, see chapter 2.3.1.4, 2.3.1.5 and figure 13. Only MGL was consistently upregulated in response to L-Thr, DL-Met and MM treatments without nematode infection. In contrast to this, with additional nematode infection the expression level of MGL was on the level of the control for all three treatments, *i.e.* not upregulated. Accordingly, the additional nematode infection clearly neutralized the upregulation of MGL. Indeed, it had been reported that MGL participates in the response towards combined abiotic stresses and *H. schachtii* infections in *A. thaliana*. Overexpressing MGL (35S::AtMGL) reduced the infection rate of J3 and J4 nematodes per plant significantly by -76%. In contrast to this, the insertion mutant line AtMGL (SALK_074592C) induced only moderate and insignificant reductions (Atkinson *et al.*, 2013).

If plants overexpress MGL to counter *H. schachtii* attacks, the expression level should be stronger upregulated in aa treated and infected plants. Indeed, the opposite reaction was observed. The expression of MGL was significantly lower in aa treated infected plants than in aa treated not infected plants. Possibly the upregulation was actively blocked or reversed by the invading nematodes. Possibly the expression of MGL was downregulated by the plant. It could be examined, if MGL is also down regulated in response to nematode associated molecular patterns (NAMPs) and aa treatments. This would allow to conclude, if the regulation was driven by the plant or indeed by the nematode.

It was argued that the reported -76% reduction of nematodes might be induced by a depletion of Met in MGL overexpressing mutants, resulting in an inhibited protein synthesis and thus developmental problems for nematodes. Mining the transcriptomic dataset (Szakasits *et al.*, 2009) revealed, that only SAMS was upregulated, whereas the Met branch as a whole and all related catabolic pathways, were downregulated or unaffected, cf. 5.2.6. If *H. schachtii* generally aims to keep the expression of Met catabolism genes low, it might have evolved a strategy to induce and establish this condition over the whole root. This could possibly by

facilitated by secretion of effector proteins. It is questionable, yet not impossible, that the upregulation of MGL in host roots upon MM, DL-Met and L-Thr treatments was sufficiently strong to generate a global Met depletion and by this reduction of -37% *H. schachtii* females per plant. Possibly, those nematodes that fail to specifically regulate the expression of MGL in their feeding site as required faced unfavorable conditions and did not develop into females.

Additional functional studies are needed to fully understand the role of MGL in nematode parasitism and in plant derived defense reactions against nematodes. Metabolomic studies might quantify selected metabolites of relevant enzymes up- and mainly downstream of MGL. It is possible, that MGL as such did not induce the effects itself, but the results clearly point towards a key involvement of MGL or the close related metabolic region.

6.4 Final conclusion

Except for the activity reduction by direct cuticle contact with Ket no tested aa induced markedly strong nematicidal effects of any kind. Direct host plant treatment with very high aa concentrations under artificial conditions provoked an average decrease of approx. -37% females per plant at no relevant control of males. Summarized, the direct and indirect potential of L-Ile, L-Hom, Ket, L-Lys, D-Lys, L-Trp, D-Trp, L-Thr, D-Thr, MM and DL-Met to control *H. schachtii* on the model plant *A. thaliana* under artificial conditions is limited. The induction of effects is most likely plant and nematode species dependent for the respective aa. Therefore, the nematode antagonistic potential of candidate aa must be determined case by case for other nematode and host plant species combinations.

Possibly exogenous applications of DL-Met, L-Thr, MM or other aa could be supportive in combination with biological or chemical nematicides. In particular MGL appears to be an important functional element of the *H. schachtii* parasitism in aa treated plants. MGL and possibly other enzymes of the aspartate pathway might yield promising targets for breeding or biotech approaches, perhaps also in combination with exogenous aa treatments.

8 REFERENCES

- Alonso, J., Stepanova, A., Leisse, T., Kim, C., Chen, H., Shinn, P., Stevenson, D., Zimmerman, J., Barajas, P., Cheuk, R., Gadrinab, C., Heller, C., Jeske, A., Koesema, E., Meyers, C., Parker, H., Prednis, L., Ansari, Y., Choy, N., Deen, H., Geralt, M., Hazari, N., Hom, E., Karnes, M., Mulholland, C., Ndubaku, R., Schmidt, I., Guzman, P., Aguilar-Henonin, L., Schmid, M., Weigel, D., Carter, D., Marchand, T., Risseeuw, E., Brogden, D., Zeko, A., Crosby, W., Berry, C., Ecker, J. (2003) Genome-wide insertional mutagenesis of *Arabidopsis thaliana*. *Science*, (301): 653-657.
- Amir, R., Galili, G. (1999) Regulation of lysine and threonine metabolism in plants. *Genetic engineering*, 21: 57–77.
- Amir, R., Hacham, Y., Galili, G. (2002) Cystathionine γ -synthase and threonine synthase operate in concert to regulate carbon flow towards methionine in plants. *Trends in plant science*, 7(4): 153–156.
- Amir, R. (2010) Current understanding of the factors regulating methionine content in vegetative tissues of higher plants. *Amino acids*, 39(4): 917–931.
- Arruda, P., Kemper, E. L., Papes, F., Leite, A. (2000) Regulation of lysine catabolism in higher plants. *Trends in plant science*, 5(8): 324–330.
- Atkinson, N. J., Lilley, C. J., Urwin, P. E. (2013) Identification of genes involved in the response of *Arabidopsis* to simultaneous biotic and abiotic stresses. *Plant physiology*, 162: 2028–2041.
- Balasubramanian, M., Myers, R. (1971) Nutrient media for plant-parasitic nematodes. II. Amino acid requirements of *Aphelenchoides* sp. *Experimental parasitology*, 29: 330–336.
- Barends, T. R., Dunn, M. F., Schlüting, I. (2008) Tryptophan synthase, an allosteric molecular factory. *Current opinion in chemical biology*, 12(5): 593–600.
- Bartlem, D., Lambein, I., Okamoto, T., Itaya, A., Uda, Y., Kijima, F., Tamaki, Y., Nambara, E., Naito, S. (2000) Mutation in the threonine synthase gene results in an over-accumulation of soluble methionine in *Arabidopsis*. *Plant physiology*, 123: 101–110.
- Bartlem, D. G., Jones, M. G. K., Hammes, U. Z. (2013) Vascularization and nutrient delivery at root-knot nematode feeding sites in host roots. *Journal of experimental botany*, 65(7): 1789–1798.
- Betka, M., Grundler, F., Wyss, U. (1991) Influence of changes in the nurse cell system (syncytium) on the development of the cyst nematode *Heterodera schachtii*: single amino acids. *Phytopathology*, 81: 75–79.
- Bleecker, A. B., Kende, H. (2000) Ethylene: a gaseous signal molecule in plants. *Annual review of cell and developmental biology*, 16: 1–18.
- Brenner, S. (1974) The Genetics of *Caenorhabditis elegans*. *Genetics*, 77(1): 71–94.

Byerly, L., Cassada, R. C., Russell, R. L. (1976) The life cycle of the nematode *Caenorhabditis elegans*. *Developmental biology*, 51(1): 23–33.

Cabrera, J., Bustos, R., Favery, B., Fenoll, C., Escobar, C. (2014) Nematic: a simple and versatile tool for the *in silico* analysis of plant-nematode interactions. *Molecular plant pathology*, 15(6): 627–636.

Cassada, R., Russell, R. L. (1975) The dauerlarva, a post-embryonic developmental variant of the nematode *Caenorhabditis elegans*. *Developmental biology*, 46(2): 326–342.

Chiba, Y., Ishikawa, M., Kijima, F., Tyson, R. H., Kim, J., Yamamoto, A., Nambara, E., Leustek, T., Wallsgrove, R., Naito, S. (1999) Evidence for autoregulation of cystathionine γ -Synthase mRNA stability in *Arabidopsis*. *Science*, (286): 1371-1374.

Chiba, Y., Sakurai, R., Yoshino, M., Ominato, K., Ishikawa, M., Onouchi, H., Naito, S. (2003) S-adenosyl-L-methionine is an effector in the posttranscriptional autoregulation of the cystathionine gamma-synthase gene in *Arabidopsis*. *Proceedings of the national academy of sciences of the United States of America*, 100(18): 10225–10230.

Chitwood, J. D. (2003) Research on plant-parasitic nematode biology conducted by the United States Department of Agriculture—Agricultural Research Service. *Pest management science*, 59: 748-753.

Crow, W., Cuda, J., Stevens, B. (2009) Efficacy of methionine against ectoparasitic nematodes on golf course turf. *Journal of nematology*, 41(3): 217–220.

Curien, G., Dumas, R., Ravanel, S., Douce, R. (1996) Characterization of an *Arabidopsis thaliana* cDNA encoding an S-adenosylmethionine-sensitive threonine synthase. Threonine synthase from higher plants. *FEBS letters*, 390(1): 85–90.

Curien, G., Job, D., Douce, R., Dumas, R. (1998) Allosteric activation of *Arabidopsis threonine* synthase by S-adenosylmethionine. *Biochemistry*, 37(38): 13212–13221.

Curien, G., Ravanel, S., Dumas, R. (2003) A kinetic model of the branch-point between the methionine and threonine biosynthesis pathways in *Arabidopsis thaliana*. *European journal of biochemistry*, 270(23): 4615–4627.

Dickman, M. B., Mitra, A. (1992) *Arabidopsis thaliana* as a model for studying *Sclerotinia sclerotiorum* pathogenesis. *Physiological and molecular plant pathology*, 41(4): 255–263.

Dolan, L., Janmaat, K., Willemse, V., Linstead, P., Poethig, S., Roberts, K., Scheres, B. (1993) Cellular organization of the *Arabidopsis thaliana* root. *Development*, 119(1): 71–84.

Doney, D., Fife, J., Whitney, E. (1970) The effect of the sugar beet nematode *Heterodera schachtii* on the free amino acids in resistant and susceptible *Beta* species. *Phytopathology*, 60: 1727-1729.

Dusenberry, D. (1975) The avoidance of D-tryptophan by the nematode *Caenorhabditis elegans*. *The journal of experimental zoology*, 193 (3): 413-418.

Elashry, A., Okumoto, S., Siddique, S., Koch, W., Kreil, D. P., Bohlmann, H. (2013) The AAP gene family for amino acid permeases contributes to development of the cyst nematode *Heterodera schachtii* in roots of *Arabidopsis*. Plant physiology and biochemistry, 70: 379–386.

Epstein, E. (1973) Effect of pretreatment with some amino acids and amino acid antimetabolites on *Longidorus africanus* infected and non-infected *Bidens tripartita*. Nematologica, 18: 555-562.

Evans, K., Trudgill, D. (1971) Effects of amino acids on the reproduction of *Heterodera rostochiensis*. Nematologica, 17: 495-500.

Félix, M. (2008) RNA interference in nematodes and the chance that favored Sydney Brenner. Journal of biology, 7(9): 34.

Fischer, W. N., Loo, D. D. F., Koch, W., Ludewig, U., Boorer, K. J., Tegeder, M., Rentsch, D., Wright, E., Frommer, W. B. (2002) Low and high affinity amino acid H⁺-cotransporters for cellular import of neutral and charged amino acids. Plant journal, 29(6): 717–731.

Gakière, B., Ravanel, S., Droux, M., Douce, R., Job, D. (2000) Mechanisms to account for maintenance of the soluble methionine pool in transgenic *Arabidopsis* plants expressing antisense cystathionine γ -synthase cDNA. Comptes rendus de l'academie des sciences - serie III, 323(10): 841–851.

Galili, G. (1995) Regulation of lysine and threonine synthesis. The plant cell, 7(7): 899–906.

Galili, G. (2002) New insights into the regulation and functional significance of lysine metabolism in plants. Annual review of plant biology, 53: 27–43.

Gallagher, D. T., Gilliland, G. L., Xiao, G., Zondlo, J., Fisher, K. E., Chinchilla, D., Eisenstein, E. (1998) Structure and control of pyridoxal phosphate dependent allosteric threonine deaminase. Structure, 6(4): 465–475.

Gördes, D., Koch, G., Thurow, K., Kolukisaoglu, U. (2013) Analyses of *Arabidopsis* ecotypes reveal metabolic diversity to convert D-amino acids. SpringerPlus, 2: 559 1-11.

Grundler, F. M. W. (1989) Untersuchungen zur Geschlechterdetermination des Rübenzysten-nematoden *Heterodera schachtii Schmidt*. PhD thesis, University of Kiel.

Grundler, F. M. W., Betka, M., Wyss, U. (1991) Influence of changes in the nurse cell system (syncytium) on sex determination and development of the cyst nematode *Heterodera schachtii*: total amounts of proteins and amino acids. Phytopathology, 81: 70–74.

Grundler, F. M. W., Sobczak, M., Golinowski, W. (1998) Formation of wall openings in root cells of *Arabidopsis thaliana* following infection by the plant-parasitic nematode *Heterodera schachtii*. European journal of plant pathology, 104(6): 545–551.

Hacham, Y., Schuster, G., Amir, R. (2006) An *in vivo* internal deletion in the N-terminus region of *Arabidopsis* cystathionine γ -synthase results in CGS expression that is insensitive to methionine. *The plant journal*, 45(6): 955–967.

Hammes, U. Z., Schachtman, D. P., Berg, R. H., Nielsen, E., Koch, W., McIntyre, L. M., Taylor, C. G. (2005) Nematode induced changes of transporter gene expression in *Arabidopsis* roots. *Molecular plant-microbe interactions*, 18(12): 1247–1257.

Hammes, U. Z., Nielsen, E., Honaas, L. A., Taylor, C. G., Schachtman, D. P. (2006) AtCAT6, a sink-tissue-localized transporter for essential amino acids in *Arabidopsis*. *The plant journal*, 48(3): 414–426.

Hanounik, S. B., Osborne, W. W. (1975) Influence of *Meloidogyne incognita* on the content of amino acids and nicotine in tobacco grown under gnotobiotic conditions. *Journal of nematology*, 7 (4): 332-336.

Hesse, H., Kreft, O., Maimann, S., Zeh, M., Hoefgen, R. (2004) Current understanding of the regulation of methionine biosynthesis in plants. *Journal of experimental botany*, 55(404): 1799–1808.

Hirner, A. (2006) *Arabidopsis* LHT1 is a high affinity transporter for cellular amino acid uptake in both root epidermis and leaf mesophyll. *The plant cell*, 18(8): 1931–1946.

Hofmann, J., El Ashry, A., Anwar, S., Erban, A., Kopka, J., Grundler, F. M. W. (2010) Metabolic profiling reveals local and systemic responses of host plants to nematode parasitism. *The plant journal*, 62, 1058–1071.

Hogenhout, S. A., Van der Hoorn, R. A. L., Terauchi, R., Kamoun, S. (2009) Emerging concepts in effector biology of plant-associated organisms. *Molecular plant-microbe interactions*, 22: 115–122.

Hol, G., Boer, W., Termorshuizen, A., Meyer, K., Schneider, J., Van der Putten, W., Van Dam, N. (2013) *Heterodera schachtii* nematodes interfere with aphid-plant relations on *Brassica oleracea*. *Journal of chemical ecology*, 39:1193–1203.

Inaba, K., Fujiwara, T., Hayashi, H., Chino, M., Komeda, Y., Naito, S. (1994) Isolation of an *Arabidopsis thaliana* mutant, mto1, that over accumulates soluble methionine. Temporal and spatial patterns of soluble methionine accumulation. *Plant physiology*, 104: 881–887.

Jones, D. L., Darrah, R. R. (1994) Amino acid influx at the soil-root interface of *Zea mays* L. and its implications in the rhizosphere. *Plant and soil*, 163: 1–12.

Joshi, V., Laubengayer, K. M., Schauer, N., Fernie, A. R., Jander, G. (2006) Two *Arabidopsis* threonine aldolases are nonredundant and compete with threonine deaminase for a common substrate pool. *The plant cell*, 18(12): 3564–3575.

Joshi, V., Jander, G. (2009) *Arabidopsis* methionine gamma-lyase is regulated according to isoleucine biosynthesis needs but plays a subordinate role to threonine deaminase. *Plant physiology*, 151(1): 367–378.

Kim, J., Leustek, T. (2000) Repression of cystathionine gamma-synthase in *Arabidopsis thaliana* produces partial methionine auxotrophy and developmental abnormalities. *Plant science*, 151(1): 9–18.

Kirschner, K., Szadkowski, H., Jardetzky, T. S., Hager, V. (1987) Phosphoribosylanthranilate isomerase—indoleglycerol-phosphate synthase from *Escherichia coli*. *Methods enzymology*, 142: 386–397.

Knippers, R. (2006) Molekulare Genetik. Thieme, Stuttgart, (9th ed.).

Koch, E., Slusarenko, A. (1990) *Arabidopsis* is susceptible to infection by a downy mildew fungus. *The plant cell*, 2(5): 437–445.

Koenning, S. R., Wrather, J. A. (2010) Suppression of soybean yield potential in the continental United States by plant disease from 2006 to 2009. *Plant health progress*, 11(1): DOI: 10.1094/PHP-2010-1122-01-RS.

Krauthausen, H. J., Wyss, U. (1982) Influence of the cyst nematode *Heterodera schachtii* on relative changes in the pattern of free amino acids at feeding sites. *Physiological plant pathology*, 21: 425–436.

Ladwig, F., Stahl, M., Ludewig, U., Hirner, A. A., Hammes, U. Z., Stadler, R., Harter, K., Koch, W. (2012) Siliques Are Red1 from *Arabidopsis* acts as a bidirectional amino acid transporter that is crucial for the amino acid homeostasis of siliques. *Plant physiology*, 158(4): 1643–1655.

Lalonde, S., Tegeder, M., Throne-Holst, M., Frommer, W. B., Patrick, J. W. (2003) Phloem loading and unloading of sugars and amino acids. *Plant, cell and environment*, 26(1): 37–56.

Lee, Y. H., Foster, J., Chen, J., Voll, L. M., Weber, A. P. M., Tegeder, M. (2007) AAP1 transports uncharged amino acids into roots of *Arabidopsis*. *The plant journal*, 50: 305–319.

Lehmann, S., Gumy, C., Blatter, E., Boeffel, S., Fricke, W., Rentsch, D. (2011) *In planta* function of compatible solute transporters of the AtProT family. *Journal of experimental botany*, 62(2): 787–796.

Liu, J. Q., Dairi, T., Itoh, N., Kataoka, M., Shimizu, S., Yamada, H. (1998) Gene cloning, biochemical characterization and physiological role of a thermostable low-specificity L-threonine aldolase from *Escherichia coli*. *European journal of biochemistry*, 255(1): 220–226.

Liu, X., Bush, D. R. (2006) Expression and transcriptional regulation of amino acid transporters in plants. *Amino acids*, 30: 113–120.

Liu, G., Ji, Y., Bhuiyan, N. H., Pilot, G., Selvaraj, G., Zou, J., Wei, Y. (2010) Amino acid homeostasis modulates salicylic acid associated redox status and defense responses in *Arabidopsis*. *The plant cell*, 22: 3845–3863.

Maeda, H., Dudareva, N. (2012) The shikimate pathway and aromatic amino acid biosynthesis in plants. *Annual review of plant biology*, 63(1): 73–105.

Marella, H. H., Nielsen, E., Schachtman, D. P., Taylor, C. G. (2013) The amino acid permeases AAP3 and AAP6 are involved in root-knot nematode parasitism of *Arabidopsis*. *Molecular plant microbe interactions*, 26(1): 44–54.

Marques De Carvalho, L., Banda, N. D., Vaughan, M. W., Cabrera, A. R., Hung, K., Cox, T., Abdo, Z., Hartwell Allen, L., Teal, P. E. A. (2015) Mi-1 mediated nematode resistance in tomatoes is broken by short-term heat stress but recovers over time. *Journal of nematology*, 47(2): 133–140.

McCarville, M. T., Marett, C. C., Mullaney, M. P., Gebhart, G. D., Tylka, G. L. (2017) Increase in soybean cyst nematode virulence and reproduction on resistant soybean varieties in Iowa from 2001 to 2015 and the effects on soybean yields. *Plant health progress*, 18(3), 146–155.

Meinke, D. W., Cherry, J. M., Dean, C., Rounsley, S. D., Koornneef, M. (1998) *Arabidopsis thaliana*: a model plant for genome analysis. *Science*, 282(5389): 679–682.

Meyerowitz, E. M. (1987) *Arabidopsis thaliana*. *Annual review of genetics*, 21: 93–111.

Milligan, S. B., Bodeau, J., Yaghoobi, J., Kaloshian, I., Zabel, P., Williamson, V. M. (1998) The root knot nematode resistance gene Mi from tomato is a member of the leucine zipper, nucleotide binding, leucine-rich repeat family of plant genes. *The plant cell*, 10: 1307–1319.

Miyazaki, J. H., Yang, S. F. (1987) The methionine salvage pathway in relation to ethylene and polyamine biosynthesis. *Physiologia plantarum*, 69(2): 366–370.

Morollo, A. A., Eck, M. J. (2001) Structure of the cooperative allosteric anthranilate synthase from *Salmonella typhimurium*. *Nature structural biology*, 8(3): 243–247.

Mudd, S. H., Datko, A. H. (1986) Methionine methyl group metabolism in *Lemna*. *Plant physiology*, 81(1): 103–114.

Mueller-Esterl, W. (2009) Biochemie. Springer-Verlag, Berlin, (1st ed.).

Müller, J., Rehbock, K., Wyss, U. (1981) Growth of *Heterodera schachtii* with remarks on amounts of food consumed. *Revue de nématologie*, 4 (2): 227-234.

Onouchi, H., Nagami, Y., Haraguchi, Y., Nakamoto, M., Nishimura, Y., Sakurai, R., Nagao, N., Kawasaki, D., Kadokura, Y., Naito, S. (2005) Nascent peptide-mediated translation elongation arrest coupled with mRNA degradation in the CGS1 gene of *Arabidopsis*. *Genes & development*, 19(15): 1799–1810.

- Osman, A. A., Viglierchio, D. R. (1981a) Foliar spray effects of selected amino acids on sunflower infected with *Meloidogyne incognita*. Journal of nematology, 13(3): 417-419.
- Osman, A. A., Viglierchio, D. R. (1981b) *Meloidogyne incognita* development on soybean treated with selected amino acids by alternate methods. Revue de nématologie, 4 (1): 172-174.
- Overman, A. J., Woltz, S. S. (1962). Effects of amino acid antimetabolites upon nematodes and tomatoes. Proceedings of the Florida state horticultural society, 75: 166-170.
- Pang, P., Meyerowitz, E. (1987) *Arabidopsis thaliana*: a model system for plant molecular biology. Nature biotechnology, 5: 1177–1181.
- Pfaffl, M. W. (2001) A new mathematical model for relative quantification in real-time RT-PCR. Nucleic acids research, 29(9): 2002–2007.
- Pollard, T. D., Earnshaw, W. C. (2008) Cell biology. Saunders/Elsevier, Philadelphia, (2nd ed.).
- Poulsen, C., Verpoorte, R. (1991) Roles of chorismate mutase, isochorismate synthase and anthranilate synthase in plants. Phytochemistry, 30(2): 377–386.
- Prasad, S. K., Webster, J. M. (1967) The effect of amino acid antimetabolites on four nematode species and their host plants. Nematologica, 13: 318-320.
- Prasad, K. S. K., Shetty, K. G. H. (1974) The effect of amino acids as foliar spray on root-knot nematode (*Meloidogyne incognita*) and tomato. Indian journal of nematology, 4: 88-107.
- Pratelli, R., Pilot, G. (2014) Regulation of amino acid metabolic enzymes and transporters in plants. Journal of experimental botany, 65(19): 5535–5556.
- Puthoff, D. P., Nettleton, D., Rodermel, S. R., Baum, T. J. (2003) *Arabidopsis* gene expression changes during cyst nematode parasitism revealed by statistical analyses of microarray expression profiles. The plant journal, 33(5): 911–921.
- Radwanski, E. R., Last, R. L. (1995) Tryptophan biosynthesis and metabolism: biochemical and molecular genetics. The plant cell, 7(7): 921–934.
- Raizen, D. M., Zimmerman, J. E., Maycock, M. H., Ta, U. D., You, Y., Sundaram, M. V., Pack, A. I. (2008) Lethargus is a *Caenorhabditis elegans* sleep-like state. Nature, 451(7178): 569–572.
- Ranocha, P., Bourgis, F., Ziemak, J. M., Rhodes, D., Gage, A. D., Hanson, A. D. (2000) Characterization and functional expression of cDNAs encoding methionine-sensitive and -insensitive homocysteine S-methyltransferases from *Arabidopsis*. Journal of biological chemistry, 275(21): 15962–15968.
- Rébeillé, F., Jabrin, S., Bligny, R., Loizeau, K., Gambonnet, B., Van Wilder, V., Douce, R., Ravanel, S. (2006) Methionine catabolism in *Arabidopsis* cells is initiated by a gamma-

cleavage process and leads to S-methylcysteine and isoleucine syntheses. *Proceedings of the National academy of sciences of the United States of America*, 103(42): 15687–15692.

Rentsch, D., Schmidt, S., Tegeder, M. (2007) Transporters for uptake and allocation of organic nitrogen compounds in plants. *FEBS letters*, 581(12): 2281–2289.

Rognes, S. E., Lea, P. J., Miflin, B. (1980) S-adenosylmethionine a novel regulator of aspartate kinase. *Nature*, 287: 357–359.

Romero, R. M., Roberts, M. F., Phillipson, J. D. (1995) Anthranilate synthase in microorganisms and plants. *Phytochemistry*, 39(2): 263-276.

Samach, A., Hareven, D., Gutfinger, T., Lifschitz, E. (1991) Biosynthetic threonine deaminase gene of tomato: Isolation, structure, and upregulation in floral organs. *Developmental biology*, 88: 2678–2682.

Sauter, M., Moffatt, B., Saechao, M. C., Hell, R., Wirtz, M. (2013) Methionine salvage and S-adenosylmethionine: essential links between sulfur, ethylene and polyamine biosynthesis. *Biochemical journal*, 451(2): 145–154.

Shaul, O., Galili, G. (1992) Threonine overproduction in transgenic tobacco plants expressing a mutant desensitized aspartate kinase of *Escherichia coli*. *Plant physiology*, 100(3): 1157–1163.

Shaul, O., Galili, G. (1993) Concerted regulation of lysine and threonine synthesis in tobacco plants expressing bacterial feedback-insensitive aspartate kinase and dihydronicotinate synthase. *Plant molecular biology*, 23: 759-768.

Shen, B., Li, C., Tarczynski, M. C. (2002) High free-methionine and decreased lignin content result from a mutation in the *Arabidopsis* S-adenosyl-L-methionine synthetase 3 gene. *Plant journal*, 29(3): 371–380.

Siddique, S., Matera, C., Radakovic, Z. S., Hasan, M. S., Gutbrod, P., Rozanska, E., Sobczak, M., Torres, M. A., Grundler, F. M. W. (2014) Parasitic worms stimulate host NADPH oxidases to produce reactive oxygen species that limit plant cell death and promote infection. *Science signaling*, 7(320), ra33 DOI: 10.1126/scisignal.2004777.

Sijmons, C. S., Grundler, F. M. W., von Mende, N., Burrows, P. R., Wyss, U. (1991) *Arabidopsis thaliana* as a new model host for plant-parasitic nematodes. *The plant journal*, 1(2): 245-254.

Simpson, R. B., Johnson, L. J. (1990) *Arabidopsis thaliana* as a host for *Xanthomonas campestris* pv. *campestris*. *Molecular plant-microbe interactions*, 3(4): 233-237.

Stiernagle, T. (2006) Maintenance of *C. elegans*. WormBook, ed. The *C. elegans* research community, WormBook, doi/10.1895/wormbook.1.101.1, <http://www.wormbook.org>

Stryer, L., Berg, J. M., Tymoczko, J. L. (2013) Biochemie. Springer Spektrum, Heidelberg, (7th ed.).

Svennerstam, H., Ganeteg, U., Näsholm, T. (2008) Root uptake of cationic amino acids by *Arabidopsis* depends on functional expression of amino acid permease 5. The new phytologist, 180(3): 620–630.

Szakasits, D., Heinen, P., Wieczorek, K., Hofmann, J., Wagner, F. M. W., Kreil, D. P., Sykacek, P., Grundler, F. M. W., Bohlmann, H. (2009) The transcriptome of syncytia induced by the cyst nematode *Heterodera schachtii* in *Arabidopsis* roots. Plant journal, 57(5): 771–784.

Talavera, M., Mizukubo, T. (2005) Effects of DL-methionine on hatching and activity of *Meloidogyne incognita* eggs and juveniles. Pest management science, 61: 413–416.

Tegeder, M., Rentsch, D. (2010) Uptake and partitioning of amino acids and peptides. Molecular plant, 3(6): 997–1011.

Tegeder, M. (2012) Transporters for amino acids in plant cells: some functions and many unknowns. Current opinion in plant biology, 15(3): 315–321.

Tegeder, M. (2014) Transporters involved in source to sink partitioning of amino acids and ureides: opportunities for crop improvement. Journal of experimental botany, 65(7): 1865–1878.

The Arabidopsis genome initiative (2000) Analysis of the genome sequence of the flowering plant *Arabidopsis thaliana*. Nature, 408: 796-815.

The *C. elegans* sequencing consortium (1998) Genome sequence of the nematode *C. elegans*: a platform for investigating biology. Science, 282: 2012-2018.

Trudgill, D. L. (1974) The Influence of DL-tyrosine on the Sex of *Heterodera rostochiensis*. Nematologica, 20: 34-38.

Untergasser, A., Cutcutache, I., Koressaar, T., Ye, J., Faircloth, B. C., Remm, M., Rozen, S. G. (2012) Primer 3 new capabilities and interfaces. Nucleic acids research, 40(15): 1–12.

Van Bel, A. J. E. (1990) Xylem-phloem exchange via the rays: The undervalued route of transport. Journal of experimental botany, 41(6): 631–644.

Vanfleteren, J. R. (1973) Amino acid requirements of the free-living nematode *Caenorhabditis briggsae*. Nematologica, 19: 93-99.

Viglierchio, D. R., Kaemmerer, P. K. (1965) On the nature of hatching of *Heterodera schachtii*. III. Principles of hatching activity. Journal of the American society of sugar beet technologists, 13(8): 698-715.

Wallsgrove, R. M., Lea, P. J., Miflin, B. J. (1983) Intracellular localization of aspartate kinase and the enzymes of threonine and methionine biosynthesis in green leaves. Plant physiology, 71(4): 780–784.

- Whalen, M. C., Innes, R. W., Bent, A. F., Staskawicz, B. J. (1991) Identification of *Pseudomonas syringae* pathogens of *Arabidopsis* and a bacterial locus determining avirulence on both *Arabidopsis* and soybean. *The plant cell*, 3(1): 49–59.
- Williamson, V. M., Gleason, C. A. (2003) Plant nematode interactions. *Current opinion in plant biology*, 6: 327–333.
- Williamson, V. M., Kumar A. (2006) Nematode resistance in plants: The battle underground. *Trends in genetics*, 22(7): 396–403.
- Wyss, U., Grundler, F. M. W. (1992a) Seminar: *Heterodera schachtii* and *Arabidopsis thaliana*, a model host-parasite interaction. *Nematologica*, 38: 488-493.
- Wyss, U., Grundler, F. M. W. (1992b) Feeding behavior of sedentary plant-parasitic nematodes. *Netherlands journal of plant pathology*, 98:165-173.
- Wyss, U., Zunke, U. (1986) Observation of the behavior of second stage juveniles of *Heterodera schachtii* inside host roots. *Revue de nematologie*, 9(2): 153–166.
- Xiang N., Lawrence K. S., Kloepper J. W., Donald P. A., McInroy J. A. (2017) Biological control of *Heterodera glycines* by spore-forming plant growth-promoting rhizobacteria (PGPR) on soybean. *PLoS ONE*, 12(7): e0181201.
- Yang, H., Postel, S., Kemmerling, B., Ludewig, U. (2013) Altered growth and improved resistance of *Arabidopsis* against *Pseudomonas syringae* by overexpression of the basic amino acid transporter AtCAT1. *Plant cell and environment*, 37(6): 1404–1414.
- Yu, H., Zhang, F., Wang, G., Liu, Y., Liu, D. (2013) Partial deficiency of isoleucine impairs root development and alters transcript levels of the genes involved in branched-chain amino acid and glucosinolate metabolism in *Arabidopsis*. *Journal of experimental botany*, 64(2): 599–612.
- Zeh, M., Casazza, A. P., Kreft, O., Roessner, U., Bieberich, K., Willmitzer, L., Hoefgen, R., Hesse, H. (2001) Antisense inhibition of threonine synthase leads to high methionine content in transgenic potato plants. *Plant physiology*, 127(3): 792–802.
- Zhang, Y., Luc, J. E., Crow, W. T. (2010) Evaluation of amino acids as turfgrass nematicides. *Journal of nematology*, 42(4): 292–297.
- Zhou, L., Yuen, G., Wang, Y., Wei, L., Ji, G. (2016) Evaluation of bacterial biological control agents for control of root-knot nematode disease on tomato. *Crop protection*, 84: 8–13.

8 APPENDIX

8.1 Materials and methods

8.1.1 NGM-medium

The stock solutions: 5 mg/ml cholesterol in ethanol, 1M stocks of MgSO₄, CaCl₂ and KPO₄ buffer (pH 6.0) were prepared. For the NGM basis mixture 3g NaCl, 17g agar, and 2.5g peptone were added 1l ddH₂O. All stock solutions and the NGM basis mixture were autoclaved. Afterwards, the flasks were cooled in 55°C water bath for 30min before 25ml KPO₄ and 1ml of CaCl₂, MgSO₄ and cholesterol in ethanol were added. The solution was stirred for 3min on a stirrer and then poured into Petri dishes under aseptic conditions. The plates were left at room temperature in a laminar flow to dry, for minimum 4h. All plates were stored in an air-tight container at room temperature.

Table 18 KPO₄ buffer(1l)

compound	volume	unit
KH ₂ PO ₄	108.3	g
K ₂ HPO ₄	35.6	g

Table 19 NGM-medium(1l)

compound	concentration	volume	unit
NaCl	-	3	g
Agar	-	17	g
Peptone	-	2.5	g
Cholesterol(in ethanol)	5 mg/ml	1	ml
KPO ₄	1M	25	ml
MgSO ₄	1M	1	ml
CaCl ₂	1M	1	ml
ddH ₂ O	-	1	l

8.1.2 LB-medium

For liquid LB-medium preparation 10g NaCl, 10g Bacto™-Tryptone and 5g YEAST EXTRACT were added to 1l ddH₂O under constant stirring on a stirrer. For solid medium

15g of agar was added. For both media pH 7 was adjusted by adding NaOH and they were autoclaved afterwards.

Table 20 LB-medium (1l)

compound	Volume	unit
Bacto™-Tryptone	10	g
YEAST EXTRACT	5	g
NaCl	10	g
NaOH	-	µl
Agar*	15	g
ddH ₂ O	1	l

8.1.3 M9 buffer

To 1l ddH₂O 5.8g Na₂HPO₄*7H₂O, 3g KH₂PO₄, 0.25g MgSO₄*7H₂O and 5g NaCl were added. The M9 buffer was autoclaved afterwards.

Table 21 M9-buffer(1l)

Compound	Volume	unit
Na ₂ HPO ₄ *7H ₂ O	5.8	g
KH ₂ PO ₄	3	g
MgSO ₄ *7H ₂ O	0.25	g
NaCl	5	g
ddH ₂ O	1	l

8.1.4 Bleach solution

Initially the NaOCl and NaOH stock solutions were prepared and filter sterilized. They were stored at +4°C fridge. To prepare 10 ml bleach solution the reagents listed above were mixed in the amounts mentioned and vortexed afterwards. The solution was prepared freshly for each synchronization.

Table 22 Bleach solution (10ml)

compound	concentration	volume	unit
NaOCl	6%	1	ml
NaOH	5M	4	ml
ddH ₂ O	-	5	ml

8.1.5 S-Basal complete medium

The preparation of S-basal complete splits into two sub steps of preparation. At first the S-Basal solution, 1M MgSO₄, 1M CaCl₂, Trace Metal Solution, Potassium citrate and Cholesterol in ethanol stocks were prepared and sterilized by autoclaving (not for cholesterol):

To prepare the S-Basal solution, the volumes of 1g K₂HPO₄, 6g KH₂PO₄ and 5.85g NaCl were added to 1l ddH₂O. Cholesterol was added under aseptic conditions past autoclaving and cooling of the solution.

The Trace Metals Solution was prepared by adding 69.2mg FeSO₄ * 7 H₂O, 186mg Na₂EDTA, 19.6mg MnCl₂ * 4H₂O and 2.4mg CuSO₄ * 5H₂O to 100ml of ddH₂O. It was autoclaved and at room temperature in the dark, for UV degradation protection.

To prepare the S-Basal complete, these solutions were combined as follows under aseptic conditions. The *E. coli* pellet was located in the 50ml tubes frozen at -80°C was dissolved in 50ml S-Basal solution. To this, 150µl MgSO₄, 150µl KH₂PO₄, 500 µl trace metal solution, 500µl Potassium citrate, 40µl Cholesterol in ethanol (5mg/ml) and 250µl freshly unfrosted streptomycin were added. The solution was homogenized by vortexing using Vortex-Genie 2 G560 E (Scientific Industries, inc., Bohemia, USA). The S-Basal complete, not the stock solutions, was prepared freshly for each experiment.

Table 23 Trace Metal Solution (100ml)

compound	volume	unit
FeSO ₄ * 7H ₂ O	69.2	mg
Na ₂ EDTA	186	mg
MnCl ₂ * 4H ₂ O	19.6	mg
CuSO ₄ * 5H ₂ O	2.4	mg
ddH ₂ O	100	ml

Table 24 S-Basal solution (1l)

compound	concentration	volume	unit
K ₂ HPO ₄	-	1	g
KH ₂ PO ₄	-	6	g
Cholesterol in ethanol	5 mg/ml	1	ml
NaCl	-	5.85	g
ddH ₂ O	-	1	l

Table 25 S-Basal complete solution (50ml)

compound	concentration	volume	unit
MgSO ₄	1M	150	μl
CaCl ₂	1M	150	μl
Trace Metal Solution	-	500	μl
Potassiumcitrate	1M	500	μl
Cholesterol in ethanol	5 mg/ml	40	μl
Streptomycin	-	250	μl

8.1.6 Knops'-medium

All stock solutions were prepared in ddH₂O and sterilized by autoclaving before they were stored at +4°C. To prepare Knops'-medium 20g sucrose, 8g Daichin agar and the stock solutions I–V were added to 1l ddH₂O under constant stirring using a stirrer. Then the pH was determined using a pH-meter, adjusted to 6.4 by supplementation of KOH. After autoclaving the medias were cooled down to 55°C using a water bath before 1ml Vitamin B5 was added under sterile conditions and homogenized by stirring on a stirrer for 3min. The medium was poured into Petri dishes and then the plates were left to dry overnight, inside a sterile bench.

Table 26 Knops'-medium protocol(1l)

compound	volume	Unit
Sucrose	20	g
Daichin Agar	8	g
Stock solution I	2	ml
Stock solution II	2	ml
Stock solution III	2	ml
Stock solution IV	0.4	ml
Stock solution V	0.2	ml
B5 Vitamins	1	ml

Table 27 Knops'-medium stock solutions (1l)

solution name	compound	volume	unit
stock solution I	KNO ₃	121.32	g
	MgSO ₄ * 7 H ₂ O	19.71	g
stock solution II	Ca(NO ₃) ₂ * 4 H ₂ O	120	g
stock solution III	KH ₂ PO ₄	27.22	g
stock solution IV	FeNaEDTA	7.34	g
stock solution V	H ₃ BO ₃	2.86	g
	MnCl ₂	1.81	g
	CuSO ₄ * 5 H ₂ O	0.073	g
	ZnSO ₄ * 7 H ₂ O	0.36	g
	CoCl ₂ * 6 H ₂ O	0.052	g
	H ₂ MoO ₄	0.052	g
	NaCl	2	g

8.1.7 DNA extraction from plant

8.1.7.1 CTAB buffer 100ml

To 40ml ddH₂O, 2g CTAB, 10ml 1M Tris, 4ml 0.5 EDTA, 28ml 5M NaCl and 1g PVP were added under constant stirring. Subsequently, the pH was adjusted to 8.0 by adding HCL and the volume was increased to 100ml with ddH₂O.

Table 28 1 M Tris (100ml)

compound	concentration	volume	unit
CTAB	-	2	g
Tris (pH 8.0)	1 M	10	ml
EDTA (pH 8.0)	0.5 M	4	ml
NaCl	5 M	28	ml
ddH ₂ O	-	40	ml
polyvinylpyrrolidone(PVP)	-	1	g

8.1.7.2 1M Tris pH 8.0

Initially, 121.1g Tris base were added to 800ml of ddH₂O. Then pH 8.0 was adjusted by adding HCL under constant stirring. The finally pH in the solution was measured at room temperature. Finally, the volume was adjusted to 1l by adding ddH₂O before the Tris was sterilized by autoclaving.

8.1.8 The NEMATIC analysis

Table 29 Marker gene dataset analyzed with NEMATIC

Gene family name	Accession no.	Gene family name	Accession no.
SAMS	AT1G02500	1-aminocyclopropane-1-carboxylate synthase	AT1G01480
	AT4G01850		AT2G22810
	AT2G36880		AT3G49700
	AT3G17390		AT3G61510
TS	AT4G29840		AT4G08040
	AT1G72810		AT4G11280
Adenosyl-homocysteinase	AT4G13940		AT4G26200
	AT3G23810		AT4G37770
Homocysteine S-methyltransferase	AT5G20980		AT5G65800
	AT3G63250	S-adenosylmethionine decarboxylase	AT3G02470
	AT3G22740		AT3G25570
MS	AT5G17920		AT5G15950

	AT3G03780		AT5G18930
	AT5G20980		AT1G69770
HK	AT2G17265		AT1G80740
			AT3G05430
CGS	AT1G33320		AT4G08990
	AT3G01120		AT4G13610
CBL	AT3G57050		AT4G14140
MGL	AT1G64660		AT4G19020
TD	AT3G10050		AT5G27650
	AT2G31810		AT5G49160
Acetolactat synthase	AT3G48560		AT1G05010
	AT5G16290		AT1G12010
Ketol-acid reductase	AT3G58610		
Ketol-acid reductoisomerase	AT3G58610	1-aminocyclopropane-1- carboxylate oxidase	AT1G62380
Dihydroxy-acid dehydrtatase	AT3G23940		T1G77330
AspArtokinase/homoserine dehydrogenase	AT1G31230		AT2G19590
	AT4G19710	Adenosyl-homocysteinase	AT3G23810
Threonine aldolase	AT1G08630		AT4G13940
	AT3G04520		

8.1.9 Primer design using Primer 3

General Primer Picking Conditions

Upload the settings from a file Keine Datei ausgewählt.

<u>Primer Size</u>	Min 18	Opt 20	Max 23
<u>Primer Tm</u>	Min 59	Opt 60	Max 61
<u>Product Tm</u>	Min -100000	Opt 0.0	Max 100000
<u>Primer GC%</u>	Min 30.0	Opt 50.0	Max 70.0

Max Tm Difference 5.0 [Table of thermodynamic parameters](#) SantaLucia 1998

Product Size Ranges 150-250 100-300 301-400 401-500 501-600 601-700 701-850 851-1000

Number To Return 5 Max 3' Stability 9.0

Max Library Mispriming 12.00 Pair Max Library Mispriming 20.00

Thermodynamic Secondary Structure Alignments

<input checked="" type="checkbox"/> <u>Use Thermodynamic Oligo Alignment</u>	<input type="checkbox"/> <u>Use Thermodynamic Template Alignment</u>		
<u>TH: Max Template Mispriming</u>	40.00	<u>TH: Pair Max Template Mispriming</u>	70.00
<u>TH: Max Self Complementarity</u>	45.0	<u>TH: Max 3' Self Complementarity</u>	35.0
<u>TH: Max Pair Complementarity</u>	45.0	<u>TH: Max 3' Pair Complementarity</u>	35.0
<u>TH: Max Primer Hairpin</u>	24.0		

Old Secondary Structure Alignments

<u>Max Template Mispriming</u>	12.00	<u>Pair Max Template Mispriming</u>	24.00
<u>Max Self Complementarity</u>	8.00	<u>Max 3' Self Complementarity</u>	3.00
<u>Max Pair Complementarity</u>	8.00	<u>Max 3' Pair Complementarity</u>	3.00

Max #N's accepted 0 Max Poly-X 4
Inside Target Penalty -1.0 Outside Target Penalty 0 Note: you can set Inside Target Penalty to allow primers inside a target.
First Base Index 1 CG Clamp 0
Max GC in primer 3' end 5
3' End Distance Between Left Primers 3 3' End Distance Between Right Primers 3
5 Prime Junction Overlap 7 3 Prime Junction Overlap 4 (Distance of the primer ends to one overlap position.)
Concentration of Monovalent Cations 50.0 Salt Correction Formula SantaLucia 1998
Concentration of Divalent Cations 1.5 Concentration of dNTPs 0.6
Annealing Oligo Concentration 50.0 (Not the concentration of oligos in the reaction mix but of those annealing to template.)
Sequencing Spacing 500 Sequencing Interval 250
Sequencing Lead 50 Sequencing Accuracy 20

Liberal Base Show Debuging Info Treat ambiguity codes in libraries as consensus
 Lowercase masking Pick anyway Print Statistics

Figure 35 Primer design parameters used for Primer 3

8.2 Results

8.2.1 Results for experiments on *C. elegans*

8.2.1.1 Effects on the activity

Rate of inactive nematodes day 1								
	Rep 1	Rep 2	Rep 3	Rep 4	Average	Stdev	Count	St. error
Control	100,0	100,0	100,0	100,0	100,0	0,0	4,0	0,0
DL-Met 20 mM	100,0	100,0	100,0	100,0	100,0	0,0	4,0	0,0
MM 1mM	100,0	100,0	100,0	100,0	100,0	0,0	4,0	0,0
L-Lys 10mM	100,0	100,0	99,0	100,0	99,8	0,5	4,0	0,3
D-Lys 10mM	100,0	100,0	100,0	100,0	100,0	0,0	4,0	0,0
L-Thr 10mM	99,516908	100,0	100,0	100,0	99,9	0,2	4,0	0,1
D-Thr 10mM	100,0	100,0	100,0	100,0	100,0	0,0	4,0	0,0
L-Trp 10mM	100,0	86,0	100,0		95,3	8,1	3,0	4,7
D-Trp 10mM	100	100	98,55769	99,54751	99,5	0,7	4,0	0,3

Rate of inactive nematodes day 2								
	Rep 1	Rep 2	Rep 3	Rep 4	Average	Stdev	Count	St. error
Control	100,0	100,0	100,0	100,0	100,0	0,0	4,0	0,0
DL-Met 20 mM	100,0	100,0	100,0	100,0	100,0	0,0	4,0	0,0
MM 1mM	100,0	100,0	100,0	100,0	100,0	0,0	4,0	0,0
L-Lys 10mM	100,0	100,0	100,0	100,0	100,0	0,0	4,0	0,0
D-Lys 10mM	100,0	100,0	100,0	100,0	100,0	0,0	4,0	0,0
L-Thr 10mM	98,550725	100,0	100,0	100,0	99,6	0,7	4,0	0,4
D-Thr 10mM	100,0	100,0	100,0	100,0	100,0	0,0	4,0	0,0
L-Trp 10mM	100,0	86,0	86,7		90,9	7,9	3,0	4,6
D-Trp 10mM	98,734177	100	100	100,0	99,7	0,6	4,0	0,3

Rate of inactive nematodes day 3								
	Rep 1	Rep 2	Rep 3	Rep 4	Average	Stdev	Count	St. error
Control	100,0	100,0	100,0	100,0	100,0	0,0	4,0	0,0
DL-Met 20 mM	100,0	100,0	98,85714	100,0	99,7	0,6	4,0	0,3
MM 1mM	100,0	100,0	100,0	100,0	100,0	0,0	4,0	0,0
L-Lys 10mM	100,0	100,0	100,0	100,0	100,0	0,0	4,0	0,0
D-Lys 10mM	100,0	100,0	100,0	100,0	100,0	0,0	4,0	0,0
L-Thr 10mM	98,550725	100,0	100,0	100,0	99,6	0,7	4,0	0,4
D-Thr 10mM	100,0	100,0	100,0	100,0	100,0	0,0	4,0	0,0
L-Trp 10mM	62,9	55	58		58,6	4,2	3,0	2,4
D-Trp 10mM	98,7	100,0	100,0	100,0	99,7	0,6	4,0	0,3

Figure 36 *C. elegans* activity in solution - detailed results

8.2.2 Results on *H. schachtii*

8.2.2.1 Activity test in solution

	Rate of inactive nematodes				Average	Stdev	Active nema	St. Error
	Rep 1	Rep 2	Rep 3	Rep 4				
Control	26,5	18,0	53,5	42,8	35,2	15,9	64,8	8,0
L-Ile 10 mM	14,4	19,7	17,1		17,1	2,6	82,9	1,5
L-Hom 10 mM	19,8	25,0	23,1		22,6	2,6	77,4	1,5
L-Lys 10 mM	22,0	18,6	50,9	38,7	32,6	15,1	67,4	7,5
DL-Met 20 mM	35,2	14,6	38,4	45,6	33,4	13,3	66,6	6,7
L-Thr 10 mM	33,3	23,0	57,2	49,7	40,8	15,5	59,2	7,7
2-Ket 0,1 mM	42,6	40,5	44,6		42,6	2,1	57,4	1,2
MM 1 mM	35,5	16,1	68,8	52,6	43,2	22,6	56,8	11,3
D-Thr 10 mM	40,5	28,6	62,5	42,1	43,4	14,1	56,6	7,0
L-Trp 10 mM	45,2	30,1	58,3	47,5	45,3	11,6	54,7	5,8
D-Lys 10 mM	35,2	24,8	70,4	57,8	47,0	20,8	53,0	10,4
D-Trp 10 mM	51,2	41,8	64,4	55,6	53,3	9,4	46,7	4,7

Figure 37 *H. schachtii* activity test in solution - detailed results

8.2.2.2 24h incubation prior to nematode inoculation

8.2.2.2.1 Infection assay

	Rate of female nematodes				Rep 5	Rep 6	Avarage	Stdev	Count	St. Error
	Rep 1	Rep 2	Rep 3	Rep 4						
Control	100,0	100,0	100,0	100,0	100,0	100,0	100,0	0,0	0,0	0,0
L-Lys 10 mM	132,4	135,4	173,5	137,7			144,7	19,3	4,0	9,6
D-Lys 10 mM	148,4	134,1	209,1	113,1	127,8	117,0	141,6	35,4	6,0	14,4
L-Ile 10 mM	92,8	163,2	112,8				122,9	36,3	3,0	20,9
L-Hom 10 mM	92,3	133,7	79,5				101,8	28,3	3,0	16,4
DL-Met 20 mM	97,8	103,8	102,9	101,6			101,5	2,6	4,0	1,3
L-Trp 10 mM	95,2	102,9	88,1	116,3			100,6	12,0	4,0	6,0
D-Trp 10 mM	88,6	97,8	85,4	100,2			93,0	7,1	4,0	3,6
D-Thr 10 mM	93,3	112,3	54,1	91,8			87,9	24,4	4,0	12,2
MM 1 mM	79,7	105,5	86,2	68,0			84,8	15,7	4,0	7,8
L-Thr 10 mM	72,0	86,4	74,3	59,0			72,9	11,2	4,0	5,6

	Rate of male nematodes				Rep 5	Rep 6	Avarage	Stdev	Count	St. Error
	Rep 1	Rep 2	Rep 3	Rep 4						
Control	100,0	100,0	100,0	100,0	100,0	100,0	100,0	0,0	0,0	0,0
L-Lys 10 mM	82,1	153,8	101,3				112,4	37,2	3,0	21,5
D-Lys 10 mM	81,4	131,8	68,8				94,0	33,3	3,0	19,2
L-Ile 10 mM	107,5	67,5	78,5	111,3			91,2	21,5	4,0	10,8
L-Hom 10 mM	102,7	75,3	83,3	102,1			90,9	13,8	4,0	6,9
DL-Met 20 mM	115,0	87,0	81,7	78,3			90,5	16,7	4,0	8,3
L-Trp 10 mM	71,5	63,4	101,8	75,0			77,9	16,6	4,0	8,3
D-Trp 10 mM	95,3	42,8	85,3	59,0			70,6	24,1	4,0	12,0
D-Thr 10 mM	86,4	49,1	80,9	61,4	45,2	85,6	68,1	18,6	6,0	7,6
MM 1 mM	89,6	64,5	38,6	79,3			68,0	22,2	4,0	11,1
L-Thr 10 mM	65,6	59,6	65,9	59,6			62,7	3,5	4,0	1,8

Figure 38 24h incubation, infection assay - detailed results

8.2.2.2.2 Infection assay - Lys treatments without of ZnCl₂ and HgCl₂

	Rate of nematodes per plant %						
	Rep 1	Rep 2	Rep 3	Average	Stdev	Count	St. Error
Control	100,0	100,0	100,0	100	0	3	0
L-Lys 10 mM female	116,0	120,3	126,7	121,0	5,4	3	3,10
D-Lys 10 mM female	131,0	135,4	132,7	133,0	2,2	3	1,29
L-Lys 10 mM male	81,5	77,2	83,2	80,6	3,1	3	1,81
D-Lys 10 mM male	105,2	98,7	94,9	99,6	5,2	3	2,99

Figure 39 24h incubation, infection assay for Lys without of ZnCl₂ and HgCl₂ - detailed results

8.2.2.2.3 Female and syncytium sizes

	Relative female sizes					Average	Stdev	Count	St. Error
	Rep 1	Rep 2	Rep 3	Rep 4	Rep 5				
Control	100,0	100,0	100,0	100,0	100,0	100,0	0,0	5,0	0,0
D-Thr 10 mM	104,0	95,3	93,8	123,9		104,2	13,9	4,0	6,9
L-Lys 10 mM	107,3	97,3	107,6			104,1	5,8	3,0	3,4
L-Trp 10 mM	106,2	104,8	90,9	112,7		103,6	9,2	4,0	4,6
D-Lys 10 mM	107,7	96,9	96,0	103,3	108,8	102,5	5,9	5,0	2,7
L-Ile 10 mM	99,2	105,2	101,1			101,8	3,1	3,0	1,8
L-Hom 10 mM	97,1	113,6	91,9			100,9	11,3	3,0	6,6
L-Thr 10 mM	104,2	97,4	99,2			100,3	3,5	3,0	2,0
MM 1 mM	100,0	97,6	94,2			97,3	2,9	3,0	1,7
DL-Met 20 mM	100,8	101,7	87,0			96,5	8,3	3,0	4,8
D-Trp 10 mM	97,3	95,5	74,3	117,2		96,1	17,5	4,0	8,8

Figure 40 24h incubations – relative female sizes at 14dpi - detailed results

	Relative syncytium sizes					Average	Stdev	Count	St. Error
	Rep 1	Rep 2	Rep 3	Rep 4	Rep 5				
Control	100,0	100,0	100,0	100,0	100,0	100,0	0,0	5,0	0,0
L-Thr 10 mM	100,2	114,5	103,2			105,9	7,6	3,0	4,4
L-Lys 10 mM	101,6	118,4	97,0			105,7	11,3	3,0	6,5
D-Trp 10 mM	113,7	108,9	96,4	103,3		105,6	7,4	4,0	3,7
L-Ile 10 mM	102,9	96,4	113,1			104,1	8,4	3,0	4,9
L-Trp 10 mM	110,8	108,0	90,8	103,7		103,3	8,8	4,0	4,4
DL-Met 20 mM	111,8	91,5	101,0			101,4	10,2	3,0	5,9
D-Lys 10 mM	91,5	96,2	87,6	105,2	112,2	98,5	10,0	5,0	4,5
L-Hom 10 mM	98,6	94,9	100,6			98,0	2,9	3,0	1,7
D-Thr 10 mM	96,2	95,2	101,5	94,3		96,8	3,2	4,0	1,6
MM 1 mM	107,3	105,9	59,3			90,8	27,4	3,0	15,8

Figure 41 24h incubations - relative syncytium sizes at 14dpi - detailed results

8.2.2.3 Test compounds supplemented to the agar

8.2.2.3.1 Invasion rate analysis

	% of invaded nematodes				Average	Count	Stdev	St. Error
	Rep 1	Rep 2	Rep 3	Rep 4				
Control	100,0	100,0	100,0	100,0	100,0	4,0	0,0	0,0
DL-Met 0.2 mM	87,1	111,0	104,2		100,8	3,0	12,3	7,1
MM 0.1 mM	59,8	90,6	120,3		90,2	3,0	30,3	17,5
L-Thr 0.1 mM	82,6	90,1	134,6	97,7	101,3	4,0	23,1	11,6
L-Ile 0.1 mM	101,4	98,2	87,3		95,6	3,0	7,4	4,3

Figure 42 Aa treated *A. thaliana*: invasion rate analysis – detailed results

8.2.2.3.2 Infection assay

	% of females per plant				Average	Stdev	Count	St. Error
	Rep 1	Rep 2	Rep 3	Rep 4				
Control	100,0	100,0	100,0	100,0	100,0	0,0	4,0	0,0
L-Lys 0.001 mM	97,6	100,2	109,9		102,6	6,5	3,0	3,7
D-Lys 0.1 mM	110,3	81,6	125,8		105,9	22,4	3,0	12,9
L-Trp 0.1 mM	54,6	76,2	117,2	112,4	90,1	29,9	4,0	15,0
D-Thr 0.1 mM	126,2	80,5	103,3	48,4	89,6	33,2	4,0	16,6
L-Hom 0.1 mM	46,7	93,0	89,7		76,5	25,8	3,0	14,9
L-Thr 0.1 mM	52,6	68,2	77,2		66,0	12,4	3,0	7,2
D-Trp 0.1 mM	60,0	66,9	53,1	81,8	65,4	12,3	4,0	6,1
L-Ile 0.1 mM	62,2	65,5	63,8		63,8	1,6	3,0	0,9
2-Ket 0.1 mM	48,9	62,6	77,4		63,0	14,3	3,0	8,2
DL-Met 0.2 mM	67,6	63,3	55,6		62,2	6,1	3,0	3,5
MM 0.1 mM	74,6	79,4	23,2		59,1	31,1	3,0	18,0

	% of males per plant				Average	Stdev	Count	St. Error
	Rep 1	Rep 2	Rep 3	Rep 4				
Control	100,0	100,0	100,0	100,0	100,0	0,0	4,0	0,0
D-Lys 0.1 mM	127,5	131,5	59,7		106,2	40,3	3,0	23,3
L-Lys 0.001 mM	125,7	88,3	109,2		107,7	18,7	3,0	10,8
DL-Met 0.2 mM	65,8	112,8	105,7		94,7	25,4	3,0	14,6
L-Ile 0.1 mM	80,1	100,2	88,3		89,5	10,1	3,0	5,8
2-Ket 0.1 mM	116,9	71,6	81,3		89,9	23,9	3,0	13,8
L-Trp 0.1 mM	118,1	76,1	97,0	47,9	84,8	30,0	4,0	15,0
D-Thr 0.1 mM	102,7	98,3	80,9	43,8	81,4	26,8	4,0	13,4
L-Hom 0.1 mM	38,9	82,4	82,5		67,9	25,2	3,0	14,5
D-Trp 0.1 mM	82,4	66,5	61,0	53,0	65,7	12,4	4,0	6,2
L-Thr 0.1 mM	33,5	34,5	99,4		55,8	37,8	3,0	21,8
MM 0.1 mM	74,9	55,6	30,9		53,8	22,0	3,0	12,7

Figure 43 Aa treated *A. thaliana*: rate of adult nematodes per plant – detailed results

8.2.2.3.3 Female and syncytium sizes

	% female sizes 14 dpi				Stdev	Count	St. Error
	Rep 1	Rep 2	Rep 3	Rep 4			
Control	100,0	100,0	100,0	100,0	100,0	5,0	0,0
D-Lys 0.1 mM	102,2	119,8	96,5		106,1	12,1	3,0
L-Lys 0.001 mM	98,0	108,1	110,8		105,6	6,8	3,0
D-Thr 0.1 mM	96,5	114,0	83,9		98,1	15,1	3,0
DL-Met 0.2 mM	100,7	83,8	97,7		94,0	9,0	3,0
L-Thr 0.1 mM	110,3	78,4	92,9		93,9	16,0	3,0
2-Ket 0.1 mM	94,9	81,5	101,3		92,5	10,1	3,0
L-Ile 0.1 mM	83,5	88,0	100,8		90,8	8,9	3,0
D-Trp 0.1 mM	76,6	99,2	81,7	99,9	89,4	12,0	4,0
L-Trp 0.1 mM	82,8	87,4	72,3	97,5	85,0	10,4	4,0
MM 0.1 mM	92,2	86,9	51,4		76,8	22,2	3,0
L-Hom 0.1 mM	62,0	85,6	82,5		76,7	12,8	3,0
							7,4

Figure 44 Aa treated *A. thaliana*: relative female sizes 14dpi – detailed results

	% female sizes 28 dpi				Average	Stdev	Count	St. Error
	Rep 1	Rep 2	Rep 3	Rep 4				
Control	100,0	100,0	100,0	100,0	100,0	0,0	4,0	0,0
DL-Met 0.2 mM	111,9	118,6	92,7		107,7	13,5	3,0	7,8
D-Lys 0.1 mM	108,9	113,9	110,0		110,9	2,6	3,0	1,5
L-Thr 0.1 mM	101,0	112,1	98,2		103,8	7,4	3,0	4,3
L-Hom 0.1 mM	76,9	107,3	115,7		100,0	20,4	3,0	11,8
D-Trp 0.1 mM	94,3	93,7	94,1		94,0	0,3	3,0	0,2
D-Thr 0.1 mM	89,0	92,7	96,6		92,8	3,8	3,0	2,2
L-Ile 0.1 mM	85,0	92,1	98,5		91,8	6,8	3,0	3,9
L-Trp 0.1 mM	83,9	94,9	89,9	88,4	89,3	4,5	4,0	2,3
MM 0.1 mM	88,3	87,6	103,5		93,1	9,0	3,0	5,2

Figure 45 Aa treated *A. thaliana*: relative female sizes 28dpi – detailed results

	% syncytium sizes					Stadev	Count	St. Error	
	Rep 1	Rep 2	Rep 3	Rep 4	Rep 5				
Control	100,0	100,0	100,0	100,0	100,0	100,0	0,0	5,0	0,0
D-Lys 0.1 mM	94,0	121,5	154,2			123,2	30,1	3,0	17,4
L-Thr 0.1 mM	103,2	110,3	108,0			107,1	3,6	3,0	2,1
L-Ile 0.1 mM	97,8	112,0	100,6			103,5	7,5	3,0	4,3
L-Lys 0.001 mM	100,3	110,5	98,4			103,1	6,5	3,0	3,7
D-Thr 0.1 mM	107,5	97,9	94,6			100,0	6,7	3,0	3,9
2-Ket 0.1 mM	92,5	86,1	107,7			95,4	11,1	3,0	6,4
DL-Met 0.2 mM	75,9	107,1	99,4	95,6	98,3	95,2	11,7	5,0	5,2
L-Trp 0.1 mM	94,6	79,1	111,6			95,1	16,3	3,0	9,4
D-Trp 0.1 mM	89,1	87,9	108,2			95,0	11,4	3,0	6,6
L-Hom 0.1 mM	80,2	96,9	96,1			91,1	9,4	3,0	5,4
MM 0.1 mM	98,8	90,0	73,3			87,4	12,9	3,0	7,5

Figure 46 Aa treated *A. thaliana*: relative syncytium sizes 14dpi – detailed results

8.2.2.3.4 Eggs per cyst

	Average eggs / 5 µl			Average / Cyst	Stdev	Count	St. Error
	Rep 1	Rep 2	Rep3				
Control	33,1	25,6	27,6	287,7	38,7	3,0	22,3
DL-Met 0.2 mM	30,8	28,6	25,4	282,8	27,0	3,0	15,6
MM 0.1 mM	21,3	29,2	27,2	258,8	41,3	3,0	23,9

	Average eggs per 5 µl			Average / Cyst	Stdev	Count	St. Error
	Rep 1	Rep 2	Rep3				
Control	36,7	40,7	37,1	381,9	22,2	3,0	12,8
L-Thr 0.1 mM	36,8	30,0	35,1	339,9	35,6	3,0	20,6
L-Ile 0.1 mM	35,1	31,5	31,9	328,1	19,5	3,0	11,3

Figure 47 Aa treated *A. thaliana*: average eggs per cyst – detailed results

8.2.2.4 Analysis of *A. thaliana* SALK_081563c and mto1-1

8.2.2.4.1 Infection assay

	female	male	St. error f	St. Error m
Control	100	100	0	0
SALK_081563c	90,5	84,7	9,1	23,7
mto1-1	87,9	73,5	15,1	18,7

Figure 48 SALK_081563c and mto1-1 infection assay, rate of adult nematodes per plant – detailed results

8.2.2.4.2 Female and syncytium sizes

	Average female sizes (mm ²)			Average	Stdev	Count	St. Error
	Rep 1	Rep 2	Rep 3				
Col-0 (for SALK)	0,116	0,121	0,11	0,116	0,005	3	0,003
SALK_081563c	0,117	0,106	0,125	0,116	0,01	3	0,006
Col-0 (for mto1-1)	0,114	0,118	0,112	0,115	0,003	3	0,002
mto1-1	0,099	0,097	0,104	0,1	0,003	3	0,002

Figure 49 SALK_081563c and mto1-1, average female sizes per plant at 14dpi (mm²). Mutants were tested individually and refer to their individual control lines: Col-0 (for SALK) and Col-0 (for mto1-1) – detailed results

	Average syncytium sizes (mm ²)			Average	Stdev	Count	St. Error
	Rep 1	Rep 2	Rep 3				
Col-0 (for SALK)	0,281	0,314	0,282	0,292	0,019	3	0,011
SALK_081563c	0,254	0,244	0,255	0,251	0,006	3	0,003
Col-0 (for mto1-1)	0,283	0,303	0,262	0,283	0,021	3	0,012
mto1-1	0,259	0,299	0,260	0,272	0,023	3	0,013

Figure 50 SALK_081563c and mto1-1, average syncytium sizes per plant at 14dpi (mm²). Mutants were tested individually and refer to their individual control lines: Col-0 (for SALK) and Col-0 (for mto1-1) – detailed results

8.2.2.5 Detailed analysis of the infection and development process

treatment	developmental stop	dpi dev. stop	exit infection site	dpi exit infection site	male	female	undetectable
Control							
Rep 1	4,0	2,5	2,0	2,5	8,0	5,0	0,0
Rep 2	4,0	3,5	2,0	1,0	4,0	6,0	3,0
Rep 3	4,0	3,8	4,0	0,8	4,0	5,0	2,0
Average		3,3		1,4			
Σ	12		8		16	16	5
DL-Met 0.2 mM							
Rep 1	3,0	3,0	3,0	1,7	1,0	9,0	3,0
Rep 2	3,0	4,3	4,0	1,3	7,0	3,0	2,0
Rep 3	6,0	2,7	5,0	1,6	3,0	2,0	3,0
Average		3,3		1,5			
Σ	12		12		11	14	8
L-Ile 0.1 mM							
Rep 1	5,0	2,8	1,0	1,0	5,0	7,0	1,0
Rep 2	4,0	4,3	3,0	1,7	3,0	6,0	3,0
Rep 3	2,0	6,0	3,0	1,3	3,0	7,0	4,0
Average	2,3	4,4		1,3			
Σ	11		7		11	20	8
L-Thr 0.1 mM							
Rep 1	5,0	3,2	4,0	1,3	5,0	4,0	1,0
Rep 2	4,0	3,3	2,0	1,5	6,0	4,0	3,0
Rep 3	5,0	2,6	2,0	1,0	4,0	6,0	2,0
Average		3,0		1,3			
Σ	14,0		8,0		15,0	14,0	6,0

Figure 51 Detailed analysis of the infection process – detailed results

8.2.2.6 Gene expression analysis by NEMATIC

Table 30 Full set of genes used for the NEMATIC based analysis. Additionally, to the fold changes given in the results, this table also includes the tested genes that had an unchanged expression rate – detailed results

gene (family)	accession no.	fold change
S-adenosylmethionine synthetase	AT1G02500	-3,1
	AT4G01850	-1,3
	AT2G36880	-2,6
	AT3G17390	No
threonine synthase	AT4G29840	3,1
	AT1G72810	No
adenosylhomocysteinase	AT4G13940	-2,4
	AT3G23810	No
homocysteine S-methyltransferase	AT5G20980	No
	AT3G63250	2,3

	AT3G22740	No
methionine synthase	AT5G17920	No
	AT3G03780	No
homoserin kinase	AT2G17265	2,2
cystathionine gamma-synthase	AT1G33320	-3,1
	AT3G01120	No
cystathionine beta-lyase	AT3G57050	1,3
methionine gamma-lyase	AT1G64660	No
threonine dehydratase	AT3G10050	2,9
	AT2G31810	No
acetolactat synthase	AT3G48560	2,3
	AT5G16290	2,6
ketol-acid reductase	AT3G58610	2,2
dihydroxy-acid dehydratase	AT3G23940	4
	AT1G31230	3,7
homoserine dehydrogenase	AT4G19710	4,5
	AT1G08630	No
threonine aldolase	AT3G04520	-1,7
	AT1G01480	No
	AT2G22810	No
	AT3G49700	No
1-aminocyclopropane-1-carboxylate synthase	AT3G61510	No
	AT4G08040	-1
	AT4G11280	No
	AT4G26200	1,2
	AT4G37770	No
	AT5G65800	No
	AT3G02470	-0,6
S-adenosylmethionine decarboxylase	AT3G25570	-1,4
	AT5G15950	No
	AT5G18930	No
	AT1G69770	No
	AT1G80740	No
DNA (cytosine-5)-methyltransferase	AT3G05430	0,5
	AT4G08990	No
	AT4G13610	No
	AT4G14140	No
	AT4G19020	No
	AT5G27650	No
	AT5G49160	No
	AT1G05010	-4
1-aminocyclopropane-1-carboxylate oxidase	AT1G12010	No
	AT1G62380	-3,3
	T1G77330	No
	AT2G19590	-2,4

8.2.2.7 qRT-PCR - gene expression analysis

Gen	fold change			Stdev			St. Error		
	DL-Met 0.2 mM	L-Thr 0.1 mM	MM 0.1 mM	DL-Met 0.2 mM	L-Thr 0.1 mM	MM 0.1 mM	DL-Met 0.2 mM	L-Thr 0.1 mM	MM 0.1 mM
Actin2	1,0	1,0	1,0	0,0	0,0	0,0	0,0	0,0	0,0
TS1	1,4	0,6	0,9	0,2	0,2	0,3	0,1	0,1	0,2
TS2	1,5	0,5	0,9	0,1	0,1	0,1	0,1	0,0	0,1
THA1	3,2	0,8	0,8	0,8	0,4	0,4	0,4	0,3	0,2
THA2	2,5	0,6	0,6	0,2	0,1	0,0	0,1	0,1	0,0
CGS	1,6	4,6	1,9	0,4	2,2	0,2	0,2	1,3	0,1
MGL	5,1	4,5	3,7	1,2	0,3	1,3	0,7	0,2	0,8
OMR	1,5	1,1	0,9	0,2	0,3	0,3	0,1	0,2	0,2
SAMS1	1,0	2,4	1,0	0,2	0,4	0,1	0,1	0,2	0,1
SAMS2	0,9	0,9	0,6	0,3	0,3	0,1	0,2	0,2	0,1
SAMS3	1,3	1,2	0,7	0,3	0,8	0,1	0,2	0,4	0,0
SAMS4	0,9	0,7	0,5	0,8	0,3	0,1	0,4	0,2	0,1

Figure 52 Gene expression analysis in uninfected *A. thaliana* roots - detailed results

Gen	fold change			Stdev			St. Error		
	DL-Met 0.2 mM	L-Thr 0.1 mM	MM 0.1 mM	DL-Met 0.2 mM	L-Thr 0.1 mM	MM 0.1 mM	DL-Met 0.2 mM	L-Thr 0.1 mM	MM 0.1 mM
Actin2	1	1	1	0	0	0	0	0	0
TS1	2,6	1,2	1,7	0,14	0,41	0,48	0,08	0,24	0,28
TS2	2,0	1,1	1,8	0,77	0,36	0,37	0,44	0,21	0,21
THA1	4,9	1,2	3,5	2,92	0,23	2,67	1,68	0,13	1,54
THA2	3,4	1,3	2,4	0,52	0,49	0,76	0,30	0,28	0,44
CGS	2,3	2,2	1,2	2,35	1,07	0,78	1,36	0,62	0,45
MGL	1,0	0,8	0,9	0,14	0,50	0,25	0,08	0,29	0,14
OMR	3,8	0,6	2,1	2,71	0,12	0,24	1,56	0,07	0,14
SAMS1	1,4	1,2	1,1	0,43	0,24	0,44	0,25	0,14	0,26
SAMS2	0,9	1,4	0,8	0,45	0,61	0,10	0,26	0,35	0,06
SAMS3	1,4	1,1	1,0	0,68	0,31	0,25	0,39	0,18	0,15
SAMS4	1,4	1,0	1,3	0,32	0,29	0,51	0,18	0,17	0,29

Figure 53 Gene expression analysis in infected *A. thaliana* roots – detailed results

8.2.2.8 Infection assays with SALK_081563c and mtol-1

As described in chapter 2.1.3, the both *A. thaliana* mutants, SALK_081563c and mtol-1, have markedly altered metabolic levels of Met, Thr and other close related metabolites. Possible effects of these artificially changed aa levels on the parasitism process of *H. schachtii* were studied by infection assay analysis. In a first step, the presence of the described mutations and the homozygosity of the plant material was confirmed.

8.2.2.8.1 Homozygosity confirmation

8.2.2.8.1 1 mto1-1

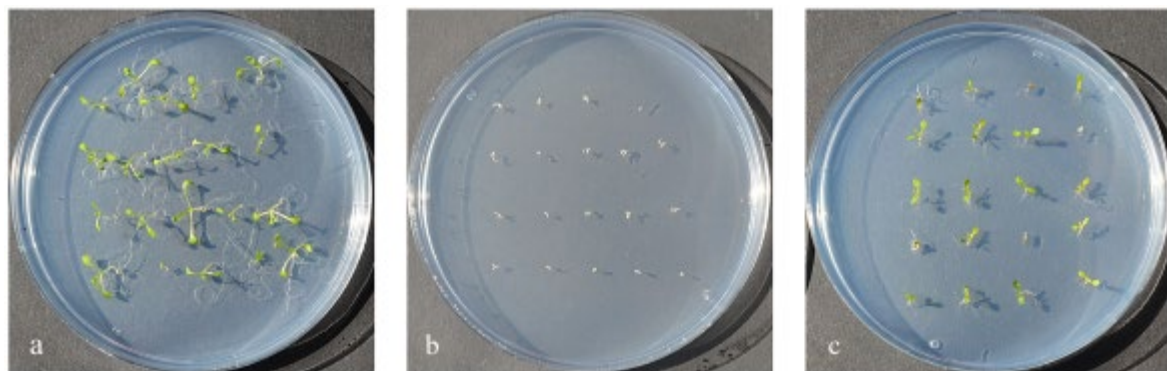


Figure 54 mto1-1 homozygosity confirmation on selective ethionine medium. Picture content description: a) *A. thaliana* (col-0) on standard Knops'-medium with functional plant development, b) *A. thaliana* (col-0) on selective 0.1 mM L-ethionine enriched Knops'-medium with inhibited plant development, c) ethionine resistant *A. thaliana* (mto 1-1) on selective 0.1mM L-ethionine enriched Knops'-medium with functional development. Plants were cultured under aseptic conditions and pictures were taken at 10dps.

As apparent from figure 26 a, all seeded *A. thaliana* (col-0) germinated and developed normally on standard Knops'-medium, proofing the integrity of this col-0 seed material. Further on, the growth inhibition for col-0 confirms the selective potential of the 0.1mM L-ethionine enriched Knops'-medium, cf. figure 26 b. All seeded mto1-1 plants germinated and developed on the ethionine selective media, cf. figure 26 b. Accordingly, the homozygosity and described mutation of the *A. thaliana* mto1-1 seed material was unambiguously proven.

8.2.2.8.1.2 SALK_081563c

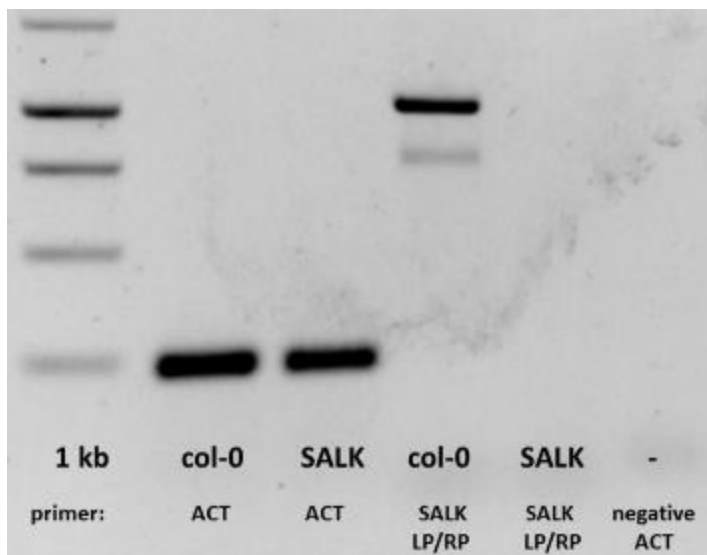


Figure 55 Homozygosity confirmation of the TS deficient SALK_081563c The positive control primer ACT generates a single amplicon on col-0 and SALK DNA. The insertion specific primer SALK LP/RP amplifies on col-0 but not on SALK DNA, proving the homozygosity of the selected SALK_081563c line. The negative ACT control proves the integrity of the reagents.

As apparent from figure 27, the positive control shows one distinct ~250bp amplicon for both, col-0 and SALK template DNA in combination with ACT. Accordingly, the functionality of both extracted DNAs was confirmed. Moreover, the negative control did not yield an amplicon proving the integrity of the applied reagents. The insertion specific primer pair SALK LP/RP did not amplify on SALK_081563c DNA but yielded two bands of 1000bp and 800bp length on col-0 template DNA. Therefore, the TS knockout in SALK_081563c was confirmed for the seed material used in the following.

8.2.2.8.2 Infection assay

8.2.2.8.2.1 Number of male and female nematodes

Cyst nematodes feed exclusively from their syncytium, dragging the needed nutrients and fluids from the surrounding host root tissue. Significantly altered metabolic Thr and Met levels might impact the underlying functional mechanistic behind, resulting in effects on the nematode development. Nematode numbers per plant and female and syncytium size measurements were conducted to screen for putative effects.

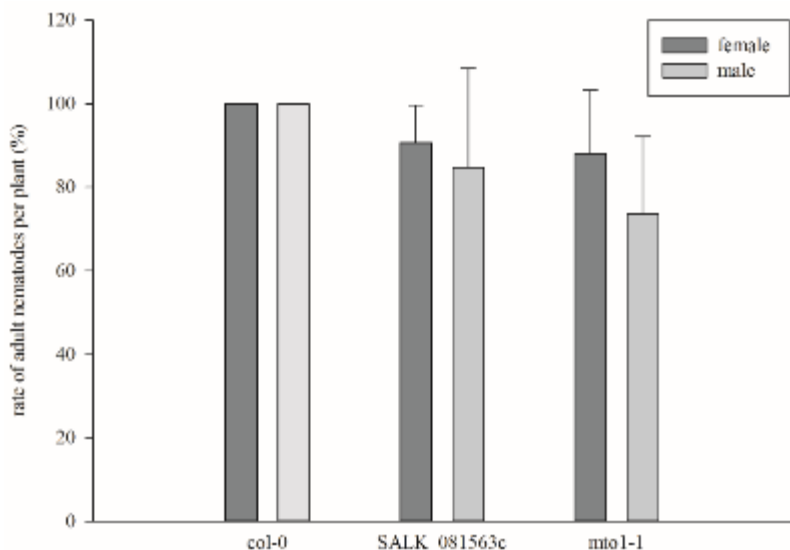


Figure 56 SALK_081563c – rate of adult nematodes / plant *A. thaliana* col-0 (control), SALK_081563c and mto1-1 were cultured on Knops medium under aseptic conditions. 60 sterile *H. schachtii* J2s were inoculated per plant at 10dps. The number of male and female nematodes per plant was counted at 12dpi. Indicated are average values \pm standard errors were calculated on the means of three biological replications.

The male and female numbers per plant, ascertained on SALK_081563c and mto1-1 were not significantly different from the ones observed on wildtype plants (col-0), cf. figure 56.

8.2.2.8.2.2 Female and syncytium sizes

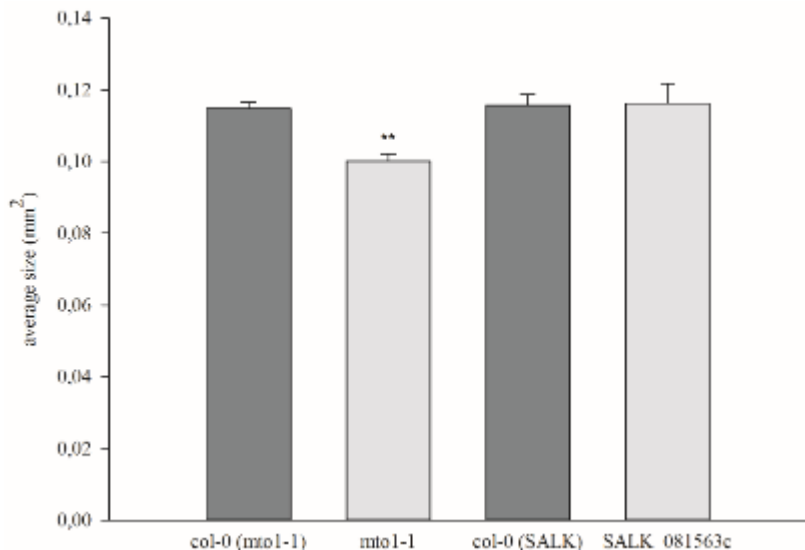


Figure 57 SALK_081563c – average female sizes *A. thaliana* col-0 (control), SALK_081563c and mto1-1 were cultured on Knops medium under aseptic conditions. 60 sterile *H. schachtii* J2s were inoculated per plant at 10 dps. Female sizes were measured at 14 dpi. The indicated are averages \pm standard errors were calculated on the means of three biological replications. The asterisk (*) refers to a significant difference according to t-Test ($P \geq 0.05$).

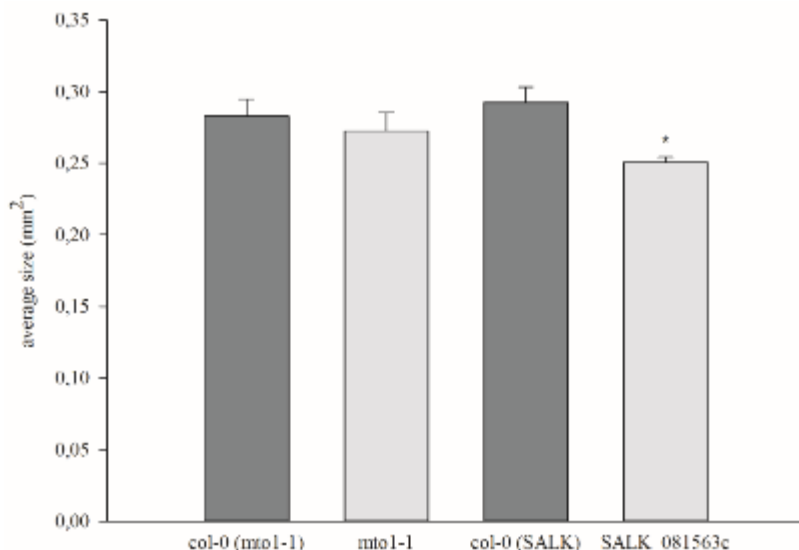


Figure 58 SALK_081563c – average syncytia sizes *A. thaliana* col-0 (control), SALK_081563c and mto1-1 were cultured on Knops medium under aseptic conditions. 60 sterile *H. schachtii* J2s were inoculated per plant at 10dps. Syncytia sizes were measured at 14dpi. The indicated are averages \pm standard errors were calculated on the means of three biological replications. The asterisk (*) refers to a significant difference according to t-Test ($P \geq 0.05$).

At 14dpi, the average female sizes were not affected on SALK (0.116mm^2), but significantly smaller on mto1-1 (0.116mm^2), cf. figure 57. As opposed to this, the mto1-1 lines (0.272mm^2) hosted normally sized syncytia whereas they were significantly reduced in size in the roots of SALK (0.251mm^2), see figure 58.

ACKNOWLEDGEMENTS

Mein besonderer Dank gilt zuerst Prof. Dr. Florian M.W. Grundler, der es mir ermöglicht hat, meine Diplomarbeit sowie meine Dissertation im Institut für Molekulare Phytomedizin der Universität Bonn durchzuführen. Mit Ihrer hervorragenden fachlichen Leitung und Ihrem offenen freundlichen Wesen haben Sie eine außerordentlich produktive und gleichzeitig angenehme Arbeitsatmosphäre geschaffen. Vielen Dank, Herr Grundler, dass Sie mir all dies ermöglicht haben.

Der Firma EVONIK gehört mein Dank für die finanzielle Unterstützung dieser Arbeit. Hier bedanke ich mich besonders bei Herrn Dr. Daniel Fischer. Auf Ihre schnelle, zuverlässige und akkurate Zuarbeit konnte ich mich stehts verlassen. Mit starkem theoretischem Wissen und Engagement haben Sie einen wichtigen Beitrag zum Gelingen dieser Arbeit geleistet.

Des Weiteren möchte ich mich vielmals bei Dr. Philipp Gutbrod bedanken. Mit deinem tiefen Fachwissen warst du ständig für mich ansprechbar, um mir bei allen aufkommenden Problemen und Ideen zu helfen. Nicht zuletzt bauen viele der hier verwendeten Methoden auf deiner wissenschaftlichen Arbeit der vergangenen Jahre auf. Es hat viel Spaß gemacht!

Auch meinen Eltern, meinen Schwestern Katharina und Rabea sowie Anjuli Bratke möchte ich an dieser Stelle ausdrücklich für die Unterstützung über all die Jahre meinen Dank aussprechen.

Bedanken möchte ich mich ebenfalls bei Dr. Abdelnaser Elashry, Dr. Shahid M. Siddique und Dr. Alexander Schouten sowie allen nicht namentlich genannten Mitarbeitern des Institutes. Ihr alle habt einen großen Anteil. Vielen Dank für Eure Mithilfe, Beratung und die schöne Zeit, die wir in den vergangenen Jahren miteinander verbracht haben. Ich habe sie sehr genossen.